AUTOMATED LABOUR DETECTION FRAMEWORK TO MONITOR PREGNANT WOMEN WITH A HIGH RISK OF PREMATURE LABOUR

by

Hisham K. Allahem

Submitted in partial fulfillment of the requirements
for the degree of Doctor of Philosophy

at

Dalhousie University
Halifax, Nova Scotia
January 2022

To my beloved Parents, Shekhah and Khalaf,

my beloved wife, Angham,

and my little angels, Nagham and Hossam, who inspired it all.

Table of Contents

List of Tables

List of Figures

List of Algorithms

Abstract

It is estimated that more than 1 in 10 babies are born prematurely worldwide. Babies that survive premature birth are more likely to face lifelong health-related disabilities. By monitoring uterine contractions, labour can be detected, which assists in reducing premature birth complications.

Several studies have been conducted on monitoring pregnant women with a high risk of premature birth. The first study focused on home monitoring of uterine activity versus nurses' frequent contact with pregnant women. The second study compared electrohysterography with intrauterine pressure catheter to monitor pregnant women by recruiting 32 pregnant women in labour for a minimum of 30 minutes and used a simple algorithm to automatically recognize uterine contractions. The third study took randomized control trials of home uterine activity monitoring for pregnant women with a high risk of premature birth from 15 studies to determine if home monitoring systems can be used to evaluate pregnancy health status. The last three studies individually proposed the use of home mobile healthcare systems to monitor pregnant women.

Machine learning techniques have recently been used to predict and detect premature labour. Recent studies have used machine learning classifiers such as Random Forest and Decision Tree to categorize and recognize electrohysterography contractions with a high accuracy rate. In addition, deep learning models such as artificial neural networks, similar to machine learning techniques, have been designed to mimic the human brain to analyze and extract complex relationships between data.

In this research, we aim to mitigate the consequences of premature birth for pregnant women and the fetus by proposing a safe, simple, home-comfortable, low-cost, and reliable monitoring framework. The system uses a non-invasive method to monitor uterine electrohysterography contractions using a wireless body sensor and a smartphone. The smartphone will analyze uterine readings, and if they contain a premature labour pattern, a warning notification will be triggered. The framework will have three schemes: an amplitude-frequency algorithm scheme, a machine learning algorithm scheme, and a deep learning scheme. A proof-of-concept prototype was designed and tested for reliability, performance and power consumption using five electrohysterography uterine contraction databases. The results show that the schemes were able to meet the framework's objectives.

Glossary

°C	Celsius
°F	Fahrenheit
AC	accuracy
AI	artificial intelligence
ANN	artificial neural network
AUC	area under the ROC curve
AUROC	area under the receiver operator curve
BC	bipolar concentric
CC	30-minute session counter check
CNN	convolutional neural network
Contr	contractions count
CPU	central processing unit
CV	conduction velocity
DL	deep learning
DT	decision trees
ECG	electrocardiogram
EHG	electrohysterography
ELM	extreme learning machine
EMD	empirical mode decomposition
EMG	electromyography
EWT	empirical wavelet transform
F	F score
FastICA	fast independent component analysis
FD	final decision
FFT	fast fourier transform

FMCU	feto-maternal care unit
FN	false negative
FNR	false negative rate
FP	false positive
FPR	false positive rate
GB	gigabyte
GLMs	generalized linear machine learning models
GMM	Gaussian mixture models
GPRS	general packet radio service network
GUI	graphical user interface
HR	heart rate
HRV	heart rate variability
IMF	intrinsic mode function
IoT	internet of things
IUPC	intrauterine pressure catheter
mAh	Milliamp/Hour
MB	megabyte
MDF	median frequency
MisCl	misclassification rate
ML	machine learning
mmHg	millimetres of mercury
MNF	mean frequency
mV	millivolt
MVU	Montevideo units
NB	Naïve Bayes

NI	national instruments
OS	operating system
P	precision
PC	personal computer
PCA	principal component analysis
PCG	phonocardiogram
PD	percentage difference
PDA	personal digital assistant
PF	peak frequency
PFM	positive force measurement
PIH	Pregnancy-induced Hypertension
PPG	photoplethysmogram
PRPD	percentage rate of pattern dissimilarities
R	recall
RBF	Radial Basis Function
RBNC	Radial Basis Function Neural Network
RF	random forest
RMS	root mean square
ROC	receiver operating characteristic
RQA	recurrence quantification analysis
RUCR	retrieved uterine contraction reading
SD	standard deviation
SSAE	stacked sparse autoencoder
SVM	support vector machine
T1D	type one diabetes

Te	end time
TH	threshold
TN	true negative
TP	true positive
TPR	true positive rate
Ts	start time
UEQ	user experience questionnaire
UI	user interface
VMD	variational mode decomposition
WBS	wireless body sensor
WBSNs	wireless body sensor networks
WPD	wavelet packet decomposition

Acknowledgements

I would like to express my sincere gratitude to my supervisor and my ideal in academic life, Dr. Srinivas Sampalli, for his support and guidance both academically and personally. From the first day he became my master's supervisor until the day I presented this thesis, he was always there to encourage me in the rough times during my graduate studies journey. He taught me how to be a student, an academic and a teacher.

I would like to express my sincere gratitude for my research aptitude, thesis proposal and Ph.D. thesis committee members: Dr. Rita Orji, Dr. Qiang Ye and Dr. Musfiq Rahman for providing valuable feedback to help guide me to improve my research from various perspectives

I would also like to thank Dr. Anjali Agarwal, from Concordia University, Canada, for graciously agreeing to be the external examiner and her thought-provoking suggestions and questions that contributed to making my thesis better.

I would like to also express my sincere gratitude to Dr. Jaume Manero from Universitat Politècnica de Catalunya, Spain; Dr. Ebtehal Hussein Aljumaai, Obstetric and Gynecology Registrar, Abha Maternity Children's Hospital, Saudi Arabia; Dr. Mohamed Elsheikh, obstetrician and fetal medicine consultant, National Guard Hospital, MRCOG, SSCOG, DIP Prenatal Genetics, Riyadh, Saudi Arabia; and Darshana Upadhyay, MCS, Faculty of Computer Science, Dalhousie University, Canada, for their help and support.

My thanks and appreciation go out to my family and friends from MyTech Lab for all the support and unforgettable days and laughs we had together.

Finally, I would like to express my sincere gratitude to Aljouf University in Saudi Arabia, which has funded this work and provided this once-in-a-lifetime opportunity to complete my Ph.D. with Saudi Arabian Cultural Bureau support in Canada. I appreciate and acknowledge the assistance provided by these organizations.

Chapter 1

Introduction

1.1 Overview of Premature Birth

Premature birth, which is a consequence of premature or preterm labour, is a serious health issue for both the fetus and the mother. It can be a major pregnancy complication [1] [2] and is the most common cause of death for neonates, even with current advanced healthcare technologies [3] [4] [5] [6] [7] [8]. Moreover, it is the leading cause of death for children under five years [9]. Worldwide, 15 million premature births occur every year, which represents about 9.6% to 11% of total births [7] [10] [11] [12] [13].

Premature birth is defined as birth before completing the 37^{th} week of gestation [5] [11] [14] [15] [16] [17]. The authors of [18] more specifically define premature birth as between the 21^{st} and 37^{th} week of gestation. Another definition of premature birth is changes in the cervix due to regular uterus contractions before the 37^{th} week of gestation [19] [20]. Thus, we can categorize premature birth based on gestational age into:

- Extremely premature (<28 weeks).
- Very premature (28 to <32 weeks).
- Moderate to late premature (32 to <37 weeks).

Premature birth is also an important perinatal healthcare issue [18] [15]. Furthermore, babies who survive a premature birth are usually not fully developed, and this can lead to short- and long-term health issues [1] [2] [13] [17] [20] [21] [22] [23] [24]. For example, premature babies can experience lifelong disabilities such as hearing and vision loss or learning and cognitive impairments [11] [20] [23] [25]. Premature babies can also suffer from growth impediments and mental health issues [26]. Other health

issues can include respiratory, cardiovascular, and neuro-developmental impairments [15] [18].

Premature birth can also have an economic impact on healthcare systems, healthcare providers, families, and societies [8] [15] [27] [28]. For instance, the cost of premature births is estimated to be between $26 billion and $50 billion per year in the United States alone [17] [23] [24] [29] and £2.95 billion per year in England and Wales [16] [30]. After defining premature birth and its complications for the fetus, the mother, and healthcare systems in general, we will present the premature birth distribution worldwide in the next section.

1.2 Premature Birth Distribution Rates around the World

Premature birth is a global issue [13]. In developed countries, the premature birth rate is between 5% and 12% and up to 40% in some developing countries [2]. When it comes to premature birth survival rates, there is a massive gap between low-income and high-income countries [11]. In high-income countries, almost all of the children born prematurely under 32 weeks survive; however, in low-income countries, the lack of a quality healthcare system contributes to the death of nearly 50% of these children. Over 90% of extremely premature babies die in low-income countries. Figure 1.1 shows the top-ten countries with the highest number of premature births [11] [31].

Although the healthcare systems in the United States and Europe are outstanding, the number of premature births is still high [32], with half a million premature births every year in the United States [6] [25] [29], which is the largest group of pediatric infants [6]. Furthermore, premature birth numbers have been increasing since 1981 from 9% to 12.7% [6] [24] [29].

Globally, 60% of premature births occur in South Asia and Africa. The rate of premature births is estimated to be 12% in low-income countries and 9% in high-income countries [11]. For example, in the USA, the premature birth rate is between 12% and 13% and between 5% and 9% in England and Wales [14] [16] [30] [33]. Figure 1.2 shows the countries with the highest premature birth rates for every 100

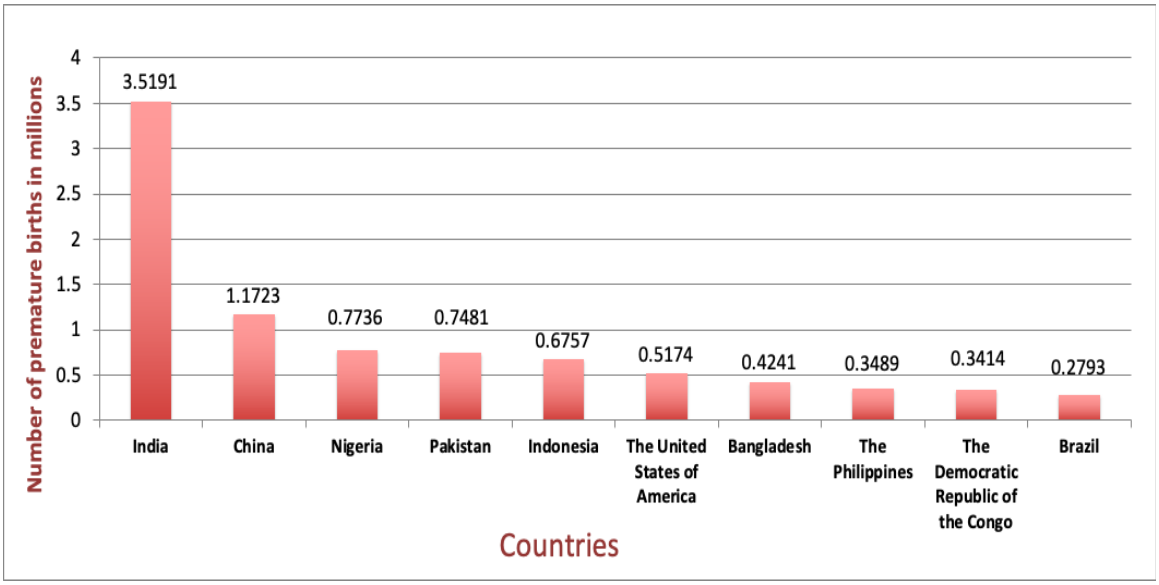

Figure 1.1: Countries with the highest number of preterm births

live births. Finally, the risk of premature birth is higher if the family has a low income [11]. In the next section, we will explain the causes of and the possible solutions for premature birth.

1.3 Causes of and Solutions for Premature Birth

Determining the causes of premature birth is difficult. It can occur spontaneously for many reasons, and the cause is usually unidentified [4] [11] [12]. However, a pregnant woman can be diagnosed with a high risk of premature birth if she or one of her family members has had a medical history of premature labour [9] [20].

1.3.1 Early detection and intervention in Premature Birth

Studies have shown that long distances from hospitals, such as in rural areas, are associated with higher mortality and a lack of healthcare access [34]. Furthermore, since it is difficult to prevent premature births, mitigating the effects and consequences of premature births on the fetus and the mother is the best solution found so far. To prevent premature births and to mitigate and reduce their consequences, we need a better understanding of this issue. One of the key factors in mitigating premature

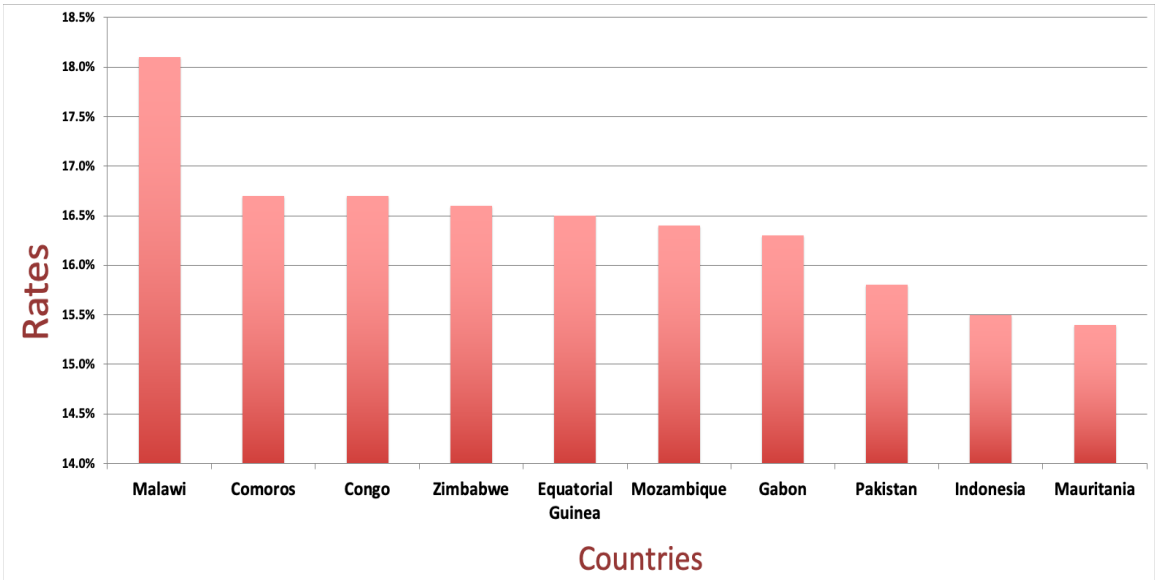

Figure 1.2: Countries with the highest rates of premature birth per 100 live births

birth issues is the early detection of labour [5] [15] [35]. Early detection can help provide medical intervention and achieve the best childbirth outcome and treatment [7] [8]. Early premature birth can be detected by monitoring the symptoms of early labour as soon as possible via the pregnant woman's biochemical or biophysical signals [4] [10] [28]. Furthermore, early detection helps mitigate the health risks for the fetus and the mother and reduces the treatment cost of premature birth complications [36].

1.3.2 Developing Countries and Illiteracy

Moreover, developing countries have 95% of the world's illiterate people [37]. We mainly target pregnant women from developing countries, and the application should be designed to their needs while keeping the prevalence of illiteracy in mind.

According to [38] and [39], studies suggest using graphical information and voice feedback when designing a user interface (UI) for illiterate users. This can also simplify information for illiterate users [40]. Furthermore, the minimal use of text can make the UI intuitive for illiterate users [41]. The combination of visual, voice feedback and minimal text can help illiterate users easily navigate the application. These recommendations will be applied to the framework's application UI.

1.4 Research Gap

As we established, premature birth is a serious health issue that threatens the life of the mother and fetus. Several studies have been conducted on monitoring pregnant women with a high risk of premature birth to address this issue.

The first study [22] was conducted in 1998 and focused on the home monitoring of uterine activity for pregnant women with a high risk of premature birth versus nurses' frequent contact with these pregnant women.

The second study conducted in 2009 by [42] compared the use of EHG and intrauterine pressure catheter (IUPC) to monitor pregnant women using a simple algorithm to measure uterine contractions.

In the third study, [43] conducted randomized control trials of home uterine activity monitoring for pregnant women with a high risk of premature birth from 15 studies to determine if using a home monitoring system would give the same results for the pregnant woman's and fetus's health status compared with the absence of such a monitoring system during pregnancy.

In the fourth study [44], the authors proposed a mobile healthcare system to monitor the health status of pregnant women with hypertensive disorders using body sensors.

The fifth study [32] designed a telemonitoring home system called Nemo Healthcare to monitor fetal heart rate, fetal electrocardiogram, maternal heart rate, and uterine contractions. They used body sensors to collect and send the pregnant woman's vital signals wirelessly to a server, where a physician could monitor the woman's health status.

The sixth study [45] proposed a system for monitoring the cardiotocograph signals of the pregnant woman. The system uses sensors to collect the pregnant woman's vital signs and sends them to the Obstetrics-Gynecology Department Information System (ObGyn) via smartphone for the physician to analyze.

The seventh study by [46] presented a long-term continuous and remote healthcare

monitoring system for pregnant women during pregnancy and postpartum using internet of things (IoT). The system monitors the stress, sleeping and physical activities of pregnant women.

The eighth study by [47] proposed a remote pregnancy risk monitoring system using wireless body sensors (WBSs) and mobile phones. The system is non-invasive, continuous and home-comfortable.

The ninth study by [30] used EHG to compare the performance of three classifiers: RF, rule-based, and penalized logistic regression. RF classifier performed the best among the three.

The tenth study by [48] classified term and preterm deliveries using EHG signals. They extracted 12 features and used seven classifiers, where Radial Basis Function Neural Network (RBNC) classifier performed the best.

The eleventh study by [49] proposed a new premature labour prediction algorithm using EHG signals. They extracted eight features using six levels of wavelet packet decomposition (WPD) and used SVM for classification.

The twelfth study by [50] used EHG and heart rate (HR) to detect labour. They used the Bloomlife sensor to collect EHG and HR for data collection and RF for classification.

The thirteenth study by [18] proposed a system for distinguishing premature patterns from term patterns using recurrence quantification analysis (RQA) and principal component analysis (PCA). They used EHG signals from 20 pregnant women and multiclass SVM for classification.

The fourteenth study by [51] proposed a machine learning system to detect labour using the Bloomlife sensor. They recruited 142 pregnant women and used generalized linear machine learning models (GLMs) for classification.

The fifteenth study by [52] classified EHG signals into term and preterm labour using SVM and RBF kernel function for classification using 300 EHG records.

The sixteenth study by [53] proposed a highly efficient and novel approach to classify EHG signals using only one feature. The authors used four classifiers, with

SVM performing the best.

The seventeenth study by [54] proposed a system classifying EHG using RF classifier. The authors used 300 EHG records and extracted 31 features for classification.

The eighteenth study by [55] proposed a low computational system for detecting premature labour using EHG. They used 300 EHG records and SVM for classification.

The nineteenth study by [56] proposed a system for monitoring the pregnant woman's uterine contractions and alerting her when the labour contractions start. They used AgC12 wearable sensors for data collection. For classification, they used five classifiers, with SVM scoring the highest.

The twentieth study by [57] proposed a system for classifying EHG signals into pregnancy or labour based on wavelet transform, sample entropy and stacked sparse autoencoder. They produced a 64-parameter feature vector and used a two-hidden-layer stacked sparse autoencoder (SSAE) deep neural network with a softmax classifier network for classification.

The twenty-first study by [58] evaluated two EHG features: contraction detection and its corresponding delineation accuracy to detect EHG contractions using five methods. Of the five methods, the square root mean square (RMS) performed the best.

The twenty-second study by [59] proposed a system for identifying EHG uterine contractions using a convolutional neural network (CNN) deep learning algorithm. They used two databases and extracted 14,016 45-second-long EHG segments. Next, they converted these segments to 482 X 482 pixel images to be fed to the algorithm.

The above proposed systems are costly, uncomfortable for pregnant women to use, or require a physician to analyze the results. To overcome these limitations, we proposed an automated, continuous, low-cost, easy-to-deploy, and reliable uterine activity home monitoring system using a wireless body sensor and a smartphone. The proposed system aims to mitigate the consequences of premature birth for both the pregnant woman and the fetus and will continuously analyze EHG readings without the need for a physician using ML and deep learning (DL) approaches, which makes

it a fully automated system that can be easily deployed in developing countries, all of which together form the novel contribution of this research.

1.5 Thesis Contributions

The proposed schemes listed above approached the prediction and detection of premature birth using the ML and DL models without a practical application to solve the premature birth issue. Our proposed framework aims to apply the ML and DL models for a real-life practical solution in the form of a smartphone application to monitor pregnant women's uterine EHG signals and trigger an alarm if they go into labour.

The thesis has three major contributions. The first contribution is the use of two mobile algorithms we designed ourselves, namely the threshold algorithm and amplitude-frequency algorithm. The threshold algorithm uses a threshold mechanism to determine if the pregnant woman is in labour. The amplitude-frequency algorithm analyzes the changes in amplitude and frequency of the pregnant women's uterine EHG signals and triggers the alarm if the uterine activity signal has a labour pattern.

The second contribution is the use of ML algorithms to increase further the reliability and accuracy detection of labour patterns in the pregnant women's uterine EHG signals. The third contribution is the use of DL models to predict and detect labour patterns and personalize them to each pregnant woman individually for more accurate results.

1.6 Report Organization

The report is organized as follows. Chapter 2 discusses the monitoring of uterine contractions, explains uterine EHG, introduces wireless body sensor networks (WBSNs), and discusses home monitoring. Chapter 3 presents the related work and literature review and discusses the research contributions and research questions. Chapter 4 discusses the research motivations, lists the research objectives and presents the details of the framework. Chapter 5 presents the threshold scheme. Chapter 6 presents

the amplitude-frequency algorithm scheme. Chapter 7 presents the machine learning scheme. Chapter 8 presents the deep learning scheme. Chapter 9 presents the obstetricians' medical opinion regarding some medical aspects of the framework. Finally, chapter 10 provides the concluding remarks and scope for future work for the proposed framework.

Chapter 2

Background

2.1 Monitoring of Uterine Contractions

As discussed in Section 1.3, the early detection approach is critical to mitigating premature birth complications. To achieve this goal, we need to develop tools and methods to better monitor pregnancy and detect early labour [18].

Abnormal uterine contractions are the first and most important sign in detecting labour progress [35] [60] [61]. By monitoring uterine contraction activity during pregnancy, we can assess and evaluate the progress of pregnancy and the health of the mother and fetus in real time [35] [61] [62] [63] [64] [65]. Labour can be detected when uterine contractions become more robust, complex, and frequent over time as pregnant women get closer to giving birth, which makes uterine contractions a crucial indicator for labour detection [60] [66] [67].

When it comes to premature birth, the monitoring of uterine contractions is vital for the fetus and pregnant woman's survival. This monitoring can provide us with vital signs of both the pregnant woman and the fetus to distinguish between premature birth and normal birth [16]. Moreover, monitoring uterine contractions can detect fetal risks of health distress or pregnancy complications such as uterine rupture, tachysystole, and placental abruption that can lead to premature birth [35] [68].

We can conclude that obstetricians monitor uterine contractions for signs of more robust and more frequent contractions to detect early premature labour [36] [66]. Furthermore, to monitor a pregnant woman's uterine contraction signals, we can use a non-invasive method to collect uterine EHG readings from the pregnant woman's abdomen. This will be discussed in detail in the next section.

2.2 Uterine Electrohysterography

Uterine electrohysterography (EHG) was developed in the 1960s [69] [70]. EHG is defined as the bioelectrical activity signals of the uterine muscle myometrial cells [27] [64] [71] [72] [73]. Obstetricians use three techniques to monitor and record pregnant women's uterine contractions:

- EHG.
- Tocodynamometer.
- Intrauterine pressure catheter (IUPC).

Of the three techniques, EHG has the advantage of being recorded externally and non-invasively from the abdomen of pregnant women [8] [74]. Moreover, EHG is more accurate and reliable than other techniques in monitoring uterine contractions since it can reflect the activity of the uterine muscle, which can reduce the treatment costs [4] [27] [33] [66] [75] [76] [77]. In addition, EHG signals can be recorded as early as 19 weeks of the pregnant woman's gestational age [15] [78] [79]. Furthermore, EHG's non-invasiveness makes it suitable for long-term pregnancy monitoring [58]. The following list summarizes the advantages of EHG:

- Non-invasive.
- Accurate.
- Reliable.
- Long-term monitoring.
- Lower healthcare costs.

Because of these advantages, EHG is a promising method for monitoring uterine contractions and detecting premature labour [7] [10] [14] [26] [51] [63] [78] [80].

However, EHG has two disadvantages. The first disadvantage is that EHG signals' filtration can be affected by the pregnant woman's tissue layers' conductivities [71]. The second disadvantage is that the quality of EHG signals can be weak and might be affected by interference [62].

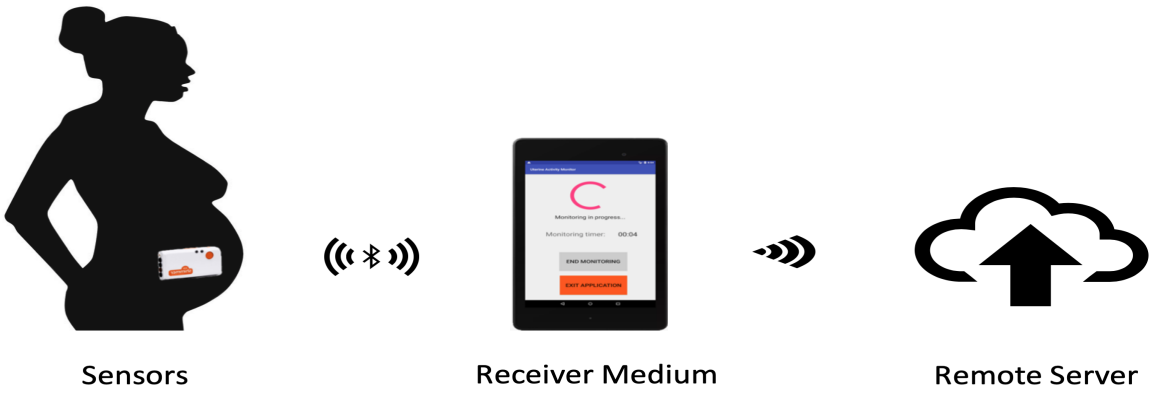

Figure 2.1: WBSN architecture

Finally, EHG has no standards for electrode location, acquisition system, or feature analysis parameters [58]. In the next section, we will discuss the recent technological advances in WBSNs that make it easier to record EHG signals non-invasively from the pregnant woman's abdomen.

2.3 Wireless Body Sensor Networks

Wireless body sensor networks (WBSNs) is an emerging wireless technology with applications in healthcare, sports, entertainment, and industry [81] [82]. One of the WBSNs' features is the continuous monitoring of the patient's vital signs. This continuous monitoring feature can help detect and lower the patient's health risks [81] [83], improve the patient's overall health status [84] and aid in the self-management of healthcare decisions [85]. Figure 2.1 shows the architecture of WBSNs. It consists of body sensors to collect and wirelessly send vital signs from the patient's body, a receiver medium to collect and analyze the patient's vital signs, and a remote server for information storage and analysis. WBSNs have several advantages such as safety, low cost, mobility, and continuous monitoring capabilities [31] [81] [83] [86].

Moreover, the wireless communication capability of WBSNs allows them to communicate with mobile devices such as smartphones. This capability will further facilitate the integration of WBSNs in healthcare systems [87]. Finally, the low cost of WBSNs will help significantly lower the cost of any system. In the next section,

we will list previous studies related to monitoring, recording, or analyzing pregnant women's uterine contractions.

2.4 Home Uterine Monitoring

Pregnant women with a high risk of premature birth visit the hospital more often to monitor their uterine contractions [88]. Such visits last for days or weeks in some cases, which will take pregnant women away from the comfort of their home [32]. Moreover, such visits can be costly, stressful and risky for the health of the pregnant woman and the fetus; for example, it can increase the risk of COVID-19 infection.

Home uterine monitoring for pregnant women has many advantages. For example, in Denmark, pregnant women's outpatient visits to the hospital were reduced, the medical staff time-of-care was reduced by 75%, and pregnant women's inpatient days were reduced by 44% without affecting the quality of healthcare [89]. Moreover, detecting false labour will help avoid unnecessary hospitalization and thus reduce financial costs[7] [90]. Researchers concluded that home uterine monitoring could help in premature birth prevention [75]. Pregnant women who used home uterine monitoring systems were less likely to give birth prematurely [91]. Using home uterine monitoring systems has also helped lower the number of infant admissions to neonatal intensive care units [91]. Only about 15% of pregnant women can detect uterine contractions, making automation a crucial feature of any home uterine monitoring system [75].

2.5 Chapter Summary

In this chapter, we present the background of monitoring uterine contractions, uterine electrohysterography, and wireless body sensor networks.

Chapter 3

Related Work and Literature Review

3.1 Overview of Studies on Monitoring Pregnant Women

Studies on monitoring pregnant women have been proposed since the 1990s. Some studies have focused on the health of the pregnant woman and her fetus, while others have focused on technical solutions that provide healthcare feedback to pregnant women. Moreover, in both developed and developing countries, digital healthcare platforms have been developed to assist pregnant women during the pregnancy period [92]. This section will give an overview of the studies that have focused on monitoring pregnant women or helping pregnant women have a safe and healthy birth.

The authors of [61] proposed a remote monitoring platform based on Virtual Instrument. The platform collects and records uterine contraction pressure from the pregnant woman using the pressure sensor. The recorded data are then sent to a personal digital assistant (PDA) wirelessly via Bluetooth. Next, the PDA sends the data to a server for a physician to diagnose and provide telemedicine services to the pregnant woman. The platform was experimentally validated in Jinhua People's Hospital, Jinhua Zhejiang, China. The authors concluded that the platform is better in terms of cost and convenience than the traditional monitoring mode.

Another author [93] proposed a system for monitoring fetal heart sounds passively and extracting the fetal heart rate. The system consists of a portable stethoscope to record fetal heart sound signals, a smartphone to upload data, a server for data storage and analysis and fetal heart rate extraction algorithms. The fetal heart signals were recorded from eight pregnant women at 37^{th} to 40^{th} weeks of gestational age. The proposed system varied about 10% in comparison to the Doppler monitor method.

The authors of [94] developed flexible concentric ring electrodes for recording

EHG signals from the pregnant woman's abdominal surface. They tested and compared the electrodes' temporal and spectral parameters with the conventional bipolar EHG recordings' parameters. The experimental results for both bipolar concentric (BC)-EHG records obtained with the new flexible TCR electrode showed that uterine electrical activity was increasing. Moreover, the BC-EHG signal showed similar spectral characteristics compared to conventional bipolar EHG recordings, but with smaller, lower-frequency content.

[95] proposed a home-based patient telemonitoring system. This system is an extension of their previously proposed obstetrical surveillance system that provides home-comfort monitoring sessions. The proposed system requires the patient to be actively involved in the monitoring process with built-in intelligence procedures for online signal analysis.

The authors of [96] designed a Pregnancy-induced Hypertension (PIH) monitoring system based on a mobile communication technology by combining wireless network technology and non-invasive hemodynamic monitoring technology. The system aims to monitor pregnant women's hemodynamic parameters in real time. The system also provides comprehensive technical means and solutions for the dynamic prediction of PIH. The system consists of three parts:

- general packet radio service network (GPRS).
- Hospital monitoring center.
- Portable monitoring terminal with two features:
  - Collect, store and deliver maternal blood parameters.
  - Display tests and feedback results in real time.

To test the system, the authors chose ten random cases of pregnant women for monitoring in a hospital's obstetrics and gynecology clinic. The experimental results show that the system is capable of monitoring blood flow parameters dynamically. The system also provides effective diagnoses and technical support for forecasting, prevention and treatment for the PIH.

The authors of [97] proposed a design and prototype for the mMamee mHealth

solution platform. The platform aims to monitor and assess the daily environmental exposures affecting the health of pregnant women. The mMamee platform has the following three distinct characteristics:

1. A smartphone application for self-reporting and monitoring of the medical condition, environmental and lifestyle habits of pregnant women in the form of easy-to-follow questionnaires via a user-friendly graphical user interface (GUI).

2. Measuring various ambient conditions via streams of urban sensing data.

3. A backbone architecture for integrating these two heterogeneous information sources.

The platform combines the user's descriptive input and urban sensing measurements. A client-server architecture is then used to collect and analyze data.

A fetus movement detector was developed by [98]. The detection is done by wrapping the pregnant woman's abdomen with an air-pressurized bag with a pressure sensor. The sensor detects the force exerted against the uterus wall in any direction. The sensor's signal is then processed and uploaded to cloud services for real-time monitoring and remote access.

The authors of [92] investigated the use of Baby+, an application for supporting pregnant women in Pakistan. The application helps pregnant women keep track of pregnancy conditions. The application was designed to meet the needs of pregnant women in the Pakistani context. The results show that pregnant women were pleased with the application's design and functionality and how the assisting tools helped them manage the pregnancy health status in the region.

The author of [99] proposed a hybrid approach to monitor pregnant women's health to protect them from possible future health risks. The system predicts risks based on pregnant women's physiological parameters to control, manage, maintain, and prevent severe health complications. The hybrid approach scored an accuracy of 0.98.

The authors in [100] used positive force measurement (PFM) to effectively filter out non-uterine contraction readings. The author designed a novel wearable device for the monitoring of uterine contractions. The proposal aims to improve accuracy and avoid unnecessary signal interference from shaking. The device sends the signal to a smartphone via Bluetooth. The data are then uploaded to the cloud. The experimental results showed that the system could allow pregnant women to accurately detect uterine contractions without interference from shaking or noise.

The authors of [101] proposed an application to non-invasively monitor the heart rate of the fetus. The application also detects pregnancy abnormalities by sending vital parameters such as the heart rate of the pregnant woman, the heart rate of the fetus and blood pressure to a hospital database.

[102] proposed a system to reduce the mortality rate in children by tracking the pregnant woman from the early stage of pregnancy until the child turns five years old. Pregnant women's health conditions, fetus growth, and child vaccinations are monitored and tracked to ensure their safety and to prevent fatal diseases. The system stores information on the cloud in real time for easy and cost-effective accessibility and quality medical care.

The authors in [103] aimed to optimize the performance of the C4.5 classification algorithm in predicting risk levels during pregnancy using a standardized and appropriate data format. The C4.5 decision trees classification algorithm achieved an accuracy rate of 0.947, which indicates that optimized results are achievable with the standardization procedure.

The authors from [104] proposed a non-invasive and multi-parameter system for telemonitoring and assessing both the mother and the fetus's health status during pregnancy and labour. They developed a prototype called feto-maternal care unit (FMCU) that uses several biomedical sensors to collect vital data from the pregnant woman such as the maternal respiration rate, maternal body temperature, abdominal electrocardiogram (ECG), fetal movement, photoplethysmogram (PPG) and phonocardiogram (PCG). For data acquisition and transmission, the authors used national

instruments (NI) myRIO, which is connected wirelessly to a personal computer (PC) running NI LabView software for signal visualization, processing and data logging in real time. For preprocessing, decomposition and the feature extraction process, the author used advanced signal processing algorithms such as Empirical empirical mode decomposition (EMD), variational mode decomposition (VMD), empirical wavelet transform (EWT), and fast independent component analysis (FastICA). Finally, the authors developed an Android-based smartphone application to synchronize data to a cloud, where experts can access the data for analysis and diagnosis. The preliminary experimental results showed that the prototype could continuously record multiple physiological parameters with excellent reliability and accuracy.

The authors of [79] analyzed and compared EHG characteristics and their variability between contraction and non-contraction in labour groups and non-labour groups. Twenty women with a singleton pregnancy were recruited at the Department of Gynecology and Obstetrics, Peking Union Medical College Hospital, Beijing. To record EHG signals, the author used Monica AN24 (Monica Healthca‹re Ltd. Nottingham, UK). Each recording was 30 minutes long. The authors found no significant difference between the term labour group and non-labour group in terms of EHG characteristics. Therefore, the non-contraction of EHG signals had similar characteristics in these two groups.

The authors in [105] presented a solution based on ontology to profile pregnant women with possible pregnancy risks. They used an ontology and medical database from maternity hospitals in Timisoara (Bega) to create profiles of women, focusing on cases with problems and high potential risks using a Visual Studio.Net application and Protégé (an open-source tool). The cloud-based application uses ontology to create pregnant women's profiles using links between the characteristics of pregnant women, medical histories, and disease and possible problems that may occur during pregnancy. The application is still in the testing stage at Bega Hospital.

A remote monitoring model for pregnant women was proposed by [106]. The model is built on current diagnostic methods and is intended to be used without

direct medical involvement. To do so, the model will solve the following tasks:

- Develop a functional monitoring system.
- Rapid fetal assessment using a description of the information and intellectual control flows.
- Assess the model's adequacy.

The author of [107] proposed a mobile-based health care monitoring system for periodically sending messages to pregnant women in rural areas. When the pregnant woman is registered and checked up, she will be given periodic counselling and reminders for safe and easy delivery. She will also be provided with guidelines for a healthy and hygienic baby delivery. These guidelines will stay with her until the baby is two years old. This will educate the pregnant woman on a healthy pre-delivery and post-delivery period, which will contribute to the healthy growth of babies in rural areas.

The author in [108] proposed a mobile personal monitoring system for pregnant women. The system will have multiple channels to record and analyze maternal and fetal abdominal ECG, photoplethysmogram and contractile activity of the uterus. The system will allow interaction between the pregnant woman and the doctor to increase the effectiveness of medical support.

The authors of [109] outlined a system that uses the IoT to monitor pregnant women in rural areas. The system aims to facilitate the receiving of health care for the first 500 days of their baby's life and positively improve pregnant women's lives. The system's prototype consists of a heart rate sensor and smartphone application for wireless data transmission to the analysis platform.

The authors of [110] proposed a system designed to aid illiterate pregnant women in rural areas. The author conducted interviews with 11 doctors and 25 pregnant women from urban and rural areas to identify their needs at a public hospital in Sialkot, Pakistan. The system is designed to be easily used in the rural areas of developing countries. The results showed that the system provided essential information and recommendations to pregnant women and improved their doctors' routine visits.

The authors from [111] proposed a mobile device framework for primary healthcare delivery using three primary healthcare services based on the population's high mortality rate. The chosen services are diagnosis, assistance and immunization modules. The diagnosis and assistance decision support system frameworks are already implemented with a preliminary disease symptom data model in a knowledge base.

An algorithm was developed by [112] to estimate the conduction velocity (CV) and direction of EHG bursts propagation occurring during uterus contractions. The authors also performed CV measurements on EHG signals before delivery. Seven pregnant women were recruited for EHG recording, and all of them gave birth within 24 hours of recording.

The authors of [113] presented a smart bracelet for monitoring pregnant women who suffer from preeclampsia, high blood pressure and cardiac diseases. The bracelet sends the heart rate and NN intervals via Bluetooth to a smartphone. Ten people were recruited to test the bracelet. The bracelet achieved an accuracy of 0.92 for the heart rate in comparison to the classical blood pressure device.

The authors from [114] highlighted pregnant women's complications by applying a random forest approach to predict hypertensive disorders. The aim of using this classification method is to reduce maternal and fetal mortality by helping to predict and diagnose risks.

The authors of [85] presented a study on the use of wearable technologies by pregnant women with type one diabetes (T1D). The wearable technologies in the study are the FreeStyle Libre™ interstitial glucose monitor, Fitbit activity tracker and a blood pressure monitor. The participants were asked to maintain physical activity to keep their blood pressure normal and keep a food diary via self-reporting using the smartphone camera to take pictures to determine the type and portions of food. The collected data will be processed using statistical and computational analysis before providing feedback using machine learning algorithms on the need for insulin or carbohydrates to maintain euglycemia.

The authors of [115] proposed a mobile application to record pregnant women's

mobility and read the weight of a scale using image processing. The authors discussed the user experience using a user experience questionnaire (UEQ) from 30 pregnant women. The results indicate that five out of six dimensions of UEQ were considered to be above average, and the novelty and efficiency of the application need major improvement.

The authors of [116] proposed a system for online real-time pregnancy mapping to monitor pregnant women. The system consists of three parts:

1. Develop a mobile application for pregnant women to record their mobility.
2. Develop a web-based interface for healthcare providers such as doctors and nurses.
3. Evaluate the user experience.

To evaluate the user experience, the authors used a UEQ with 26 questions in six dimensions. Moreover, in-depth interviews were conducted to understand user behaviour. The authors reported the following scores: Attractiveness of 0.83, pragmatic quality of 1.13 and hedonic quality of 1.25 of a range between -3 and 3. The scores are above average, except for hedonic quality, which is considered good. Therefore, the user experience needs massive improvements.

The authors in [117] proposed a multi-channel uterine electromyography (EMG) patch prototype for monitoring premature birth. The authors reported that, on average, nine significant peak points were observed in premature births and four in normal births for a monitoring window of ten minutes. To test the prototype, the authors obtained real uterine EMG data from the pregnant women. They compared the fast fourier transform (FFT) plots for uterine EMG signals for normal and uterine contraction states. They found that FFT spectral energy is significantly higher in the contraction state in the low-frequency band under 0.1 Hz.

[118] proposed a healthcare system using IoT to continuously monitor and evaluate maternal stress during pregnancy. They used an online k-means algorithm to determine the stress level using real-time heart rate measurements. Furthermore, they designed a proof of concept to evaluate the accuracy of the system. They conducted a case study by recruiting 20 pregnant women and monitoring them for six months

of pregnancy and one month postpartum. The authors reported a 71.75% accuracy rate on a validation dataset. The data from the 20 recruited women examined the performance using a 10-fold validation Random Forest and obtained an accuracy rate of 97.9%.

The authors in [119] developed a cloud-based application to help pregnant women and deprived children. Any pregnant woman can join the website for medical aid. Physicians can also use the website for remote medical aid. Finally, the system will be free of charge to support low-income families.

The authors in [120] proposed the i-bracelet machine learning system to predict the onset of preeclampsia for pregnant women. The algorithm will use blood pressure medical data as well as the age and weight of the pregnant woman for prediction. The authors used an electronic bracelet with a sensor for data collection. The sensor collects and calculates the systolic and diastolic blood pressure values and sends them wirelessly to the i-bracelet system.

The authors reported an accuracy rate of 0.8, a sensitivity rate of 0.925 and a specificity rate of 0.72.

A web-based application was proposed by [121] to non-invasively and continuously monitor the health condition of pregnant women. The application can detect any anomalies in the pregnant women's heart rate variability (HRV) parameters that can lead to complications. The collected HRV parameters are compared with the suggested normal range to determine if there are any anomalies. The application connects pregnant women and doctors. Finally, if the application detects any anomalies, it will trigger an alarm with the option for the pregnant woman to share the report with a remote doctor.

The authors in [122] proposed a reference big data architecture to facilitate adaptive health monitoring. The architecture consists of a mobile device for pregnant women, body sensors, cloud and a terminal for health professionals/researchers. Moreover, the architecture can adapt to changes in health needs by analyzing health observations and providing specific health monitoring needs for pregnant women using

ambiance awareness. Furthermore, additional analysis is conducted to continuously evaluate risk factors and contact healthcare providers in case of emergency or predicted risks. The architecture monitors the mobile device to optimize the monitoring session and adapt it to ensure the system's high availability. Finally, healthcare providers can use the terminal to perform the following:

- Communication.
- Big data analysis.
- Data visualization.
- Real-time querying/monitoring.
- Reports.

The authors from [123] proposed a mobile system to monitor pregnant women with a high risk of hypertension using sensor networks. The system uses a Naïve Bayes classifier to classify hypertensive disorder to assist physicians in emergencies. The authors recruited 25 pregnant women for data collection. The classifier achieved an accuracy rate of 0.8, a specificity rate of 0.9444 and a sensitivity rate of 0.4286.

The authors of [124] proposed to develop a simulator of fetal movements. The simulator can accurately reproduce real fetal movements.

The authors from [125] proposed a two-step method for detecting imminent labour as follows:

1. Automatically segment the contractions by analyzing the non-linear correlation between the EHG signals.
2. Classify the extracted contractions using Gaussian mixture models (GMM) based on features extracted from the segmented bursts.

The study used a database with 68 EHG records of premature births collected in France between 2017 and 2018. The system scored an accuracy rate of 0.762, a specificity rate of 0.763 and a sensitivity rate of 0.807.

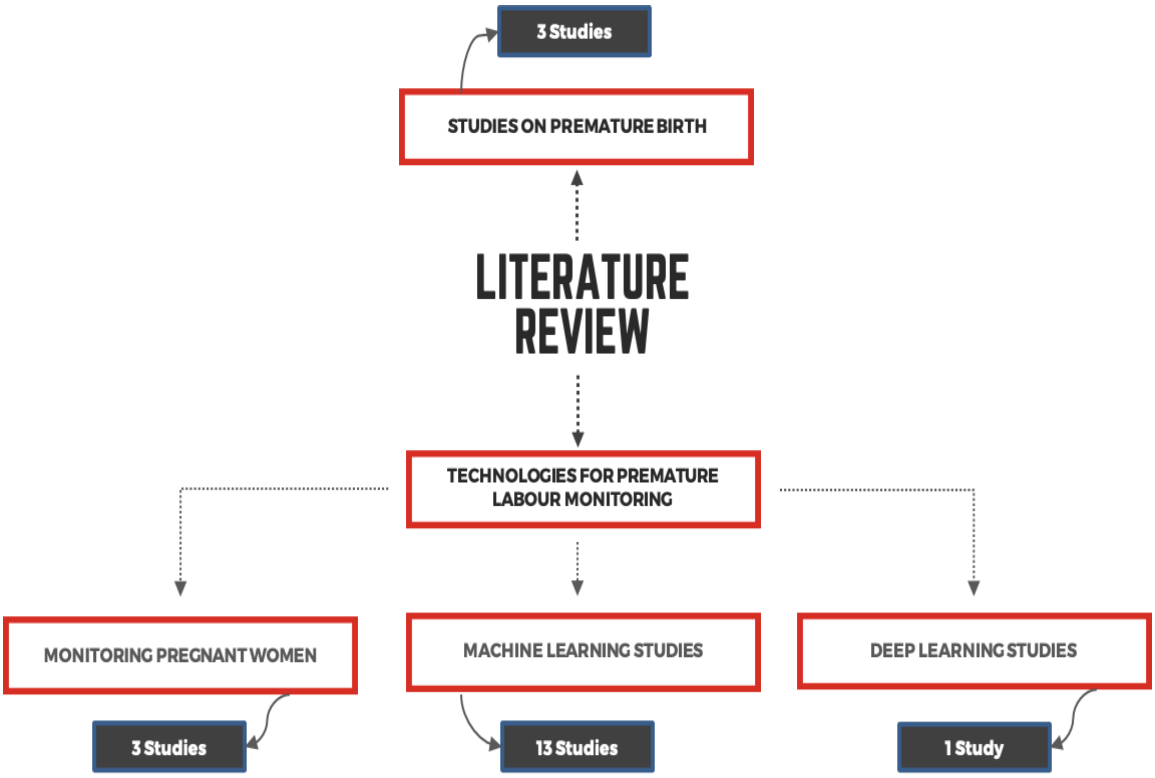

Figure 3.1: Summary of the literature review structure

3.2 Literature Review

This section will divide the literature review into two perspectives: medical and computer science perspectives. Medical studies on premature birth focus on the effectiveness of uterine activity monitoring of pregnant women's health status. Computer science studies focus on the technical side of the system, such as improving the quality of WBSNs signal filtration, signal classification, and the monitoring of uterine muscle activities. Figure 3.1 visualizes the structure of the literature review studies.

3.2.1 Studies on Premature Birth

We outline three studies that focus on the medical perspective:

The first study was conducted in 1998 [22]. It compared the effectiveness of the home monitoring of uterine activity for pregnant women with a high risk of premature birth with nurses' frequent contact with these pregnant women. The authors' goal

was to determine if the home monitoring of uterine activity would lower the premature birth rate. They randomly recruited 2422 pregnant women with a high risk of premature birth. The pregnant women received information about premature birth symptoms and signs, and they were then divided into three groups according to the following conditions:

- Weekly contact with a nurse.
- Daily contact with a nurse.
- Daily contact with a nurse and home monitoring of uterine activity.

For the home monitoring group, pregnant women were provided with Corometrics 600, a uterine monitoring device. The device records, stores, and sends information on uterine contractions to a central receiver to be diagnosed immediately. The women were asked to do a one-hour monitoring session in the morning and evening.

The study was well-constructed due to the adequate number of recruited patients and the organization of the three groups. The system was set up to monitor uterine contractions twice a day with the involvement of a nurse. This study aimed to observe if there was a difference in pregnancy progress when the pregnant woman was home monitored and determine if home monitoring can help prevent premature birth. The authors concluded that there were no differences in the outcome of the pregnancy between the three groups. They also found that the second and third groups had more unscheduled visits to the hospital.

This system, however, had the following drawbacks:

- Expensive due to the price of the monitoring device.
- Involvement of medical staff.
- Restricts pregnant women's movement while they are connected to the monitor.

The second study was conducted in 2009 by [42]. The study compared the use of EHG with IUPC to monitor pregnant women. The authors recruited 32 pregnant women in labour to record EHG and IUPC at the same time for a minimum of 30 minutes. They used a simple algorithm to automatically recognize uterine contractions. The algorithm extracted the amplitude and duration of uterine peaks.

The authors concluded that EHG is accurate in detecting uterine contractions

with a sensitivity rate of 94.5%. However, the authors did not provide results on the false positive rate (FPR) (i.e. uterine contractions that occurred but were not detected). In addition, the study is not cost-effective, as it requires hospital equipment and medical staff for monitoring, and pregnant women need to be hospitalized to be monitored. Furthermore, the monitoring is done at the time of birth, which does not make it suitable for monitoring pregnant women at any gestational age.

The third study was conducted in 2017 on the effectiveness of the home monitoring of uterine activity on the health of pregnant women with a high risk of premature birth and premature babies [43]. The authors aimed to determine if using a home monitoring system would lead to the same outcomes for the pregnant woman's and fetus's health status if such a monitoring system was absent during pregnancy.

The authors studied randomized control trials of home uterine activity monitoring for pregnant women with a high risk of premature birth from 15 studies. The authors compared the care of pregnant women with and without home uterine activity monitoring and with and without patient education programmes.

The study was well-designed and well-analyzed. The authors evaluated the trials for inclusion and risks of bias and reviewed data for accuracy. They collected and analyzed data from 6008 patients. The authors found that pregnant women who used home monitoring of uterine activity were less likely to have a premature birth at less than the 34^{th} week of pregnancy. The authors also found that babies born prematurely to women that used the home monitoring of uterine activity system were less likely to need to stay in the neonatal intensive care unit. However, pregnant women using the home monitoring of uterine activity had more unscheduled antenatal visits.

3.2.2 Technologies for Premature Labour Monitoring

We outline three studies that focus on the technologies for monitoring pregnant women, thirteen studies on using ML algorithms and one study on using DL algorithms:

Monitoring Pregnant Women

The first study by [44] proposed a mobile healthcare system to monitor the health status of pregnant women with hypertensive disorders using body sensors. Their system uses the Naïve Bayes classifier model to support decision making for physicians. To evaluate the system, the authors experimented with 25 pregnant women. Even though there was a slight improvement in the clinical condition of the pregnant women, 84% of the pregnant women did not improve. The performance analysis of the classifier showed an accuracy of 0.8.

The second study by [32] proposed the use of Nemo telemonitoring healthcare for home signals monitoring of the fetal and maternal heart rate, uterine contractions, and fetal electrocardiogram. The system consists of the Nemo Healthcare system sensors, web server, and web application. The Nemo Healthcare system sensors collect the vital signs of the pregnant woman in real time and send them wirelessly to the web server via the Internet. The physician can then monitor and diagnose the pregnant woman's health status via the web application. Pre-defined data were used to evaluate the system to simulate the signals. Although it is a well-designed system, it requires a server and physician to monitor the results, which can be expensive and would require physicians to contribute their time to monitor and analyze the results.

The third study by [45] proposed a system to monitor the pregnant woman's cardiotocograph signals. The proposal consists of three components:

- The Obstetrics-Gynecology Department Information System (ObGyn).
- Android-based application.
- Smart sensors to collect vital signs from the pregnant woman.

The smart sensor collects and analyzes data and sends an alarm to a smartphone, relaying the alarm to the ObGyn system for a physician to monitor the results. The system was validated by applying it to ten pregnant women; however, the authors did not provide any details regarding system validation results. Similar to the previous system designed by [32], this design can be expensive to implement, and the physicians must contribute their time to monitoring the results.

textbfIn the fourth study the authors presented a long-term continuous and remote healthcare monitoring system for pregnant women during pregnancy and postpartum using IoT by [46]. The system monitors the stress, sleeping and physical activities of pregnant women. Moreover, the collected data from pregnant women are stored and analyzed remotely and accessed by health providers at any time. Furthermore, the authors integrated artificial intelligence (AI) methods for data analysis such as deep learning-based quality assessment of data, personalized modelling, missing data imputation and anomaly detection. The authors recruited 28 women with high-risk pregnancies via advertisements in maternity clinics in Southwestern Finland and social media in 2019. Pregnant women were monitored during the pregnancy period and three months postpartum.

The authors designed the system to be adequate for monitoring more than one specific health issue for a long time and collecting different types of data. However, the system may not be comfortable for pregnant women since they have to wear three different types of WBSs. The system can also be expensive to set up due to the need for three WBSs, access to the Internet and servers for data storage and analysis, making the system not suitable for developing countries or remote rural areas. Besides, the system requires the efforts of a medical professional to analyze the data. Moreover, no uterine contraction signals analysis feature was added to the system design, even though they play a crucial role in pregnancy status assessment. The authors also did not provide information or evaluation regarding the machine learning or deep learning methods they used.

The authors of the fifth study [47] proposed a remote pregnancy risk monitoring system using WBSs and mobile phones. The system is non-invasive, continuous and home-comfortable. It uses the Internet to connect pregnant women to healthcare providers. Moreover, the system analyzes data using the SVM algorithm and provides data visualization for the healthcare provider to monitor the status of the pregnant women.

The system needs several WBSs to collect data, a server to store and analyze data,

Internet access and a medical professional to analyze the data. Together, this make the system expensive to deploy in developing countries or remote rural areas. Furthermore, the use of several WBSs could make it uncomfortable for pregnant women to use. The authors also claim that the collected medical data can be understood by other non-medical personnel, which raises the issue of the medical data being interpreted by someone with no medical background. The authors also claim that the system prevents complicated pregnancy risks such as stillbirth or premature birth without providing solid evidence to support this claim.

Moreover, the authors did not provide any information on or evaluation of the SVM algorithm. Furthermore, the authors did not specify if the data used in the evaluation are actual or simulated data. In addition, the authors did not provide information about the uterine contractions analysis.

Machine Learning Studies

The first study by [30] compared the performance of three classifying algorithms: the RF classifier, Rule-based classifier and Penalized Logistic Regression classifier. They used the Term-Preterm EHG database [126] from PhysioNet [127]. They extracted four features:

- RMS.
- Median frequency (MDF).
- Peak frequency (PF).
- Sample entropy.

The RF classifier had the best performance with a specificity of 86%, sensitivity of 97%, AUROC of 94% and mean square error rate of 14%. No accuracy rate, FPR or false negative rate (FNR) were reported.

The second study by [48] proposed a system for classifying term and preterm deliveries using uterine EHG. They used the Term-Preterm EHG database [126] from PhysioNet [127] and extracted the following 12 features for classification:

- Integrated EMG.
- Mean absolute value of EMG.

- Simple square integral of EMG.
- Wavelet length of EMG signal.
- Log detector of EMG signal.
- RMS of EMG signal.
- Variance of EMG.
- Difference absolute standard deviation value of EMG signal.
- Maximum fractal length of EMG signal.
- Average amplitude change of EMG signal.
- PF of EMG signal.
- MDF.

The authors used seven advanced artificial neural network classifiers. RBNC performed the best with 90% accuracy, 85% sensitivity, 80% specificity, 90% area under the ROC curve (AUC), and a 17% mean error rate. No results were reported on the FPR and FNR.

The third study by [49] proposed a new algorithm to use to predict premature labour for women with a high risk of premature labour using term and preterm EHG signals. They used the Term-Preterm EHG database [126] from PhysioNet [127]. The author extracted the following eight features using six levels of WPD:

- Fractal dimension.
- Fuzzy entropy.
- Interquartile range.
- Mean absolute deviation.
- Mean energy.
- Mean Teager-Kaiser energy.
- Sample entropy.
- Standard deviation.

SVM was used to classify uterine EHG signals into term and preterm and reported an accuracy of 96.25%, sensitivity of 95.08%, and specificity of 97.33%.

The fourth study by [50] proposed a method for labour detection using both EHG and fetus HR. They used a Bloomlife wearable sensor to collect uterine EHG

and FHR from 37 pregnant women (19 labour and 18 non-labour). The extracted features are:

- RMS.
- Normalized range.
- Mean crossing rate.
- Power of the EHG signal.
- Mean HR.

The authors then summarized the features in terms of the mean and standard deviation over 20-minute windows into the power of the EHG and the frequency and amplitude of the main peak. They used the RF classifier and achieved an accuracy of 79% for EHG only, 81% for HR only and 87% for both. No results were reported for FPR and FNR.

The fifth study by [18] proposed a system to distinguish between premature and term birth patterns using RQA and PCA. They used EHG signals from 20 pregnant women with a risk of premature birth between the 24th and 28th weeks of pregnancy. The authors used Support Vectors Machine classifications (multiclass SVM) to train the classifiers with the following five parameters:

- Recurrence Rate.
- Determinism.
- Laminarity.
- Entropy.
- Recurrence Period Density Entropy.

The accuracy of the classification was 83.32%. On the other hand, the authors did not report other essential results, such as FPR and FNR, on how the classifiers performed.

The sixth study by [51] proposed a machine learning model to non-invasively detect labour in unsupervised free-living settings using a Bloomlife wearable body sensor device. The proposed model has two phases. In the first phase, the researchers used data collected under supervised laboratory settings to develop artifact and labour

probability estimation models. They combined EHG and HR data collected at different gestational ages and showed a high accuracy in identifying artifacts and labour. In the second phase, they deployed the models on 142 pregnant women from week 22 to delivery. Pregnant women had an average of seven hours of data. The authors used the GLMs with the following features extracted over 16-second windows before being summarized in terms of mean and standard deviation over windows of 20 minutes:

- RMS of the EHG signal.
- Normalized range of the EHG signal.
- Mean crossing rate of the EHG signal.
- Power of the EHG signal.
- Frequency and amplitude of the main peak.
- Mean HR .

The authors concluded that within the last 24 hours of pregnancy, labour probability is consistently higher than in any other gestational weeks. The authors recruited an adequate number of pregnant women for the study; however, the proposed system cannot be applied for monitoring premature labour since it can detect labour only 24 hours before delivery, and premature labour can occur spontaneously at any pregnancy week. Furthermore, the authors did not provide any results on accuracy, sensitivity, specificity, false positive (FP) or false negative (FN) rates.

The seventh study by [52] proposed a system using SVM classifier with RBF kernel function to classify EHG signals into term and preterm delivery. The Term-Preterm EHG database [126], which contains 300 records, from PhysioNet [127] was used in the study. The authors used the autoregressive model (AR) for feature extraction and used the particle swarm optimization (PSO) algorithm to find the optimal features. The authors did not list the selected features. The authors reported a 97.1% accuracy rate, 95% sensitivity, and 99% specificity. No results were reported regarding FPR or FNR.

The eighth study by [53] proposed a novel and highly efficient approach that uses one feature to classify EHG signals. It is based on the centroid frequency, a single time-varying feature extracted using spectral analysis. They used the Term-Preterm

EHG database [126] from PhysioNet [127]. The authors used four classification algorithms. SVM performed the best with a 99.74% accuracy rate, 99% sensitivity, and 99% F score (F). They used only one feature that is used in the classification algorithms, which could imply a bias in the results since EHG signals have several features that could change how the algorithm would classify the signals. Furthermore, no FPR and FNR were reported.

The ninth study by [54] proposed a study to evaluate EHG signals for term and preterm delivery recognition using the RF classification algorithm. They used the Term-Preterm EHG database [126], which contains 300 records, from PhysioNet [127]. Thirty-one features were extracted with time domain, frequency domain, time-frequency domain and nonlinear analysis such as:

- RMS.
- Autocorrelation zero-crossing.
- PF.
- MDF.
- Mean frequency (MNF).

The authors reported an accuracy of 93%, sensitivity of 89%, specificity of 97%, and AUC of 80%. However, neither FPR nor FNR was reported.

The tenth study by [55] proposed a low computational and efficient algorithm to detect premature labour using EHG signals. The authors used the Term-Preterm EHG database (TPEHGDB) with 300 datasets of pregnant women's EHG signals. Two hundred sixty-two of these datasets are from term delivery and 38 are from premature delivery. The authors also used EMD for features extraction and RMS of the first two intrinsic mode function (IMF) of decomposed EHG signals as features. SVM was used for classification.

The authors reported an accuracy rate of 99.5%, sensitivity rate of 98.9% and specificity rate of 99.3%. It should be noted that the authors did not provide any results on the FPR and FNR. Moreover, the achieved rates could have some bias towards the term or premature datasets because, from what we learned from research papers, each woman's EHG is different and detecting premature labour is highly

complex. More rates such as FPR and FNR could clear these viewpoints. Finally, the rates are from one small database only; hence, more testing on other available databases is required.

The eleventh study by [56] proposed a system to monitor pregnant women's uterine EHG signals and alert them when the initial contractions of labour occur. The system consists of AgC12 wearable electrodes, EHG data captured by the electrodes and a smartphone application, and the pregnant woman's details to alert the health-care provider. The authors used the Term-Preterm EHG Database (TPEHGDB) with 300 datasets to extract features and classify the term and preterm datasets using the following machine learning classifiers: SVM, Naïve Bayes classifier, K-NN classifier, Gradient Boost and Decision Tree.

The SVM performed the best, with an accuracy rate of 96%, a specificity rate of 94% and a sensitivity rate of 92%. Naïve Bayes performed the worst, with an accuracy rate of 85%, a specificity rate of 84% and a sensitivity rate of 80%. There was no reporting of FPR or FNR. The datasets are relatively small, and more testing is needed with available databases.

The twelfth study by [57] proposed a novel method to classify EHG signals into pregnancy or labour signals. They built their method based on wavelet transform, sample entropy and stacked sparse autoencoder. The authors used the Icelandic 16-electrode Electrohysterogram Database [128] of PhysioNet [127]. To produce a 64-parameter feature vector, the authors applied the following steps:

1. Perform, using db1, 3-level wavelet decomposition of a time series.
2. Compute level-3 approximation coefficients of a time series.
3. Compute the sample entropy of detail coefficients at levels 1, 2 and 3.

The authors extracted 150 pregnancy EHG samples and 150 labour EHG samples. For training, 100 feature vectors were randomly chosen, and the other 50 feature vectors were used for testing. A two-hidden-layer SSAE deep neural network with a softmax classifier network was chosen to automatically classify EGH signals. The SSAE algorithm was compared with two widely used classification algorithms: the extreme learning machine (ELM) and SVM. The results show that SSAE performed

the best, with 90% accuracy, 92% sensitivity and 88% specificity. However, there were no results reported for the FPR and FNR. Furthermore, the number of datasets for training and testing is too low (300 in total), which can cause biases or overfitting. More datasets are needed to further confirm and generalize the results.

The thirteenth study by [58] proposed a methodology to automatically detect EHG contractions using signal envelope features. They evaluated two main features: contraction detection and its related delineation accuracy using the following five methods:

1. Wavelet energy.
2. Teager energy.
3. RMS.
4. Squared RMS.
5. Hilbert envelope.

The authors used the Icelandic 16-electrode Electrohysterogram Database [128] of PhysioNet [127]. They selected datasets of gestational age between 29 and 41 with 20 subjects, which represent 16% of the datasets. From those 20 subjects, the authors obtained 2383 contractions. The five methods were then applied to detect contractions using the associated energy bursts as a feature with a sample window of 70 seconds.

Of the five methods, the squared RMS gave the best results with an accuracy rate of 97.15% for contractions detection and 89.43% for delineation. Furthermore, the paper is very well explained; however, no specificity or sensitivity rates were given. Moreover, the authors talked about the FPR in the abstract; however, they reported the same rates in the results section as FNR, not FPR. Another issue is that the datasets are too small, which can cause biases or overfitting. There are other available datasets the authors could use to further confirm and generalize the results.

Deep Learning Studies

The study by [59] used CNN to identify uterine contractions in EHG signals from two databases. The first database is the Icelandic 16-electrode Electrohysterogram

database [128] from PhysioNet [127]. The second database was collected by recruiting 20 pregnant women with singleton pregnancies at the Department of Gynecology and Obstetrics, Peking Union Medical College Hospital, Beijing. The authors created 14,016 45-second-length segments from the first database: 7008 with uterine contractions and 7008 without uterine contractions. The segments with the uterine contractions were extracted based on the uterine contractions' peak corresponding with the tocodynamometer signals from the same database. The author extracted a total of 308 segments from the second database: 154 with uterine contractions and 154 without uterine contractions. All EHG segments were saved and normalized by resizing to 482 X 482 pixel images.

Furthermore, CNN's ability to recognize uterine contractions was evaluated using five-fold cross-validation using the first database. The CNN model was then applied to the second database for testing the model. The results for the first database are 98% accuracy, 87% sensitivity, 93% specificity, 92% AUC, FP value of 121 and FN value of 903. For the second database, there was 93% accuracy, 88% sensitivity, 97% specificity, 87% AUC, FP value of 5 and FN value of 18. The study is well written and designed. The authors were able, to an extent, to increase the input datasets to the CNN models from the first database since the size of EHG data from pregnant women is hard to collect in large quantities to use in deep learning approaches. However, the authors did not provide any information on the average recording time; hence, more testing is needed to evaluate the proposed approach's ability to detect if a pregnant woman is in labour. Furthermore, the proposed approach needs tocodynamometer signals, which will make it more expensive and unusable in home-monitoring scenarios due to the high demand for medical devices and medical staff for data collection.

3.3 Literature Review Comparision and Research Questions

Table 3.1 summarizes the proposed studies and their limitations. The "ease of use" and "designed for developing countries" criteria were added to the comparison table based on the studies recommendations in Section 1.3.2. These two criteria are

Proposed systems	Continuous	Mobility	Home comfortable	Use of EHG	Designed for premature birth	Auto. (no physician)
Dyson et al. [22]			✓		✓	
Jacod et al. [42]				✓		
Urquhart et al. [43]			✓		✓	
Rodrigues et al. [44]						
Vermeulen-Giovagnoli et al. [32]	✓	✓	✓			
Ni et al. [45]	✓	✓	✓			
Idowu et al. [30]				✓	✓	
Fergus et al.[48]				✓	✓	
Acharya et al. [49]				✓	✓	
Altini et al. [50]				✓		
Borowska et al. [18]				✓	✓	
Altini et al. [51]				✓		
Hoseinzadeh and Amirani [52]				✓	✓	
Degbedzui and Yüksel [53]				✓	✓	
Peng et al. [54]				✓	✓	
Shahbakhti et al. [55]				✓	✓	
Sheryl Oliver et al. [56]				✓	✓	✓
Chen et al. [57]				✓		
Esgalhado et al. [58]				✓		
Hao et al. [59]				✓		
Sarhaddi et al. [46]	✓	✓				
Veena and Aravindhar [47]	✓	✓				

Table 3.1: Summary of the related work studies

reflected on the framework's application UI.

As can be seen from the table, most of the proposed systems are costly, uncomfortable for pregnant women to use, or need a physician to analyze the results. Moreover, none of them is designed for developing countries, which is where most premature births occur.

To overcome these limitations, we propose an automated, low-cost, easy-to-deploy, and reliable home uterine EHG activity monitoring system for pregnant women with a high risk of premature birth using WBSNs. The proposed system also aims to mitigate the consequences of premature birth for the pregnant woman and the fetus. The proposed system will continuously analyze EHG readings without the need for a physician using ML and DL approaches. Furthermore, the proposed system will be suitable for use in developing countries due to its low budget. The following list is the advantages of the framework:

- Reduce the system cost to be affordable for developing countries.
- Eliminate the need for a physician for continuous monitoring.
- System design suitable for low-end smartphones.
- Integrating the smartphone with ML and DL for an accurate and fast pregnancy health status decision.

3.3.1 Research Questions

As concluded in Section 1.3, preventing premature births is difficult; however, labour itself is detectable. Moreover, the health of the pregnant woman and the fetus is the central issue in premature birth alongside the financial burden that comes afterward. Therefore, we need a system that continuously monitors the uterine contractions of the pregnant woman and detects if she is in labour, which would allow for the early detection of premature birth and provide a chance for medical intervention that can reduce premature birth outcomes. This analysis leads us to the following research questions:

RQ1: Will the use of WBSNs and smartphones to continuously monitor uterine contractions of pregnant women at a high risk of premature birth lower the outcomes of premature birth?

RQ2: Will the use of ML and DL algorithms improve the detection and prediction of labour for pregnant women with a high risk of premature birth?

3.4 Chapter Summary

This chapter discussed the related work and literature review of previous studies in monitoring pregnant women for both medical and computer science fields. We also presented the research contributions and research questions. In the next chapter, we will present our previously proposed system.

Chapter 4

Research Focus

4.1 Motivation

With practical and cost-effective care, researchers suggest that over three-quarters of babies born prematurely could be saved [11]. Furthermore, researchers have suggested that premature birth rates could be lowered by improving the care of pregnant women before, during, and after pregnancy [11] [19] [21] [43] [88]. Therefore, there is a crucial need for an automated approach to non-invasively, continuously and reliably monitor pregnant women at a high risk of premature birth [32] [74]. Such an approach can help mitigate the consequences of premature birth and thus provide better healthcare for both the pregnant woman and the fetus [35] [51]. Furthermore, with over three billion smartphone users worldwide, the use of smartphones to deliver healthcare services and solutions has been increasing in recent years [92].

4.2 Objectives

We propose an automated framework for monitoring pregnant women with a high risk of premature birth using WBSNs and a smartphone with the following objectives:

- Continuously monitor uterine contractions.
- Reliably record uterine contractions.
- Accurately analyze and detect if the pregnant woman is in labour.
- Being fully mobilized: The pregnant woman can be monitored from the comfort of her home.
- Being cost-effective: Affordable to be deployed in developing countries.
- Easily installed and used.
- Effectively consume WBSNs' and smartphone's resources.

Building upon these objectives, we will present in detail our proposed framework in the next section.

4.3 Framework Overview

As established in Chapter 1, premature birth has serious health issues for both the pregnant women and the fetus with an infant mortality rate of 85%. It can also lead to lifelong health complications for surviving infants. Furthermore, healthcare systems and families suffer from a substantial economic burden by having to take care of surviving babies.

Currently, there is no permanent treatment to prevent premature birth. Therefore, the best treatment is to prevent or mitigate the consequences of premature birth through early detection using monitoring systems [19]. Authors have suggested monitoring uterine contractions as a solution to reduce the health and economic consequences of premature birth. The monitoring system must be automated and reliable in order to evaluate pregnancy progression and detect labour [6] [21] [71]. Furthermore, the monitoring of uterine contractions has been proven to be an efficient method for detecting labour [23] and allows a significant percentage of pregnant women to give birth at term, which means such monitoring will help pregnant women with a high risk of premature birth avoid or mitigate premature birth-related health and economic issues [75].

Uterine contractions change during pregnancy [75]. The changes in uterine contractions occur as frequency spikes increase over time when the pregnant woman is going into labour. Extracting data on such spike frequencies will lead to the efficient detection of labour [78]. Moreover, uterine contraction frequencies are higher for pregnant women who deliver prematurely and start earlier than pregnant women who deliver at term [75].

To use uterine contractions' EHG in predicting and detecting premature birth, we need to extract uterine contractions' quantitative parameters from EHG readings [1] [64] [42]. Specifically, we need to extract two contraction parameters used by

obstetricians to evaluate pregnancy progress [35] [60] [64]:

- Amplitude.
- Frequency.

Over time, the intensity of uterine contractions increases when the pregnant woman gets closer to labour [90]. In particular, uterine contractions become more frequent with larger amplitudes [33]. Measuring the changes in these readings as they get more intense over time will enable us to detect labour. In the next section, we will describe our framework based on monitoring EHG characteristics.

4.3.1 Framework

The two main challenges associated with premature birth are detection and prediction [1]. Therefore, based on the advantages of WBSNs listed in Section 2.3 and the parameters extracted from EHG signals, we propose an automated wireless home uterine monitoring framework to use to detect when a pregnant woman with a high risk of premature birth is in labour using WBS and a smartphone.

The WBS will be attached non-invasively to the pregnant woman's abdomen using bipolar electrodes to collect uterine contraction information in the form of EHG signals and send them wirelessly to a smartphone via Bluetooth. The smartphone will then analyze the received data from the WBS for 30 minutes. The 30-minute monitoring period was chosen based on the two studies conducted by [33] and [90], which generally mimics how obstetricians monitor pregnant women before deciding if they are going into labour. After the 30-minute monitoring period, the smartphone will trigger a warning if the pregnant woman's EHG readings resemble consistent patterns of uterine contraction spikes (i.e. she is in labour).

The framework is fully portable and hence will not restrict the pregnant woman from moving around freely. The pregnant woman can also be monitored while she is in the comfort of her home. Moreover, due to the low cost of the WBS, the framework will be deployable and affordable for use in developing countries. Furthermore, there is no need for obstetricians to contribute their valuable time to continuously analyze results and determine if the pregnant woman is in labour as the smartphone will do

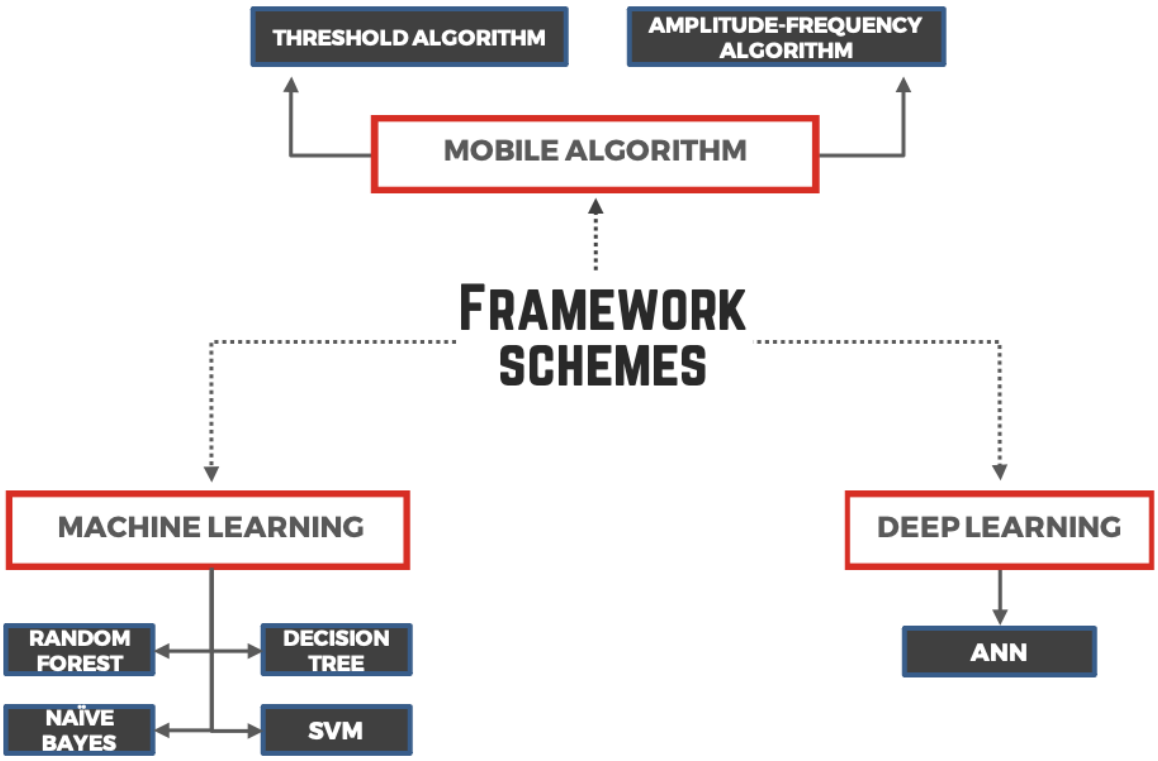

Figure 4.1: Framework's proposed schemes

the analysis automatically. To the best of our knowledge, there is no mobile uterine activity system designed to detect premature labour with the advantages mentioned earlier in Section 4.2.

The framework consists of three proposed schemes to analyze uterine EHG signals:

1. Designing our mobile algorithms with two approaches:

   (a) Threshold algorithm.

   (b) Amplitude-frequency algorithm.

2. Using machine learning algorithms.
3. Using deep learning algorithms.

Figure 4.1 shows the framework's proposed schemes. Each scheme will be explained in detail in the following chapters.

4.4 Chapter Summary

In this chapter, we presented the motivation and listed the objective of the research. We also presented the framework's three schemes. The framework is designed to be portable, cheap, and reliable. Finally, we will explain each scheme in a separate chapter. The next chapter will discuss the threshold algorithm scheme presented previously in the research aptitude defence (RAD).

Chapter 5

Threshold Algorithm Scheme

5.1 Introduction

In this scheme, we used a threshold to determine the number of contractions every ten minutes in a half-hour period. Our first paper entitled *"Framework to monitor pregnant women with a high risk of premature birth using sensor networks"* [129] was published from this scheme. In the next section, we will present the scheme in detail.

5.2 Proposed Scheme

As established in Chapter 1, premature birth has severe health impacts on pregnant women and babies. Babies born prematurely can have long-life health complications. Therefore, we designed an algorithm to detect if a pregnant woman with a high risk of premature labour is in labour based on a predefined threshold. The system is continuous, home-comfortable, cost-effective, and reliable. We designed a proof-of-concept smartphone prototype application to collect and analyze EHG readings and trigger a warning if the result of the analysis of the readings is above a predetermined threshold.

5.3 Scheme implementation

We designed and implemented a proof-of-concept prototype application using Java programming language for the Android operating system (OS). The programming platform was the Android Studio version. The application was deployed and tested on an Asus Nexus 7 tablet.

The application will continuously analyze the dataset inputs for uterine contractions. Each monitoring session will last for 30 minutes. Each 30-minute session will be divided into three 10-minute phases. During each 10-minute phase, the application will count uterine contraction readings above a predefined criterion. At the end of the 30-minute session, the application will calculate the average of the contraction readings counted in the three 10-minute periods (30 minutes). If the average is equal to or above 5, a warning will be triggered to notify the pregnant woman. Figure 5.1 shows the flow chart of the system, where:

- Contractions count (Contr).
- 30-minute session counter check (CC).
- Retrieved uterine contraction reading (RUCR).
- Threshold (TH).
- Start time (Ts).
- End time (Te).

5.3.1 Scheme User Interface

In total, the proposed prototype has four interfaces. The recommendations from the studies in Section 1.3.2 were applied to the application's UI as follows:

- We used green and red colours for visual representation, similar to the traffic lights, to be globally and easily recognized and interpreted by illiterate users.
- We used minimal text to represent the functions of the buttons.
- We used colours and voice feedback in the warning interface for easy recognition by illiterate users.

The first one is the main interface at the beginning of the application. On this interface, there are three options: start monitoring, exit application, and show the electrohysterogram wave plot. Figure 5.2 shows the main interface.

When the user clicks on the start monitoring button, the monitoring process will begin with two options. The first option will be monitoring without showing the electrohysterogram wave plot (i.e., the electrohysterogram wave plot option checkbox is unchecked). In this case, the screen will switch to the monitoring screen as shown

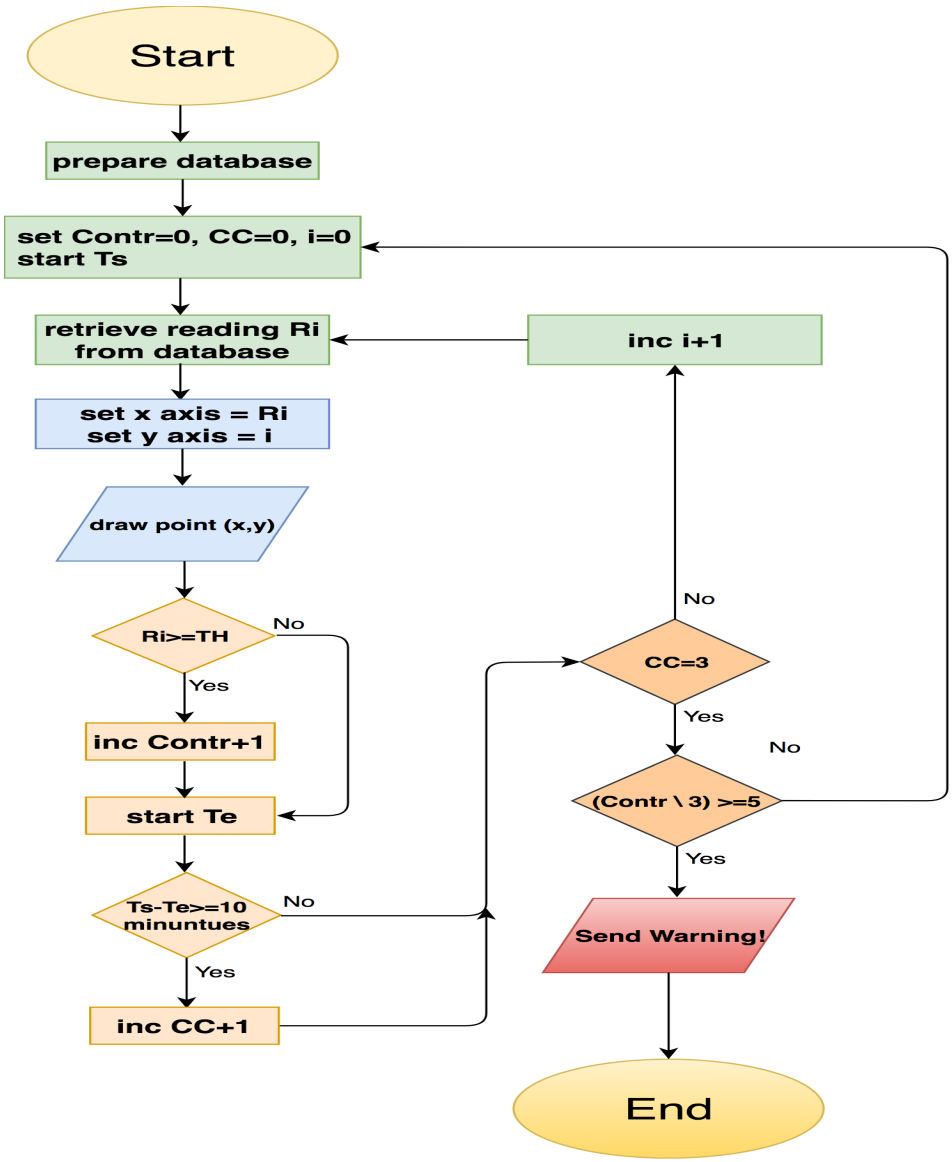

Figure 5.1: Threshold scheme flowchart

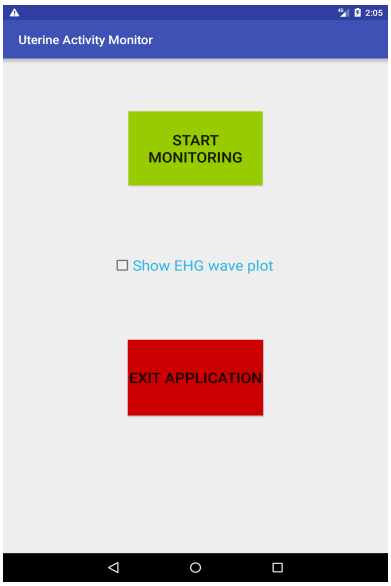

Figure 5.2: Application main interface - Threshold scheme

in figure 5.3. There is only one button on this screen that will cancel the monitoring process and go back to the main screen.

The second option will be monitoring while showing the electrohysterogram wave plot (i.e., the electrohysterogram wave plot option checkbox is checked). The wave plot screen will start, as shown in figure 5.4.

In both options, the application will be continuously analyzing uterine contraction readings. After finishing data analysis, the warning interface will be triggered, as shown in figure 5.5 with an alarm sound. The mute button will stop the alarm sound, end data analysis, and return to the main interface.

5.4 Data Selection and Preprocessing

To test the application, we used a uterine contraction signals dataset of pregnant women from PhysioNet [127]. The database we used was the Icelandic 16-electrode Electrohysterogram (EHG) Database [128]. Figure 5.6 shows a sample of the uterine contraction readings database.

The Icelandic 16-electrode Electrohysterogram (EHG) Database [128] has 45 recordings of pregnant women performed between 2008 and 2010. Each recording consists

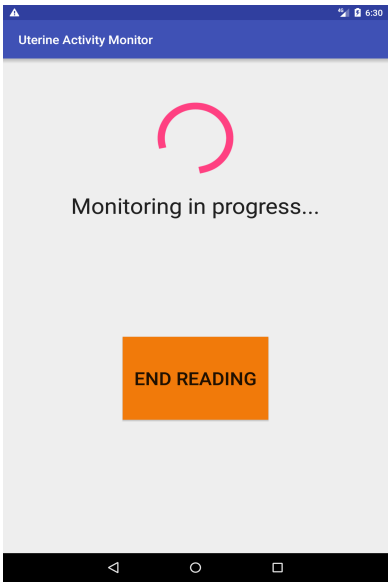

Figure 5.3: Application monitoring interface - Threshold scheme

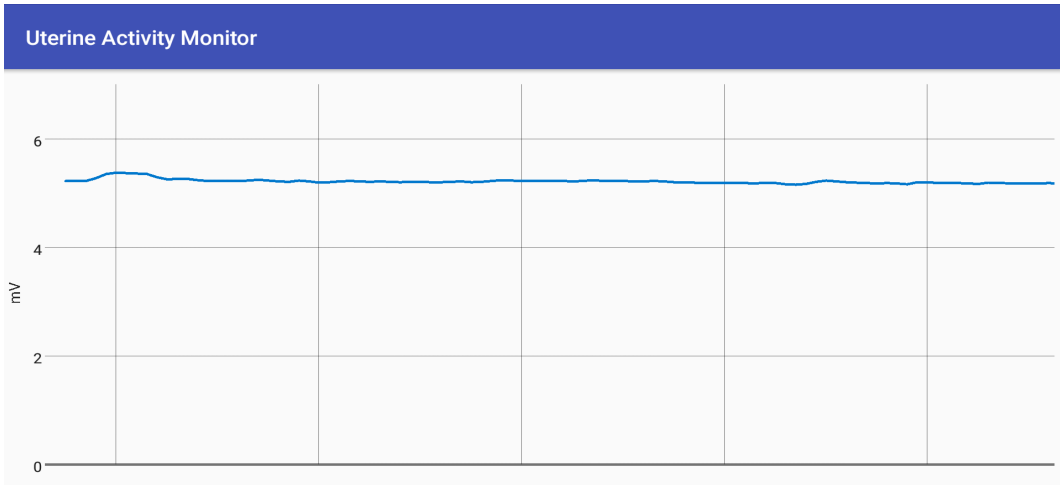

Figure 5.4: Application wave plot interface

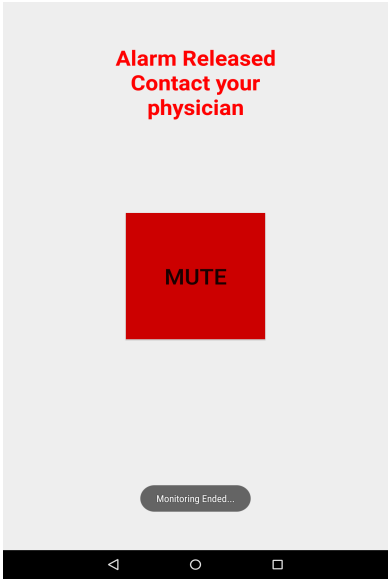

Figure 5.5: Application alarm interface - Threshold scheme

Elapsed time	EHG1	EHG10	EHG11	EHG12	EHG13	EHG14	EHG15	EHG16	EHG2	EHG3	EHG4	EHG5	EHG6	EHG7
hh:mm:ss.mmm	(mV)	(mV)	(mV)	(mV)	(mV)	(mV)	(mV)	(mV)	(mV)	(mV)	(mV)	(mV)	(mV)	(mV)
23:00.000	14.512	6.684	4.189	6.485	10.002	5.707	6.554	5.234	5.173	5.928	4.532	10.521	6.844	2.853
23:00.005	14.527	6.661	4.189	6.462	9.987	5.692	6.531	5.211	5.181	5.913	4.509	10.559	6.821	2.831
23:00.010	14.481	6.676	4.181	6.485	10.002	5.715	6.531	5.234	5.150	5.921	4.517	10.498	6.821	2.831
23:00.015	14.527	6.691	4.166	6.500	10.025	5.722	6.546	5.257	5.158	5.928	4.540	10.552	6.844	2.846
23:00.020	14.512	6.684	4.181	6.485	10.002	5.707	6.554	5.234	5.173	5.921	4.532	10.521	6.844	2.853
23:00.025	14.527	6.668	4.196	6.462	9.987	5.692	6.531	5.211	5.181	5.913	4.509	10.559	6.821	2.838
23:00.030	14.481	6.676	4.181	6.485	10.010	5.715	6.531	5.242	5.150	5.921	4.517	10.498	6.821	2.831
23:00.035	14.527	6.691	4.166	6.500	10.025	5.722	6.546	5.257	5.158	5.928	4.540	10.552	6.844	2.846
23:00.040	14.512	6.684	4.181	6.485	9.995	5.707	6.554	5.234	5.173	5.928	4.532	10.521	6.844	2.853
23:00.045	14.527	6.668	4.196	6.462	9.987	5.692	6.531	5.219	5.181	5.913	4.509	10.559	6.821	2.838
23:00.050	14.481	6.676	4.173	6.485	10.002	5.715	6.523	5.234	5.150	5.921	4.517	10.498	6.821	2.831
23:00.055	14.527	6.691	4.166	6.508	10.018	5.722	6.546	5.264	5.158	5.928	4.540	10.559	6.844	2.853
23:00.060	14.512	6.684	4.189	6.485	10.002	5.707	6.554	5.242	5.173	5.928	4.532	10.521	6.836	2.853
23:00.065	14.527	6.661	4.196	6.470	9.987	5.692	6.539	5.219	5.181	5.913	4.509	10.552	6.821	2.838
23:00.070	14.481	6.676	4.181	6.485	10.010	5.715	6.531	5.242	5.150	5.921	4.517	10.491	6.829	2.831
23:00.075	14.542	6.691	4.166	6.500	10.018	5.722	6.546	5.264	5.165	5.928	4.540	10.567	6.844	2.853
23:00.080	14.504	6.684	4.181	6.485	9.995	5.707	6.554	5.242	5.165	5.921	4.532	10.521	6.829	2.853
23:00.085	14.519	6.661	4.189	6.462	9.980	5.684	6.531	5.211	5.173	5.905	4.501	10.544	6.813	2.831
23:00.090	14.473	6.668	4.173	6.478	10.002	5.707	6.523	5.234	5.142	5.913	4.517	10.491	6.836	2.823
23:00.095	14.527	6.691	4.166	6.500	10.018	5.722	6.546	5.257	5.158	5.928	4.532	10.552	6.844	2.846
23:00.100	14.512	6.684	4.181	6.485	9.995	5.707	6.554	5.242	5.173	5.921	4.532	10.521	6.821	2.853
23:00.105	14.527	6.661	4.189	6.462	9.980	5.692	6.531	5.219	5.181	5.913	4.509	10.552	6.813	2.838
23:00.110	14.481	6.676	4.173	6.478	10.002	5.707	6.523	5.242	5.150	5.913	4.517	10.491	6.836	2.831
23:00.115	14.527	6.691	4.166	6.500	10.018	5.722	6.546	5.257	5.158	5.928	4.540	10.559	6.836	2.846
23:00.120	14.504	6.684	4.181	6.485	9.995	5.699	6.554	5.242	5.165	5.921	4.532	10.514	6.821	2.853

Figure 5.6: Uterine contraction readings data sample

Figure 5.7: Data noise at the beginning of the readings

of 16 datasets of uterine contractions readings labelled from EHG1 to EHG16. We arbitrarily chose the EHG1 dataset from the ice001_1_1of1 recording to be our simulation data.

The beginning of the dataset contains noisy data. These noisy data can negatively affect the outcome of the simulation. Figure 5.7 shows the electrohysterogram of the beginning of the dataset readings where the noise data exist. To avoid such an outcome, we selected the readings with fewer noise data (i.e., removed the first readings where the noisy data exist).

Finally, the dataset used in the simulation has a list of 99467 uterine contraction readings in millivolt (mV).

5.4.1 Data Analysis

In general, the system data analysis is divided into three 10-minute phases and a 30-minute session. At the end of the 30-minute session, the simulation will either trigger a warning or not depending on the output result. The details of each phase are as follows:

10-minute phase

The first phase consists of three sub-phases. Each sub-phase lasts for 10 minutes. During each sub-phase, the program retrieves and counts uterine contraction readings from the database. The program also draws each reading on x and y axes to simulate

a real-time chart of the uterine contractions. Algorithm 1 illustrates the 10-minute phase.

Algorithm 1 10-minute Phase

Require: RUCR from the dataset

repeat
  start Ts
  retrieve $RUCRi$
  set x axis = $RUCRi$
  set y axis = i
  draw point (x,y)
  if $RUCR >= 5.7$ **then**
    $Contr++$
  end if
  start Te
  if $Ts - Ts >= 10$ **then**
    $CC++$
  end if
  $i++$
until $CC = 3$

30-minute phase

This is the second phase of the uterine contraction readings analysis. Each simulation session will last for 30 minutes. At the end of the session, the application will calculate and analyze the average of the uterine contraction readings count over the three 10-minute phases. If the average is equal to or above 5, the application will trigger a warning. Otherwise, no warning will be triggered. Algorithm 2 illustrates the calculation and analysis of the uterine contractions for each 30-minute session.

Algorithm 2 30-minute Session

Require: 30-minute session counter check CC

if $(Contr/3) >= 5$ **then**
  return $true$ {trigger warning}
else
  return $false$ {no warning}
  set $Contr = 0$, $CC = 0$, $i = 0$
end if

5.5 Evaluation Methodology

A proof of concept was implemented in the Java programming language to evaluate the proposed scheme. A dataset from the Icelandic 16-electrode Electrohysterogram database [128] was used to test the implementation.

The dataset we used was the ice001_1_1of1 dataset. The dataset has a list of 99467 uterine contraction EHG readings in mV of a pregnant woman in labour. The following aspects will be used to evaluate the proposed scheme:

- Threshold's false positive rate.
- central processing unit (CPU) Memory performance.
- Power consumption.

5.5.1 Threshold's false positive rate

To detect a uterine contraction occurring in the dataset, we need to choose a threshold. If a reading from the dataset is equal to or above the threshold, this reading is considered a uterine contraction. Moreover, since each patient has a different threshold for uterine contractions detection [74], we can modify the application based on the patient's threshold preferences. The threshold we chose was 5.7 mV.

According to [74], the threshold is selected based on the false positive rate. To evaluate the selected threshold accuracy in detecting the occurrence of a uterine contraction, we will calculate the false positive rate of the threshold.

5.5.2 CPU and Memory performance

As we mentioned in Chapter 4, the proposed scheme should be cheap and reliable. In addition, our proposed scheme is deployed on a smartphone that has limited resources. For these reasons, we need to evaluate the simulation of the proposed scheme in terms of CPU and memory consumption. The simulation should efficiently consume CPU and memory resources to be deployed even on cheap, lower-end smartphones.

Finally, we will use the Android Monitor tool from the Android Studio platform to analyze the CPU and memory consumption.

5.5.3 Power consumption

The simulation should efficiently consume the smartphone's power resources. This will also make the proposed scheme deployable on high-end as well as low-end smartphones. To perform the power consumption analysis, we will use a tool called Battery Historian.

5.6 Results

In this section, we present the results of the evaluation methodology for the scheme. The aspects covered in this section will be the threshold false positive rate, CPU and memory performance, and power consumption. The application was running for 30 minutes during the testing and triggered a warning at the end of the 30 minutes. Figure 5.8 shows the application running time at the beginning and the end of the monitoring session with a triggered warning.

5.6.1 Threshold and false positive rate

We chose the threshold of 5.7 mV from the possible thresholds listed on the record we chose from the dataset. Table 5.1 shows the contractions count for the thresholds.

Threshold mV	**Count of Contractions from the Application**
6.0	0
5.9	0
5.8	16
5.7	82
5.6	901
5.5	2278

Table 5.1: Thresholds contractions count

As we mentioned in Section 5.5, the research outcomes of [74] suggest that the

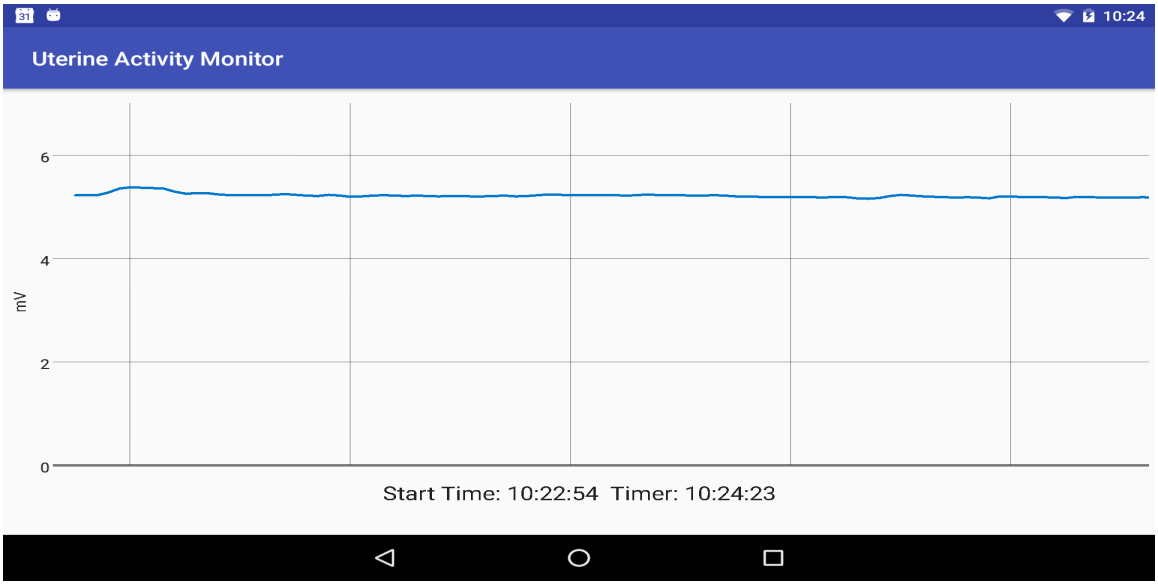

(a) The beginning

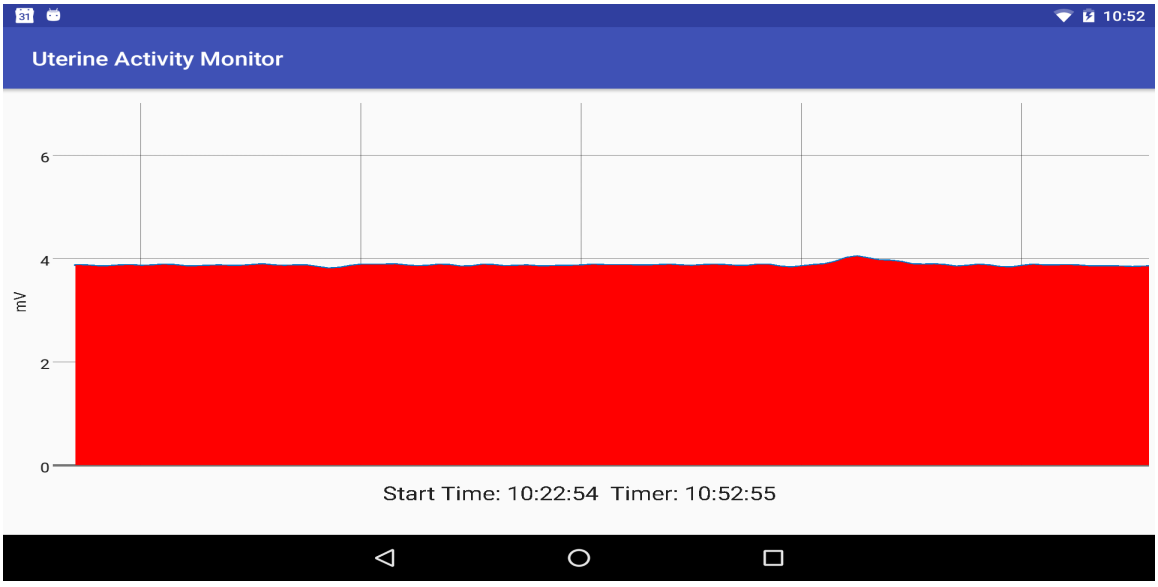

(b) The end

Figure 5.8: application running time at the beginning and the end of the monitoring session

Threshold mV	False Positive Rate
6.0	0 %
5.9	0 %
5.8	0 %
5.7	3.79 %
5.6	0.22 %
5.5	0.32 %

Table 5.2: Thresholds false positive rate

threshold is to be chosen based on its false positive rate. Our choice of 5.7 mV as a threshold has a false positive rate of 3.79%. Table 5.2 shows the false positive rate for the thresholds.

5.6.2 CPU and Memory performance

We analyzed the application's CPU and memory performance at the beginning, the middle, and the end of the application running time (i.e., the warning was triggered). As seen in Figure 5.9, the application at the beginning uses about 60% of the CPU and allocates a maximum of 26.64 MB out of 1.80 GB of the device's memory.

The X axis is the running time on both the memory and CPU charts. The Y axis is "Memory Size" on the memory chart and "Usage Percentage" on the CPU chart.

After 10 minutes of running time, the application used 40% of CPU power and used the same amount of memory (26.64 MB). Figure 5.10 shows the CPU and memory usage in the middle of the application running time.

Figure 5.11 shows the end of the application's running time. CPU consumption is still the same with 40% usage until the 30-minute period where we notice a slight increase due to the warning being triggered. Memory usage is also still the same, with 26.64 MB.

5.6.3 Power consumption

The device has a battery capacity of 3448 mAh. As seen in Figure 5.12, the application took 30 minutes from start to finish. During execution time, the device screen was

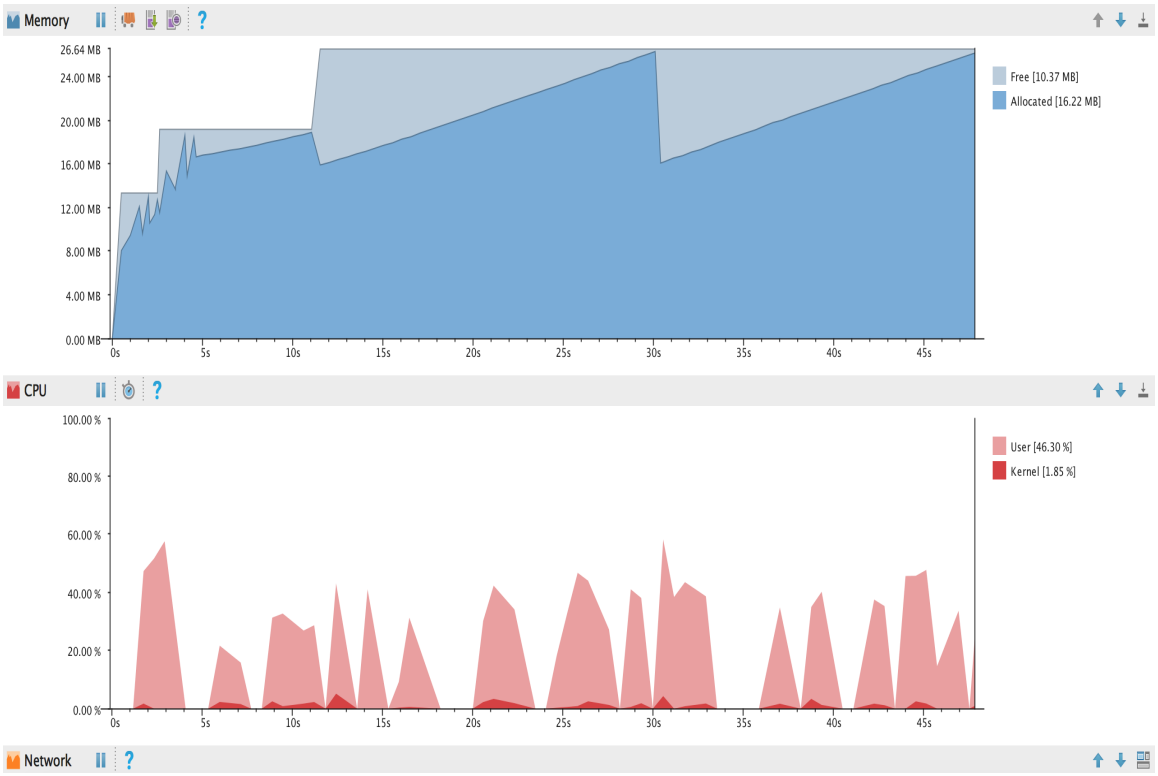

Figure 5.9: The beginning of the application's running time

Figure 5.10: The middle of the application's running time

Figure 5.11: The end of the application's running time

on and the charger was off. The application consumed between 103.44mAh (3%) and 137.92mAh (4%) of the battery charge.

Figure 5.13 shows the complete analysis of the application battery consumption. The screen bar shows that the screen was on all the time. The Audio bar shows that the warning was not triggered until the end of the 30 minutes. The device temperature was 24.4 °C (75.9 °F). Finally, the "charging on" bar shows that the device was not charging while the application was running.

5.7 Discussion

This chapter will discuss the results of the proposed scheme's simulation and how the proposed scheme met the goals set in Chapter 4.

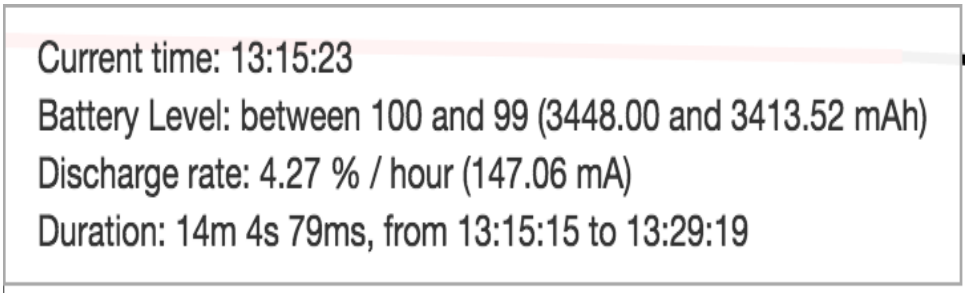

(a) Start

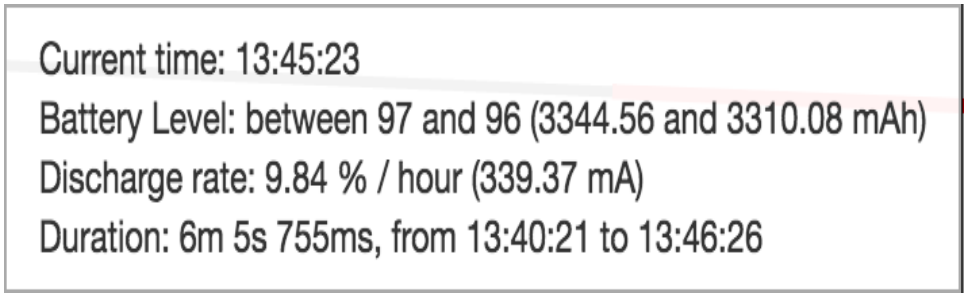

(b) End

Figure 5.12: Battery status at the beginning and the end of the application's running time

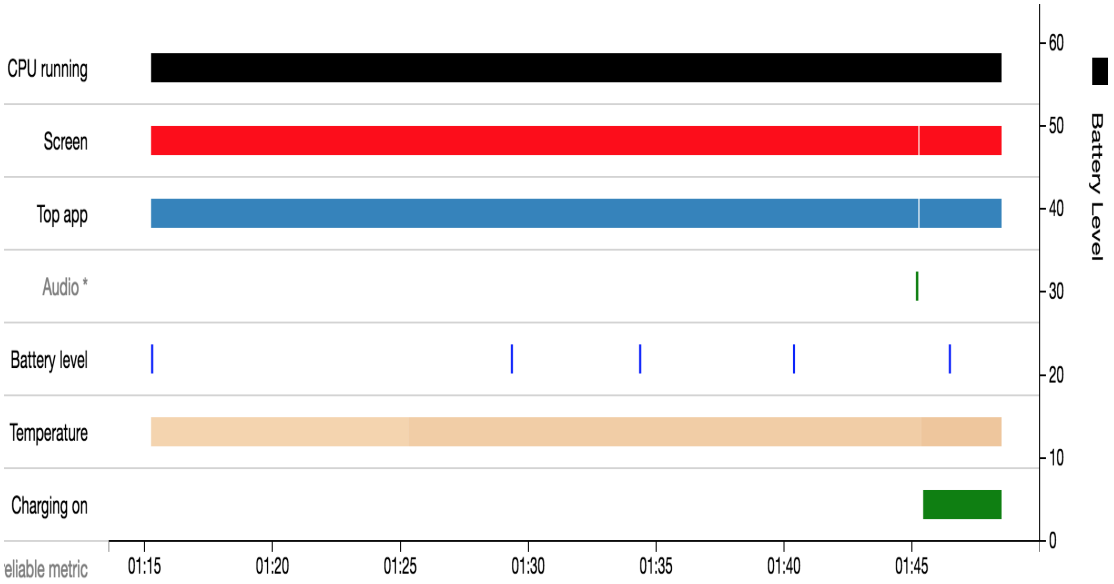

Figure 5.13: The full analysis of the application's battery consumption

5.7.1 Threshold and false positive rate

Each pregnant woman can has a specific threshold. Our analysis results indicate that 5.7 mV has the optimum false positive rate of 3.79%, and that is why we chose this value from the dataset to be our threshold. As shown in Table 5.1, any value lower than 5.7 mV will result in very high contraction counts, which will always result in a warning whether there is labour or not. With 5.8 mV as a threshold, the contractions count is low, which will result in no warning. That contradicts the dataset properties, indicating that the pregnant woman was in labour at the time of recording. Finally, any result above 5.8 mV will result in no contraction counts.

In Table 5.2, we can notice that, other than 5.7 mV, all the thresholds have low false positive rates. However, we can not choose them since these thresholds already contradict the dataset properties mentioned in the previous paragraph. For these reasons, 5.7 mV as a threshold is the optimum choice.

5.7.2 CPU and Memory performance

CPU performance

Regarding CPU performance, the application initially used up to 60% of CPU power. This relatively high usage is due to the preparation of the large number of uterine contraction readings (99,467 readings) from the dataset before the start of contractions monitoring. The dataset is large, especially when we deploy it on the Android OS's limited resources. However, this peak decreases to 40% after the dataset is prepared. The application then works smoothly until the end where a warning is triggered. This 40% usage is justified since the application kept the device screen on, and the device temperature was average throughout execution time during the application running time. This indicates that the CPU was running efficiently.

Memory performance

The application allocates 26.64 MB out of 1.80 GB of the device's memory. This is about 1.44% of the memory usage, which is considered low, especially if it is deployed

on other devices with lower hardware specifications.

5.7.3 Power consumption

Power consumption results show that the application consumed 4% of the battery's charge. Considering that the screen was always on and the device temperature was average, we can conclude that it efficiently consumes battery charge.

5.7.4 Results implication on the threshold algorithm scheme

Although the threshold algorithm scheme met the goals described in Chapter 4, we need to make sure the system design can be generalized to other uterine contraction EHG databases. Moreover, a threshold has to be chosen for each pregnant woman, which adds more setup time for the system. Thus, we need to elevate the system design and make it able to analyze EHG readings of pregnant women without individually assigning thresholds to each pregnant woman. In the next chapter, we will present the amplitude-frequency algorithm scheme to automatically read and analyze EHG readings of pregnant women without the need for assigning thresholds individually.

5.8 Chapter Summary

This chapter presented the threshold algorithm scheme to monitor pregnant women with a high risk of premature birth based on a predefined threshold. We showed the system design and implementation, evaluation results and discussed the pros and cons of the scheme design. In the next chapter, we will present the amplitude-frequency algorithm scheme in detail.

Chapter 6

Amplitude-frequency Algorithm Scheme

6.1 Introduction

In this scheme, we extracted EHG signals' amplitude and frequency features over a 30-minute monitoring session and used them in determining if the pregnant woman is in labour. From this scheme, our second journal paper entitled *"Automated uterine contractions pattern detection framework to monitor pregnant women with a high risk of premature labour"* [130] was published in the journal "Informatics in Medicine Unlocked". In the next section, we will present the scheme in detail.

6.2 Proposed Scheme

As mentioned before, it is challenging to detect or predict premature birth [1]. Our previous threshold algorithm scheme results were promising in labour detection [129]; however, the proposed scheme lacked some aspects to be generalized. The first aspect is that it needs more testing with a larger sample of databases. The second aspect is that the algorithm needs more features and complexity to independently decide the pregnancy's progress. Therefore, based on the parameters extracted from EHG signals, we proposed an automated wireless home uterine monitoring scheme to detect when a pregnant woman with a high risk of premature birth is in labour.

6.3 Scheme implementation

As we discussed before, EHG is a vital measurement for non-invasively detecting labour from the pregnant woman's abdomen [19] [63]. In the amplitude-frequency

algorithm implementation, we will be extracting two features from EHG uterine contractions readings, namely amplitudes (which we will refer to as "peaks") and frequencies. In terms of time-frequency methods, these two were found to be the most-used parameters to predict premature birth [4] [8]. Additionally, these two parameters change throughout pregnancy [70]. They go from weak and uncoordinated signals to more intense and coordinated as they get closer to labour [27]. According to [68] [90], the accurate analysis of these parameters is critical in evaluating pregnancy progress.

Building upon this knowledge, we designed and implemented a proof-of-concept prototype application using the Java programming language. The application was built using the Android Studio programming platform and was deployed and tested on an Asus Nexus 7 tablet with Android OS version 6.0.1.

The application continuously reads the dataset inputs of uterine contractions for a 30-minute session. After the 30-minute monitoring session, the application analyzes EHG readings and extracts the two features: peaks and frequencies then decides if the pregnant woman is in labour. If she is in labour, the application triggers a warning to notify the pregnant woman to go to the hospital. In the following sections, we will present the scheme UI.

6.3.1 Scheme User Interface

We designed the application's UI to have only three interfaces. The first interface is the application's start interface, which has two options: start monitoring and exit application buttons. Figure 6.1 shows the main interface.

When the user presses the start monitoring button on the application's main interface, the application switches to the second interface shown in Figure 6.2 and starts the 30-minute monitoring session. This interface has a monitoring timer, end monitoring button, and exit the application button.

When the 30-minute monitoring session ends with a warning, the application triggers the alarm sound, turns the screen on and shows a warning message, as shown in Figure 6.3. In the following sections, we will explain data selection and preprocessing.

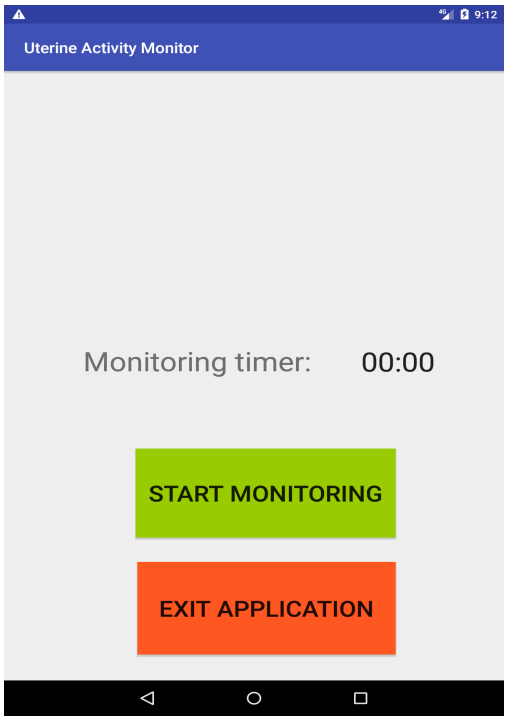

Figure 6.1: Application main interface - Amplitude-frequency scheme

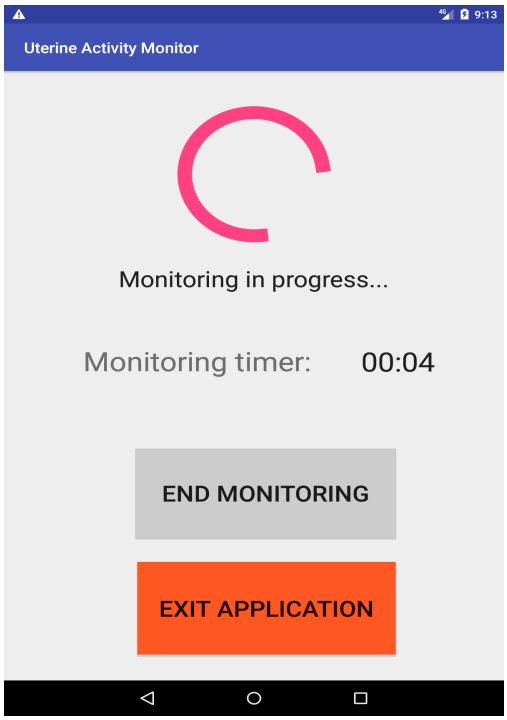

Figure 6.2: Application monitoring interface - Amplitude-frequency scheme

Figure 6.3: Application alarm interface - Amplitude-frequency scheme

6.4 Data Selection and Preprocessing

6.4.1 Data Selection

To test the scheme, we used three publicly available uterine contraction EHG signals databases of pregnant women from the PhysioNet repository [127]. The three databases are:

- Icelandic 16-electrode Electrohysterogram Database [128].
- Term-Preterm EHG Database [126].
- Term-Preterm EHG DataSet with Tocogram [131].

The Icelandic 16-electrode Electrohysterogram database has 45 recordings of pregnant women performed between 2008 and 2010. Each recording consists of 16 datasets of uterine contraction EHG signals shown in the data sample in Figure 6.4.

The Term-Preterm EHG database contains 300 uterine EHG recordings of pregnant women obtained from 1997 to 2005 at the University Medical Centre Ljubljana, Department of Obstetrics and Gynecology. Each record is 30 minutes long and has

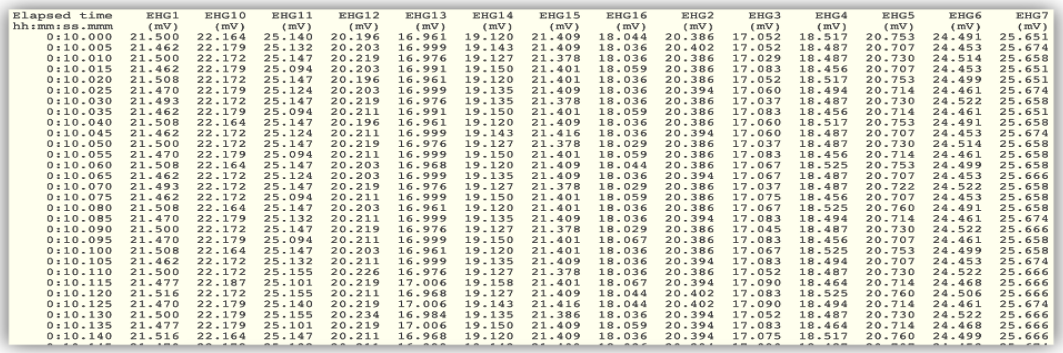

Elapsed time	EHG1	EHG10	EHG11	EHG12	EHG13	EHG14	EHG15	EHG16	EHG2	EHG3	EHG4	EHG5	EHG6	EHG7
hh:mm:ss.mmm	(mV)	(mV)	(mV)	(mV)	(mV)	(mV)	(mV)	(mV)	(mV)	(mV)	(mV)	(mV)	(mV)	(mV)
0:10.000	21.500	22.164	25.140	20.196	16.961	19.120	21.409	18.044	20.386	17.052	18.517	20.753	24.491	25.651
0:10.005	21.462	22.179	25.132	20.203	16.999	19.143	21.409	18.036	20.402	17.052	18.487	20.707	24.453	25.674
0:10.010	21.500	22.172	25.147	20.219	16.976	19.127	21.378	18.036	20.386	17.029	18.487	20.730	24.514	25.658
0:10.015	21.462	22.179	25.094	20.203	16.991	19.150	21.401	18.059	20.386	17.083	18.456	20.707	24.453	25.651
0:10.020	21.508	22.172	25.147	20.196	16.961	19.120	21.401	18.036	20.386	17.052	18.517	20.753	24.499	25.651
0:10.025	21.470	22.179	25.124	20.203	16.999	19.135	21.409	18.036	20.394	17.060	18.494	20.714	24.461	25.674
0:10.030	21.493	22.172	25.147	20.219	16.976	19.135	21.378	18.036	20.386	17.037	18.487	20.730	24.522	25.658
0:10.035	21.462	22.179	25.094	20.211	16.991	19.150	21.401	18.059	20.386	17.083	18.456	20.714	24.461	25.651
0:10.040	21.508	22.164	25.147	20.196	16.961	19.120	21.409	18.036	20.386	17.060	18.517	20.753	24.491	25.658
0:10.045	21.462	22.172	25.124	20.211	16.999	19.143	21.416	18.036	20.394	17.060	18.487	20.707	24.453	25.674
0:10.050	21.500	22.172	25.147	20.219	16.976	19.127	21.378	18.029	20.386	17.037	18.487	20.730	24.514	25.658
0:10.055	21.470	22.179	25.094	20.211	16.999	19.150	21.401	18.059	20.386	17.083	18.456	20.714	24.461	25.658
0:10.060	21.508	22.164	25.147	20.203	16.968	19.120	21.409	18.044	20.386	17.067	18.525	20.753	24.499	25.658
0:10.065	21.462	22.172	25.124	20.203	16.999	19.135	21.409	18.036	20.394	17.067	18.487	20.707	24.453	25.666
0:10.070	21.493	22.172	25.147	20.219	16.976	19.127	21.378	18.029	20.386	17.037	18.487	20.722	24.522	25.658
0:10.075	21.462	22.172	25.094	20.211	16.999	19.150	21.401	18.059	20.386	17.075	18.456	20.707	24.453	25.658
0:10.080	21.508	22.164	25.147	20.203	16.961	19.120	21.401	18.036	20.386	17.067	18.525	20.760	24.491	25.658
0:10.085	21.470	22.179	25.132	20.211	16.999	19.135	21.409	18.036	20.394	17.083	18.494	20.714	24.461	25.674
0:10.090	21.500	22.172	25.147	20.219	16.976	19.127	21.378	18.029	20.386	17.045	18.487	20.730	24.522	25.666
0:10.095	21.470	22.179	25.094	20.211	16.999	19.150	21.401	18.067	20.386	17.083	18.456	20.707	24.461	25.658
0:10.100	21.508	22.164	25.147	20.203	16.961	19.120	21.401	18.036	20.386	17.067	18.525	20.753	24.499	25.658
0:10.105	21.462	22.172	25.132	20.211	16.999	19.135	21.409	18.036	20.394	17.083	18.494	20.707	24.453	25.674
0:10.110	21.500	22.172	25.155	20.226	16.976	19.127	21.378	18.036	20.386	17.052	18.487	20.730	24.522	25.666
0:10.115	21.477	22.187	25.101	20.219	17.006	19.158	21.401	18.067	20.394	17.090	18.464	20.714	24.468	25.666
0:10.120	21.516	22.172	25.155	20.211	16.968	19.127	21.409	18.044	20.402	17.083	18.525	20.760	24.506	25.666
0:10.125	21.470	22.179	25.140	20.219	17.006	19.143	21.416	18.044	20.402	17.090	18.494	20.714	24.461	25.674
0:10.130	21.500	22.179	25.155	20.234	16.984	19.135	21.386	18.036	20.394	17.052	18.487	20.730	24.522	25.666
0:10.135	21.477	22.179	25.101	20.219	17.006	19.150	21.409	18.059	20.394	17.083	18.464	20.714	24.468	25.666
0:10.140	21.516	22.164	25.147	20.211	16.968	19.120	21.409	18.036	20.394	17.075	18.517	20.760	24.499	25.666

Figure 6.4: The Icelandic 16-electrode Electrohysterogram data sample

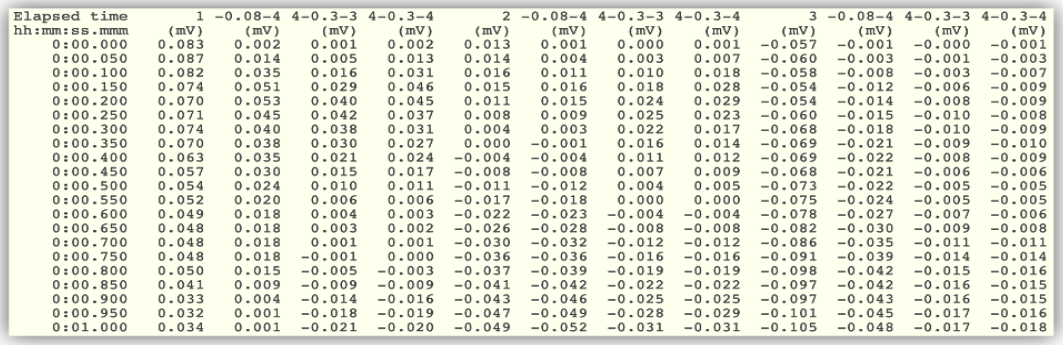

Elapsed time	1	-0.08-4	4-0.3-3	4-0.3-4	2	-0.08-4	4-0.3-3	4-0.3-4	3	-0.08-4	4-0.3-3	4-0.3-4
hh:mm:ss.mmm	(mV)	(mV)	(mV)	(mV)	(mV)	(mV)	(mV)	(mV)	(mV)	(mV)	(mV)	(mV)
0:00.000	0.083	0.002	0.001	0.002	0.013	0.001	0.000	0.001	-0.057	-0.001	-0.000	-0.001
0:00.050	0.087	0.014	0.005	0.013	0.014	0.004	0.003	0.007	-0.060	-0.003	-0.001	-0.003
0:00.100	0.082	0.035	0.016	0.031	0.016	0.011	0.010	0.018	-0.058	-0.008	-0.003	-0.007
0:00.150	0.074	0.051	0.029	0.046	0.015	0.016	0.018	0.028	-0.054	-0.012	-0.006	-0.009
0:00.200	0.070	0.053	0.040	0.045	0.011	0.015	0.024	0.029	-0.054	-0.014	-0.008	-0.009
0:00.250	0.071	0.045	0.042	0.037	0.008	0.009	0.025	0.023	-0.060	-0.015	-0.010	-0.008
0:00.300	0.074	0.040	0.038	0.031	0.004	0.003	0.022	0.017	-0.068	-0.018	-0.010	-0.009
0:00.350	0.070	0.038	0.030	0.027	0.000	-0.001	0.016	0.014	-0.069	-0.021	-0.009	-0.010
0:00.400	0.063	0.035	0.021	0.024	-0.004	-0.004	0.011	0.012	-0.069	-0.022	-0.008	-0.009
0:00.450	0.057	0.030	0.015	0.017	-0.008	-0.008	0.007	0.009	-0.068	-0.021	-0.006	-0.006
0:00.500	0.054	0.024	0.010	0.011	-0.011	-0.012	0.004	0.005	-0.073	-0.022	-0.005	-0.005
0:00.550	0.052	0.020	0.006	0.006	-0.017	-0.018	0.000	0.000	-0.075	-0.024	-0.005	-0.005
0:00.600	0.049	0.018	0.004	0.003	-0.022	-0.023	-0.004	-0.004	-0.078	-0.027	-0.007	-0.006
0:00.650	0.048	0.018	0.003	0.002	-0.026	-0.028	-0.008	-0.008	-0.082	-0.030	-0.009	-0.008
0:00.700	0.048	0.018	0.001	0.001	-0.030	-0.032	-0.012	-0.012	-0.086	-0.035	-0.011	-0.011
0:00.750	0.048	0.018	-0.001	0.000	-0.036	-0.036	-0.016	-0.016	-0.091	-0.039	-0.014	-0.014
0:00.800	0.050	0.015	-0.005	-0.003	-0.037	-0.039	-0.019	-0.019	-0.098	-0.042	-0.015	-0.016
0:00.850	0.041	0.009	-0.009	-0.009	-0.041	-0.042	-0.022	-0.022	-0.097	-0.042	-0.016	-0.015
0:00.900	0.033	0.004	-0.014	-0.016	-0.043	-0.046	-0.025	-0.025	-0.097	-0.043	-0.016	-0.015
0:00.950	0.032	0.001	-0.018	-0.019	-0.047	-0.049	-0.028	-0.029	-0.101	-0.045	-0.017	-0.016
0:01.000	0.034	0.001	-0.021	-0.020	-0.049	-0.052	-0.031	-0.031	-0.105	-0.048	-0.017	-0.018

Figure 6.5: Term-Preterm EHG data sample

12 datasets of uterine contractions EHG signals shown in the data sample in Figure 6.5.

The Term-Preterm EHG DataSet with tocogram has 24 uterine EHG recordings of pregnant women and another five uterine EHG recordings of non-pregnant women. It was developed at the Faculty of Computer and Information Science (Laboratory for Biomedical Computer Systems and Imaging), University of Ljubljana, Ljubljana. The records themselves were collected at the University Medical Centre Ljubljana, Department of Obstetrics and Gynecology in 2018 shown in the data sample in Figure 6.6.

There are 376 datasets in the three databases ranging in recording time from less

Elapsed time	EHG1	-0.08-5	EHG2	-0.08-5	EHG3	-0.08-5	TOCO	-0.08-5
hh:mm:ss.mmm	(mV)	(mV)	(mV)	(mV)	(mV)	(mV)	(mV)	(mV)
0:00.000	0.028	0.021	0.069	0.041	-0.401	-0.100	-0.335	-0.101
0:00.050	0.010	0.017	0.061	0.058	-0.393	-0.216	-0.344	-0.210
0:00.100	0.001	0.007	0.059	0.054	-0.391	-0.201	-0.352	-0.212
0:00.150	0.003	0.007	0.061	0.050	-0.393	-0.166	-0.360	-0.190
0:00.200	0.010	0.015	0.064	0.054	-0.397	-0.173	-0.366	-0.199
0:00.250	0.013	0.018	0.063	0.056	-0.399	-0.185	-0.373	-0.216
0:00.300	0.003	0.010	0.059	0.052	-0.394	-0.174	-0.380	-0.218
0:00.350	-0.005	0.001	0.056	0.048	-0.389	-0.160	-0.385	-0.217
0:00.400	-0.007	-0.001	0.054	0.046	-0.388	-0.158	-0.389	-0.222
0:00.450	-0.008	-0.002	0.052	0.045	-0.388	-0.157	-0.393	-0.226
0:00.500	-0.012	-0.004	0.051	0.044	-0.386	-0.151	-0.395	-0.227
0:00.550	-0.015	-0.007	0.050	0.042	-0.384	-0.144	-0.397	-0.226
0:00.600	-0.017	-0.008	0.047	0.041	-0.382	-0.140	-0.398	-0.227
0:00.650	-0.019	-0.011	0.045	0.039	-0.382	-0.137	-0.398	-0.226
0:00.700	-0.020	-0.012	0.044	0.037	-0.382	-0.133	-0.400	-0.226
0:00.750	-0.020	-0.007	0.042	0.036	-0.381	-0.131	-0.398	-0.224
0:00.800	-0.006	0.003	0.042	0.038	-0.386	-0.131	-0.396	-0.221
0:00.850	-0.002	0.006	0.046	0.038	-0.389	-0.129	-0.394	-0.217
0:00.900	-0.017	-0.002	0.039	0.034	-0.382	-0.123	-0.392	-0.214
0:00.950	-0.021	-0.010	0.033	0.029	-0.381	-0.117	-0.388	-0.210
0:01.000	-0.017	-0.005	0.032	0.027	-0.384	-0.116	-0.385	-0.205

Figure 6.6: Term-Preterm EHG DataSet with Tocogram data sample

than 30 minutes to 1 hour. The following section will explain data preprocessing and how we extracted the final datasets for testing.

6.4.2 Data Preprocessing

As we explained in Section 6.3, the amplitude-frequency scheme's primary goal is to detect premature birth by analyzing EHG signals for consistent labour contraction spikes for the 30-minute monitoring session. We need to extract the datasets from the three databases and prepare them to be 30-minute-long single columns of readings.

To illustrate further, each dataset in the three databases has several columns of EHG readings, as shown in Figure 6.4, for example. The length of these datasets ranges from less than 30 minutes to an hour. Based on that, the datasets extraction process has the following steps:

1. Extract each column separately from each dataset.
2. Split each column to the length of 30 minutes following these rules:
   (a) If the length of the dataset is less than 30 minutes, then discard the dataset.
   (b) If the length of the dataset is 30 minutes, then extract the dataset as it is.
   (c) If the length of the dataset is more than 30 minutes, then extract the first 30 minutes of the dataset.
   (d) If the dataset has more readings after the first 30 minutes, repeat the steps starting from process number 2a.

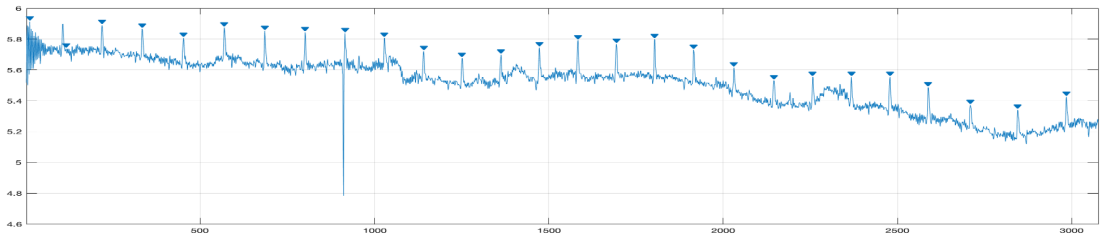

(a) EHG consistent pattern (labour)

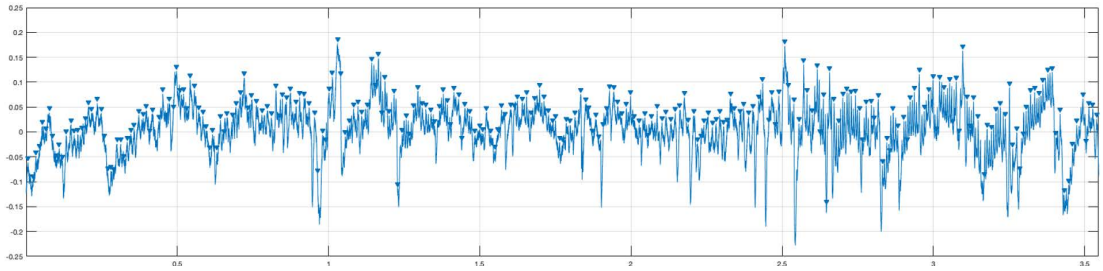

(b) EHG random pattern (non-labour)

Figure 6.7: Datasets EHG signal types

From the three databases' 376 datasets, we extracted a total of 6169 30-minute-long datasets. In the next section, we will detail the data analysis process for EHG feature extraction and final decision (FD) selection for labour detection.

6.4.3 Data Analysis

In general, the extracted EHG signals datasets have either a consistent pattern (labour) or a random pattern (non-labour). Figure 6.7 shows both types of EHG signal pattern datasets.

Based on this observation, we divided data analysis into two phases, as shown in the scheme's general flowchart in Figure 6.8, where SD stands for standard deviation, and FD stands for final decision. The scheme's general flowchart is divided into four sections:

1. Data streaming section (coloured green), where the application reads EHG signals.
2. Phase 1 analysis section (coloured blue).
3. EHG feature extraction Section (coloured orange).

4. Phase 2 analysis section (coloured gray).

If the dataset does not pass Phase 1, it has a random EHG signal pattern, and the final decision will not trigger the alarm. If the dataset passes Phase 1, it goes into feature extraction, followed by Phase 2. If the dataset does not pass Phase 2, then the final decision will be to not trigger the alarm. Otherwise, the final decision will be to trigger the alarm since the dataset has passed Phase 2. The following sections will go into detail for each phase and feature extraction process.

6.4.4 Phase 1 Analysis

To optimize the proposed scheme, we need to first recognize if the dataset's EHG signal pattern is consistent or random. We need a value that can determine if the pattern of the EHG signals is random and can be efficiently calculated using the smartphone's limited resources. Standard deviation (SD) is one of the commonly calculated attributes when analyzing uterine contractions [33] [42] and can be efficiently calculated using the smartphone's limited resources.

To find out if the SD value can indicate the randomness of the pattern of the EHG signals, we calculated the SD value for several randomly chosen datasets from our 6169 datasets. We noticed that datasets with a random EHG signal pattern scored SD values of less than 0.1, while the datasets with consistent EHG signal patterns scored higher SD values. Therefore, we chose the SD value of 0.1 to be the threshold to determine if the dataset's EHG signal has a pattern and therefore whether Phase 1 will be passed or not. Figure 6.9 shows the plot of the SD value for all the datasets. Notice that the threshold value of 0.1 (represented by the red dotted line) distinguishes the datasets with pattern readings from those with random readings.

Standard Deviation Analysis

To calculate the SD value, we will use the following equations, where N is the size of the dataset:

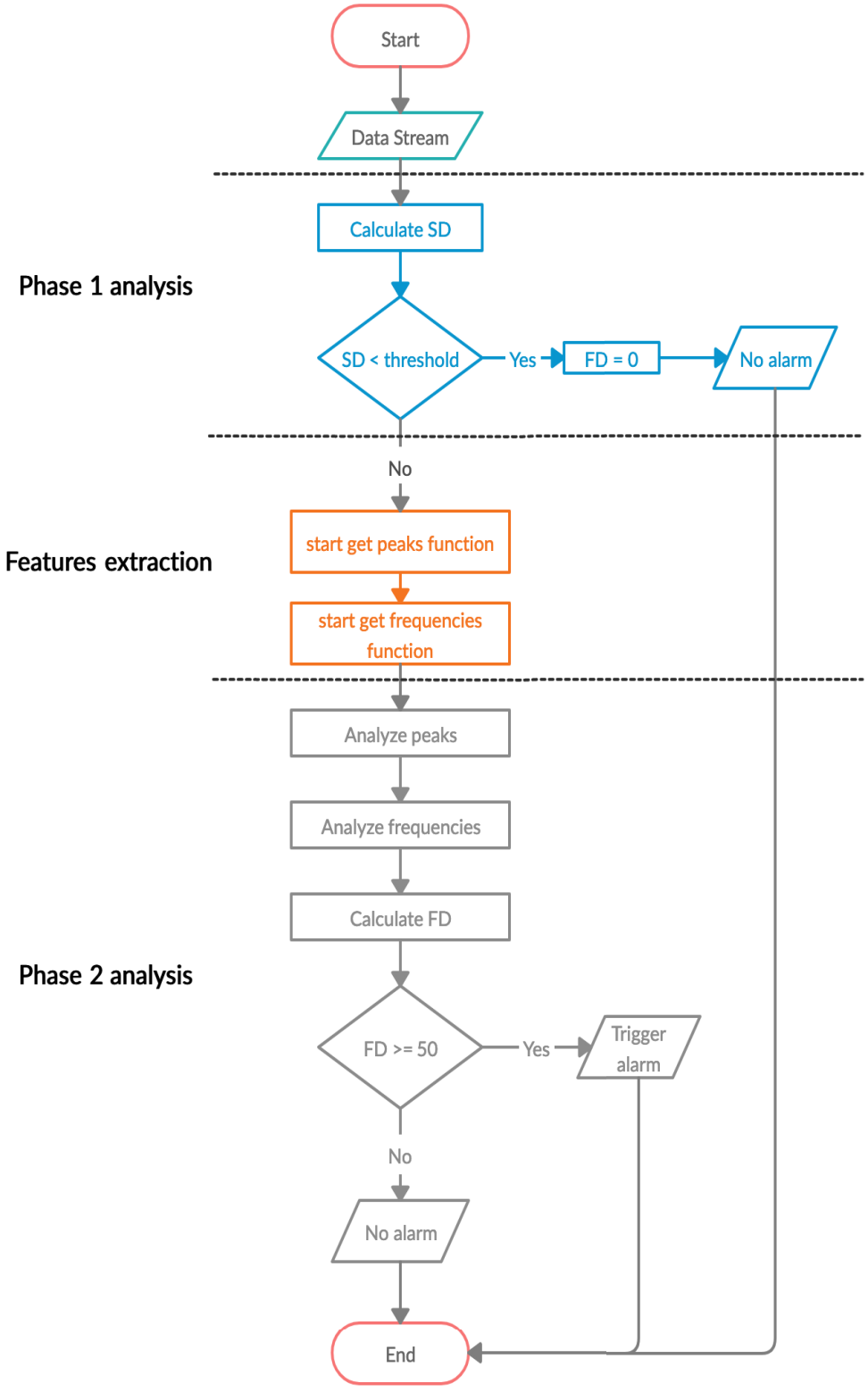

Figure 6.8: Amplitude-frequency scheme general flowchart

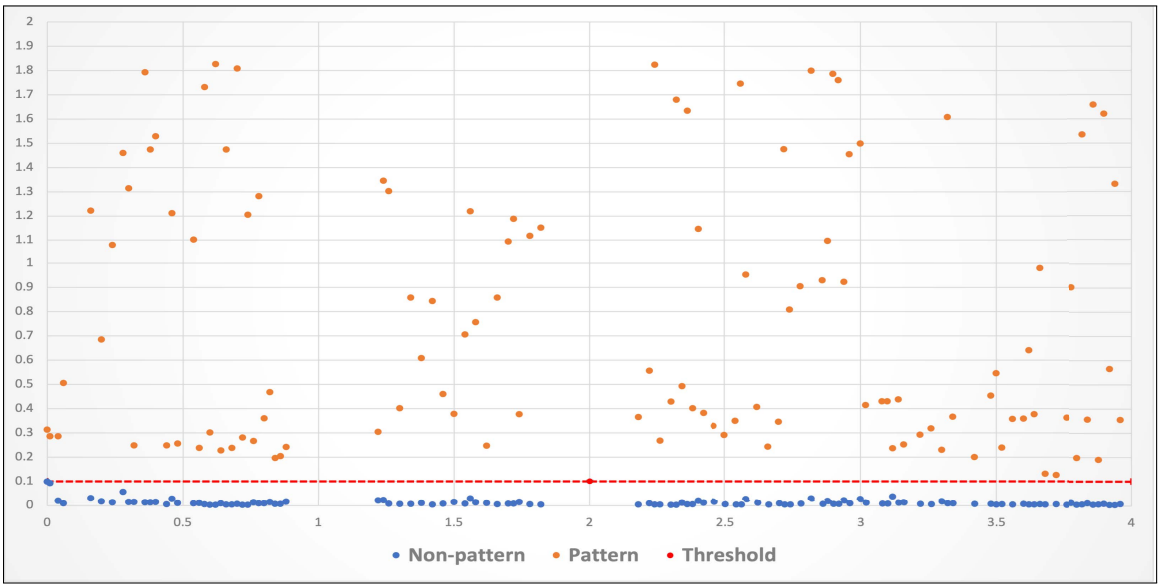

Figure 6.9: SD values plot

1. Sum of all dataset readings:

$$sum = \sum_{i=1}^{N} x_i \tag{6.1}$$

2. Mean of the dataset readings:

$$\mu = sum/N \tag{6.2}$$

3. SD value:

$$\sigma = \sqrt{\frac{1}{N}\sum_{i=1}^{N}(x_i - \mu)^2} \tag{6.3}$$

If the SD value is higher than the threshold of 0.1, then the dataset will pass Phase 1 and proceed to feature extraction and then Phase 2. Otherwise, the dataset will not pass Phase 1, and no alarm will be triggered.

6.4.5 Feature extraction

After passing Phase 1, the dataset will go through the process of feature extraction. As we mentioned in Section 6.3, we will be using peaks and frequency to determine if the pregnant woman is in labour. Notice that each feature extraction iteration will be done in a window of 100 EHG readings until the end of the dataset.

Peaks

During labour, the uterine contraction amplitude will peak before decreasing again. Contractions close to each other will have similar peak levels. The peaks algorithm will look for the highest reading in the 100 reading range and mark its position as a peak. Figure 6.10 shows the flowchart of peak extraction, and Algorithm 3 illustrates the peak extraction process. The following section will define what a frequency is and illustrate the frequency feature extraction process.

Algorithm 3 Peaks extraction algorithm

Require: dataset EHG signals readings

```
1: for i ← 0 to < sataset_size do
2:     isPeak ← ture
3:     l ← max(0, i − range)
4:     r ← min(datasetSize − 1, i + range)
5:     for j ← l to <= r do
6:         if i = j then
7:             continue
8:         end if
9:         if Dataset_i < dataset_j then
10:            isPeak ← false
11:            break
12:        end if
13:    end for
14:    if isPeak = true then
15:        store peak value
16:        store peak position
17:        i+ = range
18:    end if
19: end for
```

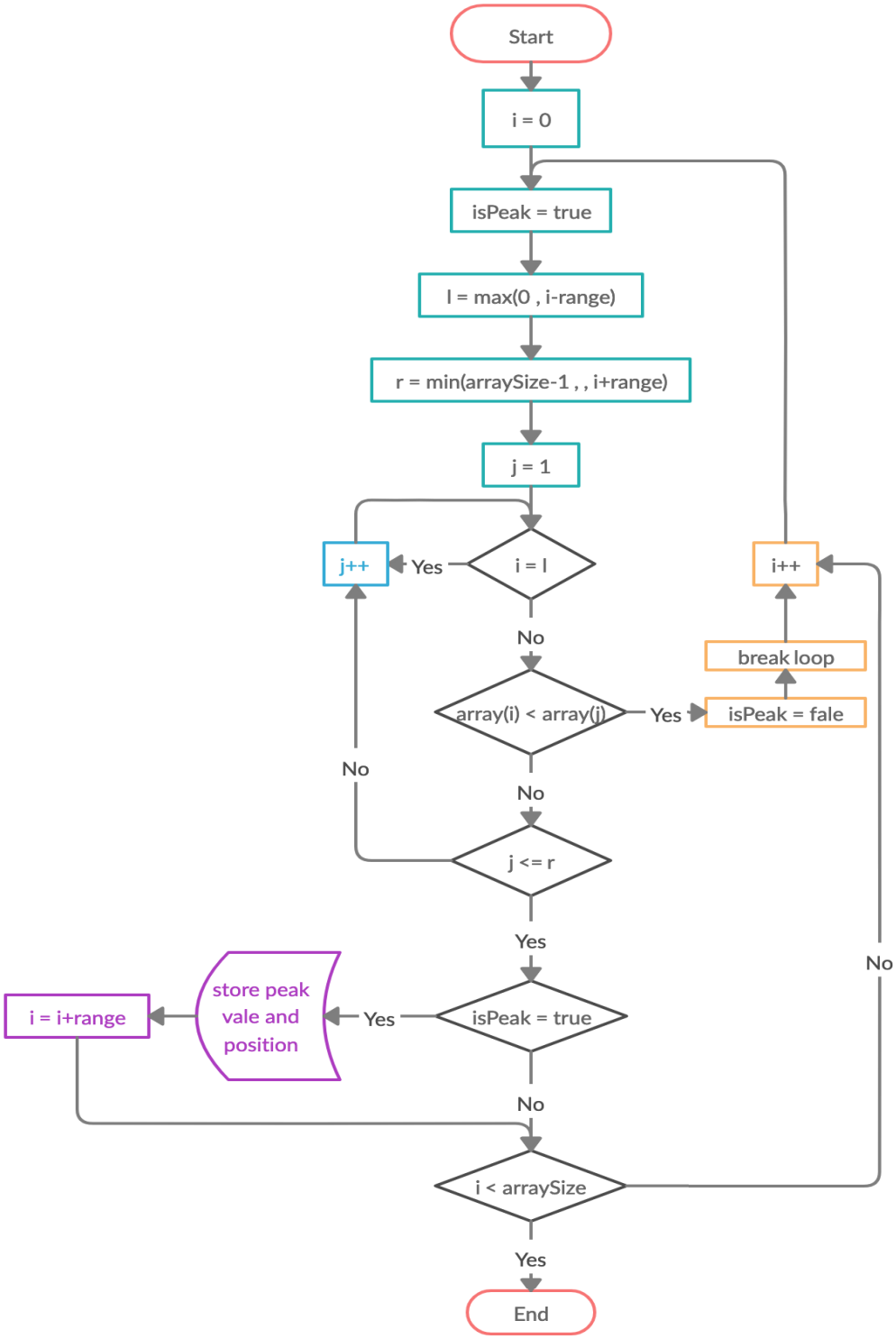

Figure 6.10: Peaks extraction flowchart

Frequency

Frequency is defined as the time from one peak to the next peak. Similar to the peaks, contractions closer to each other will have similar frequency values. The frequency algorithm will calculate the distance from one peak position to the next peak position. Figure 6.11 shows the flowchart of frequencies extraction, where pp refers to peak position, and Algorithm 4 demonstrates the frequency extraction process.

Algorithm 4 Frequency extraction algorithm

Require: peaks positions
1: **for** $i \leftarrow 0$ to $< PeaksSize - 1$ **do**
2: $frequency \leftarrow Peaks_i + 1 - Peaks_i$
3: *store frequency value*
4: **end for**

6.4.6 Phase 2 Analysis

Phase 2 is designed to calculate three statistical values used for the final decision (FD). The three statistical values are:

- The percentage difference between two peaks or two frequencies values next to each other.
- The percentage rate of pattern dissimilarities (PRPD) of extracted features.
- The final decision (FD) rate.

Each value is the baseline for the next one. We will use the above list of statistical values to determine if the dataset has a consistent pattern for each extracted feature.

Percentage Difference

This is the first statistical value to be calculated. To illustrate how the percentage difference (PD) is calculated, we will check the similarity of each value with the following value and calculate the PD between the two values. Figure 6.12 shows the PD flowchart, where:

- *valP is value1 + value2.*
- *valM is value1 - value2.*

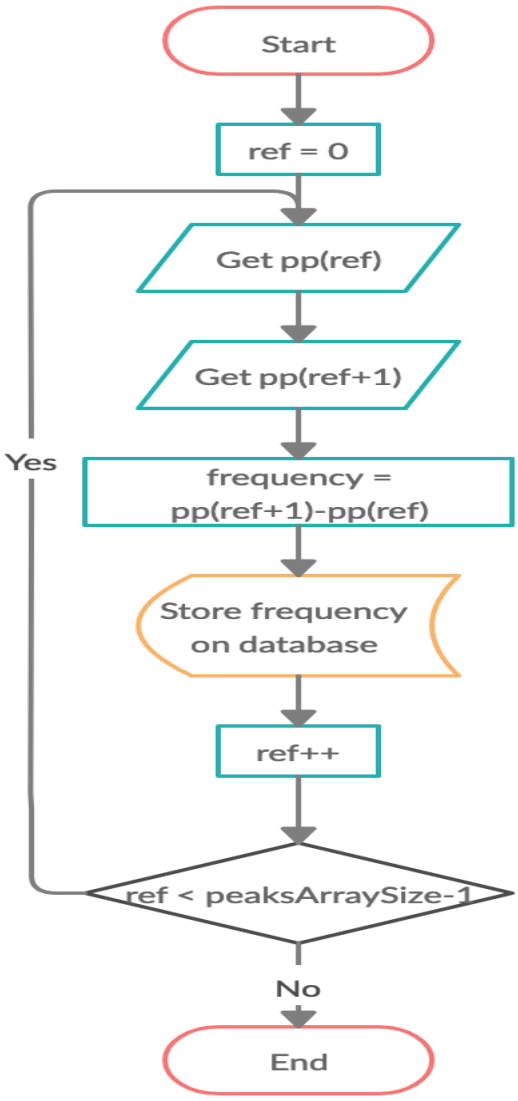

Figure 6.11: Frequency extraction flowchart

- *perDiff is the PD result.*

Algorithm 5 illustrates the percentage difference calculation:

Algorithm 5 Percentage difference algorithm

Require: two values

1: $valM \leftarrow |val1 - val2|$
2: $valP \leftarrow (|val1 + val2|)/2$
3: **if** $valP \neq 0$ **then**
4: $perDiff \leftarrow (valM/valP) * 100$
5: *return perDiff*
6: $i+ = range$
7: **end if**

The lower the PD, the more similar the two values are. If the PD is more than 14%, then we consider the two values as not similar. In the end, we will count how many dissimilarities there are in order to calculate PRPD using the following equation:

$$PRPD = \frac{dissimilarities * 100}{extracted\_values\_size}$$

PRPD should be 25% or less to consider the values consistent. Before calculating the final decision (FD), both PD and PRPD will be calculated for peaks and frequencies.

Peaks Analysis

We defined peaks in Section 6.3 as uterine contraction spikes. They are one of the essential features used in detecting labour. As we mentioned in the previous chapter, PD and PRPD will be calculated to determine if the peaks have consistency. Figure 6.13 shows the peaks analysis flowchart, where:

- *PFC is the count of dissimilar peaks.*
- *PDR is the peaks percentage difference rate.*
- *PeaksFD is the peaks final decision.*

Algorithm 6 illustrates the peaks analysis process.

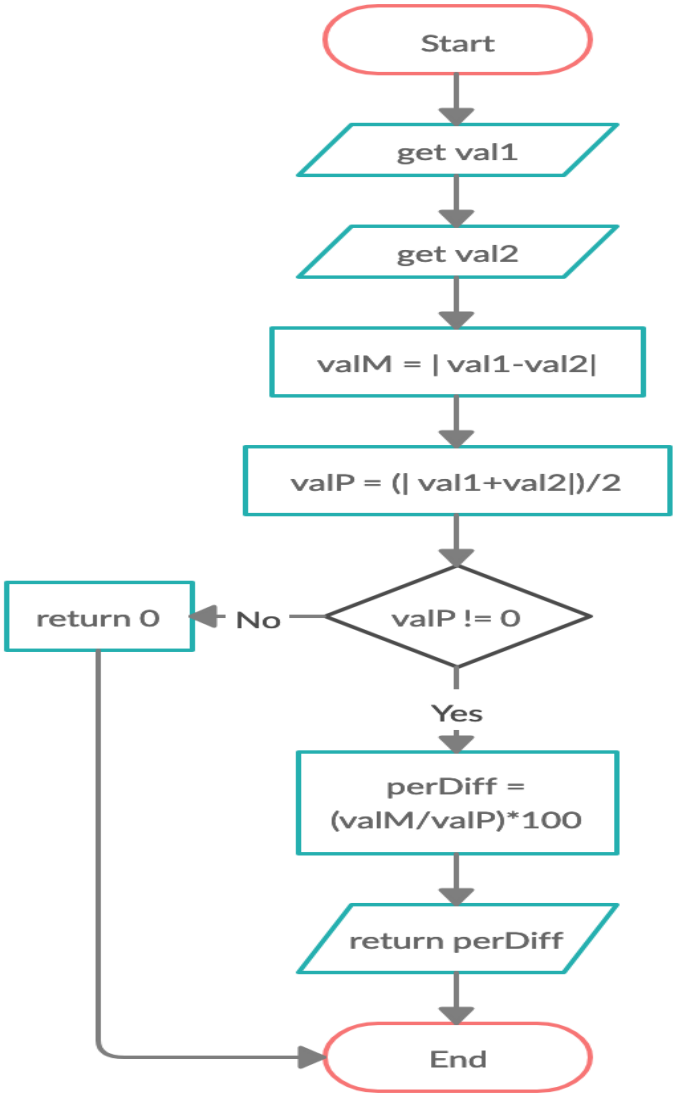

Figure 6.12: Percentage difference flowchart

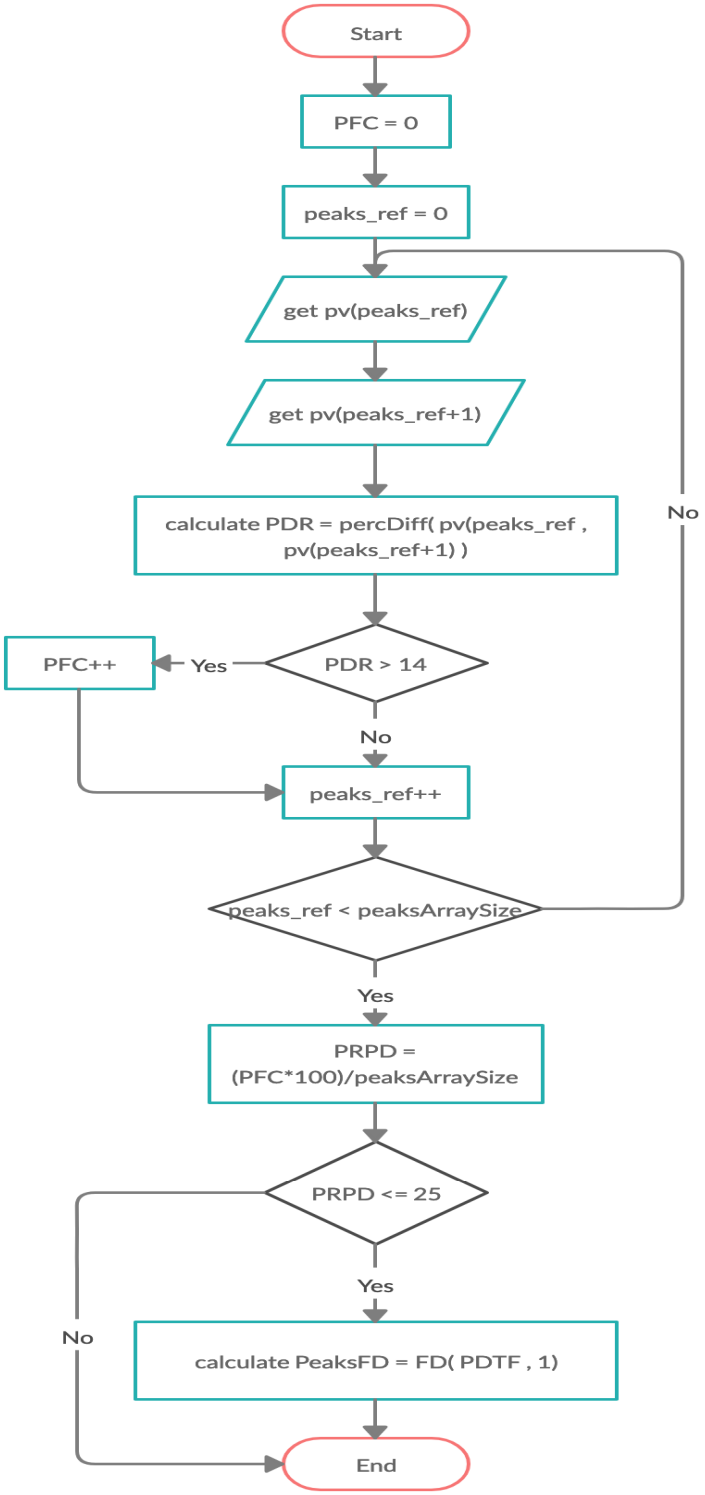

Figure 6.13: Peaks analysis flowchart

Algorithm 6 Peaks analysis algorithm

Require: peaks values

1: $PFC \leftarrow 0$
2: **for** $i \leftarrow 0$ to $< peaks\_size - 1$ **do**
3: $peak1 \leftarrow peak_i$
4: $peak2 \leftarrow peak_{i+1}$
5: $PDR \leftarrow percDiff(peak_i, peak_{i+1})$
6: **if** $PDR > 14$ **then**
7: $PFC++$
8: **end if**
9: **end for**
10: $PRPD \leftarrow (PFC * 100)/peaks\_size$
11: **if** $PRPD <= 25$ **then**
12: $PeaksFD \leftarrow FD(PRPD, 1)$
13: **end if**

Frequency Analysis

In Section 6.3, we explained the importance of frequencies in detecting labour. A uterine frequency is a distance from one peak to the next. Similar to peaks analysis, PD and PRPD will be used to determine the consistency of the frequencies of the dataset. Figure 6.14 shows the frequency analysis flowchart, where:

- FFC is the count of dissimilar frequencies.
- FDR is the frequencies percentage difference rate.
- FreqFD is the frequency final decision.

Algorithm 7 illustrates the frequency analysis process:

6.4.7 Final Decision Analysis

This is the last step in dataset analysis. After calculating the peaks FD and frequencies FD, we will calculate the FD of the dataset's consistency and trigger the alarm. We will combine the peaks FD (PeaksFD) and frequencies FD (freqFD) to calculate the FD. If the result is higher than or equal to the FD threshold, the alarm will be triggered. Our choice of the FD threshold is based on the framework's design goal to monitor pregnant women with a high risk of premature birth. As we explained in Section 1.3, premature birth can happen spontaneously without a known reason

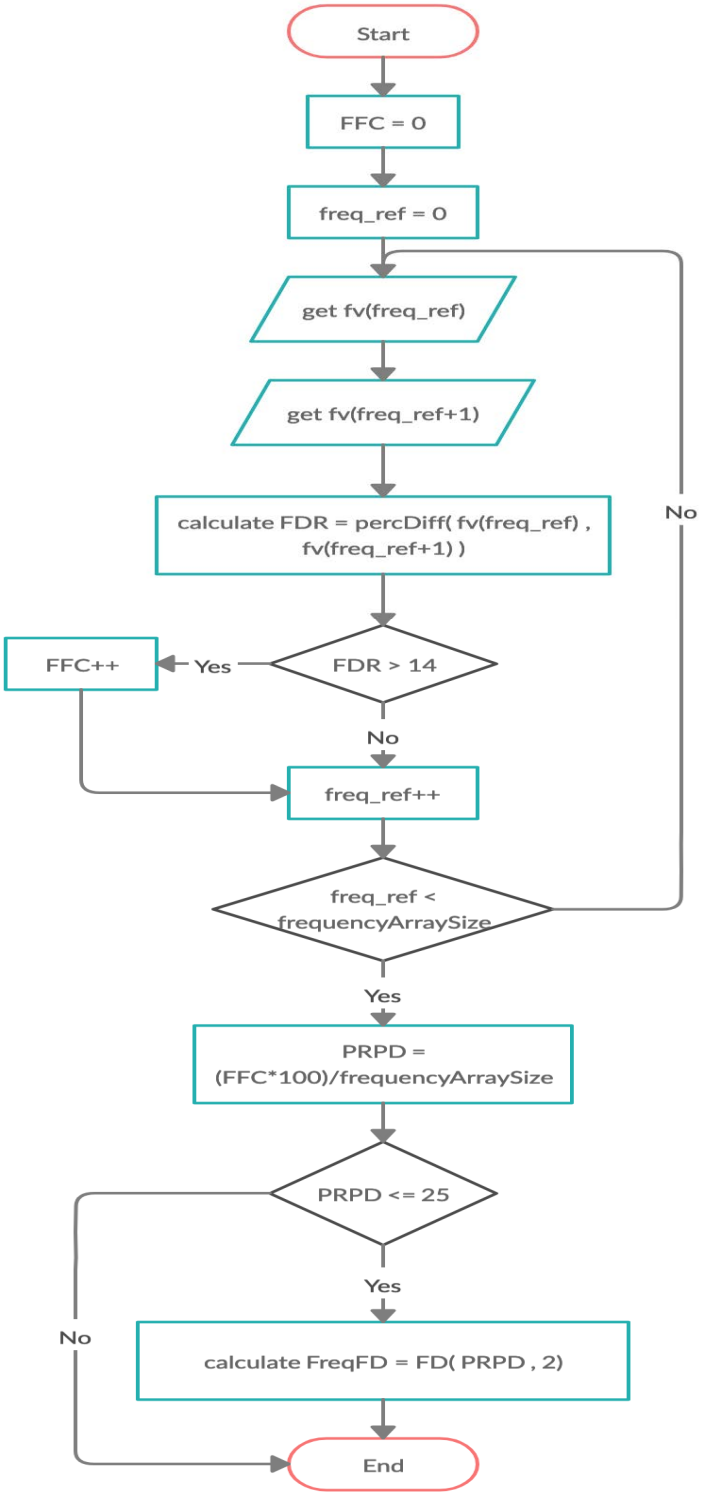

Figure 6.14: Frequency analysis flowchart

Algorithm 7 Frequency analysis algorithm

Require: frequeny values

1: $FFC \leftarrow 0$
2: **for** $i \leftarrow 0$ to $< frequency\_size - 1$ **do**
3: $\quad freq1 \leftarrow frequency_i$
4: $\quad freq2 \leftarrow frequency_{i+1}$
5: $\quad FDR \leftarrow percDiff(frequency_i, frequency_{i+1})$
6: $\quad$ **if** $FDR > 14$ **then**
7: $\quad\quad FFC++$
8: $\quad$ **end if**
9: **end for**
10: $PRPD \leftarrow (FFC * 100)/frequency\_size$
11: **if** $PRPD <= 25$ **then**
12: $\quad FreqFD \leftarrow FD(PRPD, 2)$
13: **end if**

and at a very early gestational age. Considering this, we believe that the threshold must be reasonable to ensure the safety of pregnant women and premature babies, considering the high risk that could threaten their well-being. Figure 6.15 shows the application FD analysis flowchart, and Algorithm 8 illustrates the application FD analysis process. In the next section, we will present the scheme evaluation methodology.

6.5 Evaluation Methodology

To meet our research goals listed in Chapter 4, we need to evaluate the proposed scheme in terms of two aspects:

- Scheme algorithms' reliability and accuracy in detecting labour patterns.
- Smartphone resources performance.

We will implement a proof-of-concept application in the Java programming language using a Nexus 7 tablet and use the uterine EHG datasets derived from the three databases from [127] to evaluate the application.

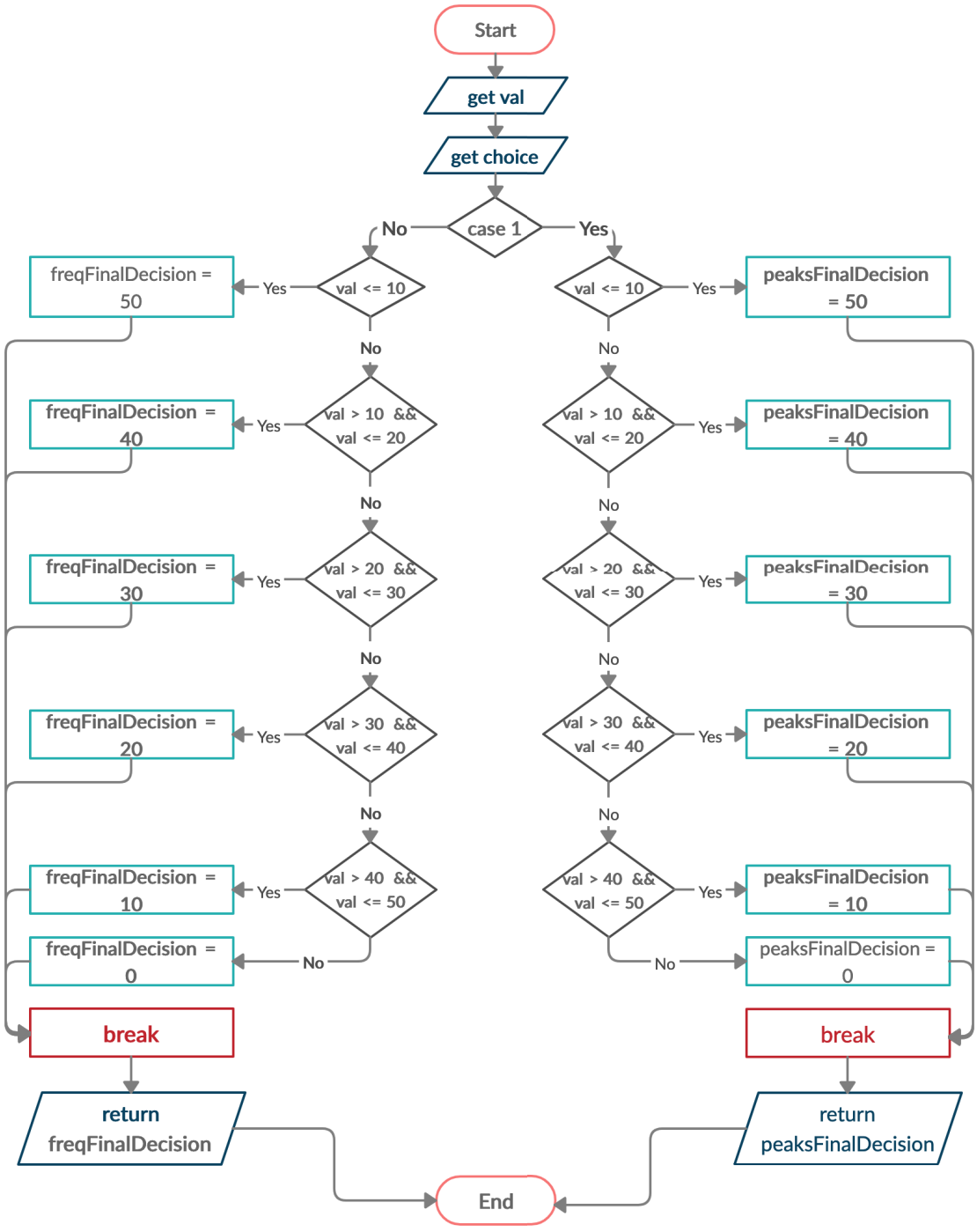

Figure 6.15: FD analysis flowchart

Algorithm 8 FD analysis algorithm

Require: value (PeaksFD or freqFD), choice

```
switch (choice)
case 1:
    if value <= 10 then
        peaksFinalDecision ← 50
    else if value > 10 and value <= 20 then
        peaksFinalDecision ← 40
    else if value > 20 and value <= 30 then
        peaksFinalDecision ← 30
    else if value > 30 and value <= 40 then
        peaksFinalDecision ← 20
    else if value > 40 and value <= 50 then
        peaksFinalDecision ← 10
    else
        peaksFinalDecision ← 0
    end if
case 2:
    if value <= 10 then
        freqFinalDecision ← 50
    else if value > 10 and value <= 20 then
        freqFinalDecision ← 40
    else if value > 20 and value <= 30 then
        freqFinalDecision ← 30
    else if value > 30 and value <= 40 then
        freqFinalDecision ← 20
    else if value > 40 and value <= 50 then
        freqFinalDecision ← 10
    else
        freqFinalDecision ← 0
    end if
end switch
```

	Classified pattern	**Classified no pattern**
Pattern	true positive (TP)	FN
No pattern	FP	true negative (TN)

Table 6.1: Confusion matrix

6.5.1 Reliability and Accuracy Analysis

We will be using a confusion matrix, a two-dimensional matrix table used to rate the performance of a classifier based on test data [132], to evaluate the scheme algorithms' performance. Table 6.1 represents the confusion matrix we will be using.

From this table, we will calculate the following equations to measure the system algorithm performance:

- Accuracy (AC) is the percentage of how often the classifier is correct overall to identify the dataset as having a pattern or no pattern. AC is given by Equation 6.4:

$$AC = \frac{TP + TN}{TP + TN + FP + FN} \tag{6.4}$$

- Misclassification rate (MisCl) is the percentage of how often the classifier is wrong overall to identify the dataset as having a pattern or no pattern. MisCl is given by Equation 6.5:

$$MisCl = \frac{FP + FN}{TP + TN + FP + FN} \tag{6.5}$$

- Recall (R) is the percentage of how often the classifier identifies the dataset as having a pattern when it is has a pattern. R is given by Equation 6.6:

$$R = \frac{TP}{TP + FN} \tag{6.6}$$

- Precision (P) is the percentage of how often the classifier is correct when it identifies the dataset as having a pattern. P is given by Equation 6.7:

$$P = \frac{TP}{TP + FP} \tag{6.7}$$

- F is the balance between the precision (P) and the recall (R) values. A higher F value indicates a classifier is more accurate, especially since we care more about patterned datasets in our results. F is given by Equation 6.8:

$$F = 2 * \frac{P * R}{P + R} \tag{6.8}$$

- False negative rate (FNR) is the percentage of how often the classifier identifies the dataset as not having a pattern when it has a pattern. This evaluation parameter is important because if it is high, it means the application will not trigger an alarm, even though dataset has a pattern. FNR is given by Equation 6.9:

$$FNR = \frac{FN}{TP + FN} \tag{6.9}$$

- False positive rate (FPR) is the percentage of how often the classifier identifies the dataset as having a pattern when it has no pattern. This evaluation parameter is important because if it is high, it means the application will trigger an alarm, even though the dataset has no pattern, resulting in pregnant women having more unscheduled visits to the hospital for no reason. FPR is given by Equation 6.10:

$$FPR = \frac{FP}{FP + TN} \tag{6.10}$$

We used the NetBeans 8.2 platform to test all 6169 datasets and obtain the results for the confusion matrix. In the next section, we will present the smartphone resources performance criteria.

6.5.2 Smartphone Resources Performance

As we mentioned in Chapter 4, the proposed scheme should be cheap and reliable. Moreover, the proposed scheme will be deployed on a smartphone that has limited resources. For these reasons, we need to evaluate the application in terms of CPU, memory, and battery power consumption. The application should efficiently consume the smartphone's resources so it can be deployed on low-cost, lower-end smartphones,

which are commonly used in developing countries. We will use two tools to analyze the smartphone's resource consumption: the Android monitor tool and Battery Historian.

Furthermore, since we need to deploy the algorithm and the datasets on the smartphone for resource evaluation, we cannot use all 6169 datasets individually for testing. Therefore, we will choose a set of datasets for resource evaluation. This set will contain the different varieties of datasets to cover all possible outcomes, i.e. did not pass Phase 1, did not pass Phase 2, and passed Phase 2 with alarm.

CPU and Memory Performance

We will monitor the application CPU and memory consumption at the beginning, middle, and end of the 30-minute monitoring session. We will take the overall average CPU and memory consumption rate for all the testing datasets to evaluate the smartphone's CPU and memory resources' application consumption efficiency.

Battery Power Consumption

The Batterystats and Battery Historian tools will provide us with the percentage and quantity (in mAh) of the application's battery power consumption. For each chosen dataset, we will monitor the application at the beginning, middle, and end of the 30-minute monitoring session. We will take the overall average battery power consumption rate for all the datasets to evaluate how efficiently the application consumes battery power. In the next section, we will present the results of the simulation experiment.

6.6 Results

In this section, we will present the results of the scheme we obtained based on our evaluations. The application was running for 30 minutes. Since the Android Studio monitoring tool needs the tablet to be connected to the laptop and the battery monitoring tool needs the tablet to be disconnected, we used two identical Asus Nexus 7 tablets with no noticeable difference in performance for evaluation. One tablet was

	Classified pattern	**Classified no pattern**
Pattern	2795	581
No pattern	0	2793

Table 6.2: The threshold of 70% confusion matrix for the amplitude-frequency algorithm

used to collect CPU and memory performance, and the other was used for battery power consumption.

6.6.1 Reliability and Accuracy Analysis

We need to ensure that the algorithm can recognize the uterine contractions labour pattern. The final decision (FD) represents this crucial point. Furthermore, as we explained in Section 6.4.7, the risk of premature birth is high for some pregnant women, and they need to be monitored more carefully than pregnant women with low premature birth risk. Therefore, we need to ensure that pregnant women with a high risk of premature birth will have the highest possible probability of getting a warning from the application. For that reason, our analysis results of reliability and accuracy will be divided into two FD thresholds:

- FD threshold of 70%.
- FD threshold of 50%.

The threshold of 70% or higher means that 70% of the dataset has a pattern consistency. Table 6.2 represents the confusion matrix of the threshold of 70% we will be using to calculate the evaluation equations described in Section 6.5.1.

As with the threshold of 70%, the threshold of 50% or higher means that 50% of the dataset has pattern consistency. Table 6.3 represents the confusion matrix of the threshold of 50%. Table 6.4 shows the reliability and accuracy analysis evaluation results derived from both confusion matrix Tables 6.2 and 6.3. In the next section, we will present the smartphone's resource performance.

	Classified pattern	Classified no pattern
Pattern	3350	26
No pattern	0	2793

Table 6.3: The threshold of 50% confusion matrix for the amplitude-frequency algorithm

	Threshold of 70%	Threshold of 50%
AC	0.905	0.995
MisCl	0.094	0.004
R	0.827	0.992
P	1	1
F	0.905	0.996
FNR	0.172	0.007
FPR	0	0

Table 6.4: Reliability and accuracy analysis evaluation results for the amplitude-frequency algorithm

6.6.2 Smartphone's Resources Performance

Since the smartphone is the primary resource the proposed scheme uses to analyze uterine contractions, we need to make sure the application uses the smartphone's resources efficiently. The next smartphone resource consumption evaluation results are the same for both thresholds of 70% and 50%.

Because we are testing the application for 30 minutes, it is not practical to run the test for all 6169 datasets. Therefore, we randomly chose 13 datasets, making sure they represent the following:

- All three different databases.
- All three FD situations, i.e., did not pass Phase 1, did not pass Phase 2, and passed Phase 2.

We will show the results at the beginning, middle, and end of the application's running time and divide them into "with alarm" and "with no alarm" resource consumption.

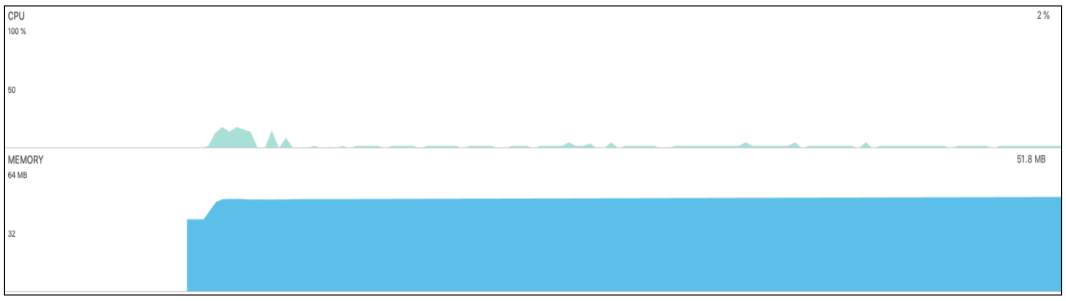

Figure 6.16: Beginning of the application's running time - with alarm - amplitude-frequency algorithm

Figure 6.17: Middle of the application's running time - with alarm - amplitude-frequency algorithm

CPU and Memory Performance

With Alarm

As seen in Figure 6.16, the application at the beginning uses 2% of the CPU with a small spike representing the launch of the application and allocates 51.8 MB out of 1.80 GB of the device's memory. The application at the middle uses 2% of the CPU and allocates 60.7 MB out of 1.80 GB of the device's memory, as shown in Figure 6.17.

Figure 6.18 shows that the application at the end uses 2% of the CPU, with a short spike of 50% of the CPU representing data analysis and alarm triggering with the screen turning on, and allocates 67.7 MB out of 1.80 GB of the device's memory. Notice that at the top of Figure 6.18, the alarm was triggered.

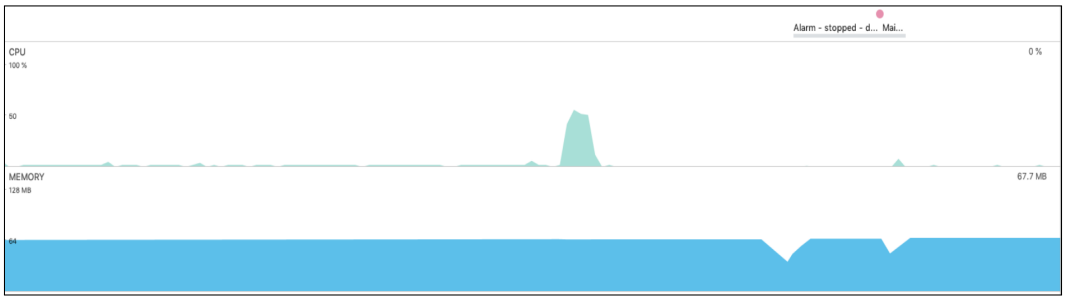

Figure 6.18: End of the application's running time - with alarm - amplitude-frequency algorithm

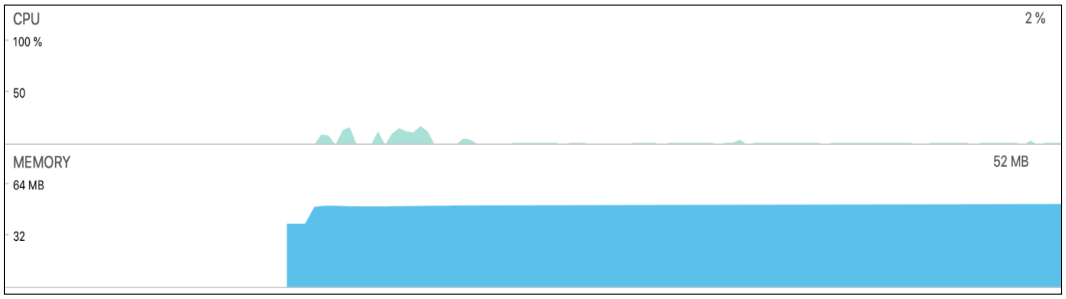

Figure 6.19: Beginning of the application's running time - with no alarm - amplitude-frequency algorithm

With no Alarm

As seen in Figure 6.19, the application at the beginning where it used 2% of the CPU with a small spike representing the launch of the application and allocated 52 MB out of 1.80 GB of the device's memory.

Figure 6.20 represents the application in the middle where it used 2% of the CPU and allocated 52.1 MB out of 1.80 GB of the device's memory.

Figure 6.20: Middle of the application's running time - with no alarm - amplitude-frequency algorithm

Figure 6.21: End of the application's running time - with no alarm - amplitude-frequency algorithm

Figure 6.21 shows the application at the end where it used 2% of the CPU, with a short spike representing data analysis, and allocated 53.4 MB out of 1.80 GB of the device's memory. Notice that there is no alarm indicator at the top of Figure 6.18 since the alarm was not triggered. On average, the application used 2% of CPU power and allocated 60 MB out of 1.80 GB of the smartphone's memory.

Battery Power Consumption

The device has a battery capacity of 3448 mAh. On average, the application consumed 0.84% or 34.5 mAh of battery capacity. In the next section, we will discuss the results.

6.7 Discussion

In this section, we will discuss the results of the scheme and how the scheme met the objectives set in Section 4.2. We will also compare the results of the smartphone application with the studies in the literature review and the results from the previously proposed scheme [129] that we detailed in Chapter 5.

6.7.1 Reliability and Accuracy Analysis

On the one hand, with normal labour, pregnant women have an expected date of birth determined by the obstetrician. On the other hand, labour for a pregnant woman with a high risk of premature birth can happen spontaneously at an early gestational age without her noticing labour until later. This uncertainty will put her health and

the fetus's health in danger. Due to this unpredictable nature of premature birth, we need to make sure we give the pregnant woman the highest possible chance of knowing if she is starting to go into labour. For these reasons, we chose the minimum of 50% pattern consistency of the uterine contraction datasets since, in our assumption, 50% is enough for the pregnant woman to be checked by an obstetrician due to the high risks that can follow a premature birth. This decision could increase unscheduled hospital visits if the application gave a false warning after analyzing the dataset.

Based on the above, the application's reliability and accuracy analysis results are critical for the proposed scheme to meet our design objectives. Moreover, the framework's ultimate goal is to mitigate the consequences of premature birth for pregnant women and babies. Therefore, we chose the two FD thresholds of 70% and 50% to detect if the pregnant woman is going into labour or not. The following will discuss the thresholds' confusion matrices' results, as shown in Table 6.4.

In general, the FD threshold of 50% has better results than the 70% threshold in all the above criteria except FPR. Starting with the AC rate, the application is 9% more accurate with the threshold of 50% than 70% in classifying the datasets, with an accuracy rate of 0.995 and 0.905, respectively. On the other hand, the threshold of 70% has a misclassified rate of 0.094, and the threshold of 50% has a misclassified rate of 0.004.

The R rate is 0.827 for the threshold of 70% and increases to 0.992 for 50%, with a total of 2795 and 3350 correctly predicted pattern datasets, respectively. That means the application with the threshold of 50% has a better rate of predicting a pattern in a dataset.

For both thresholds, the P rate has a possibility of 1. This indicates that both the thresholds are always correct when they classify a dataset as patterned.

The F score for the threshold of 70% is 0.905, and it increases to 0.996 for 50%. This score indicates that R and P are balanced more in the 50% threshold, which means the threshold of 50% has a better classifier than 70%.

Of all the evaluation results in the above table, FNR is the most important result

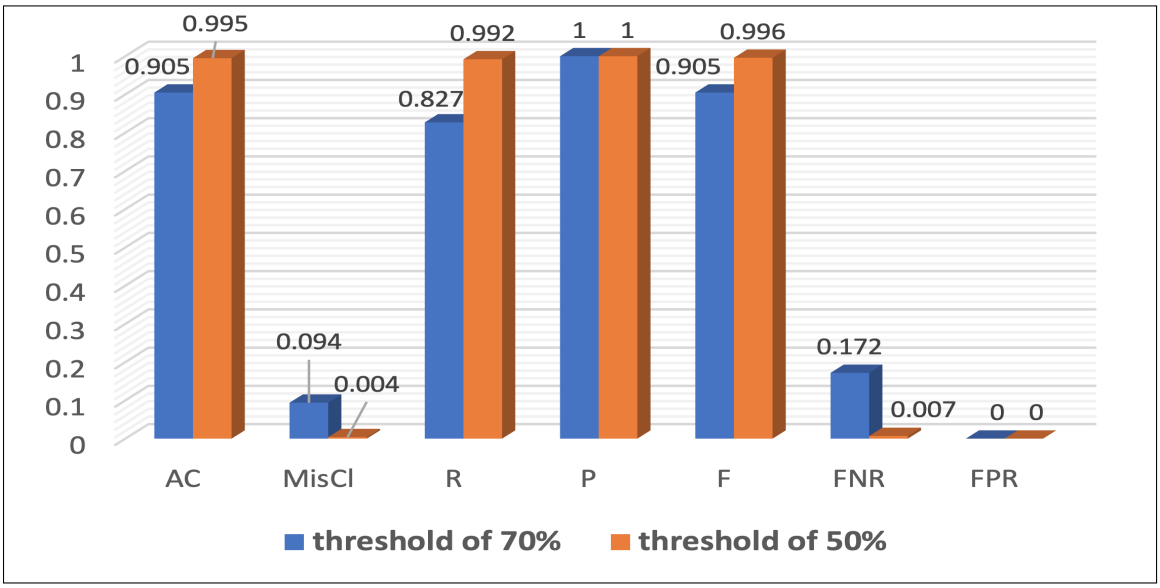

Figure 6.22: FD thresholds result in comparison - amplitude-frequency algorithm

because it represents the percentage of the application not triggering a warning when the dataset has a labour pattern. This rate indicates that the pregnant woman has started going into labour, but the application failed to notify her through a warning. This error could jeopardize her life and the life of the fetus, thereby failing to meet the core goal of the framework. The FNR for the threshold of 50% is 0.007 with a total of 26 misclassified patterned datasets and 0.172 for the threshold of 70% with 581 misclassified patterned datasets.

On the other hand, the FPR for both thresholds is 0 since both thresholds did not classify any non-patterned datasets into patterned datasets. Finally, the chart in Figure 6.22 visualizes the differences between the two thresholds.

Finally, compared to the previously proposed system [129], the smartphone application's proposed scheme is more reliable and accurate. The application extracts more features with higher precision and analyzes them with more complicated algorithms. The application was also tested with more datasets derived from three different databases, making the application more reliable and generalized.

In conclusion, the threshold of 50% has been shown to be a more suitable choice

that meets the proposed scheme's objectives. It has a lower possibility of misclassifying a patterned dataset into non-patterned while maintaining a reasonable pattern detection threshold. In the next section, we will discuss how efficient the application is in consuming the smartphone's resources.

6.7.2 Smartphone's Resources Performance

Since the amplitude-frequency algorithm scheme is designed to be deployed on smartphones, the application must be optimized to efficiently consume smartphone resources to meet the framework's design objectives. The scheme will not be practical if the application quickly drains the smartphone's resources.

There are two main reasons for the optimum usage of the smartphone's resources:

- The scheme will be continually monitoring pregnant women.
- The scheme is designed to be suitable for developing countries, where low-end smartphones are widely used.

For these reasons, we need to ensure that the monitoring application will not intensively consume the smartphone's resources. In comparison to the proposed studies listed in Chapter 3, none of the proposed studies have used a smartphone to analyze uterine EHG signals for labour detection. Furthermore, our proposed system is fully automated and has a wireless design so it does not require the pregnant woman to stay at home or go to the hospital regularly to monitor her uterine activity. The proposed systems in [42] and [44] require the pregnant woman to stay home to be monitored, which will restrict her from moving around freely and comfortably. Moreover, we designed our system to work on any smartphone that operates on Android OS and collect uterine EHG signals using a cost-effective wireless body sensor. These two features make our system cost-effective and suitable for deployment in developing countries where low-cost, low-end Android smartphones are commonly used. All of the proposed studies in the literature review are expensive and cannot be deployed in developing countries.

To measure the application's resource consumption, we focused on the smartphone's CPU, memory performance, and battery power consumption, which will be

discussed in the following three sections.

CPU

Throughout the 30-minute monitoring sessions, the application managed to use only 2% of the CPU on average. Although the proposed scheme has a more complex data analysis process than the previous scheme, its CPU usage was significantly lower than the threshold algorithm scheme due to the optimization of the application. However, there is a short spike in CPU usage to a maximum of around 50% at the end of the monitoring session. This is due to the more complicated calculations of the algorithm.

Memory Performance

The application used an average of 60 MB of memory, which is about 3.33% of the smartphone's memory. However, compared to the threshold algorithm scheme, the complicated data analysis process increased the memory usage by about 130% or 34 MB, which is still considered low compared to the smartphone's memory capacity of 1.80 GB.

Battery Power Consumption

The continuous monitoring of pregnant women requires the application to consume the smartphone's battery efficiently. If the smartphone battery cannot keep up with the application's power demands, the scheme will not meet its objectives. Across the 13 testing datasets, the application consumed 0.84% or 34.5 mAh of battery capacity on average. The application's battery consumption was efficient, and compared to the threshold algorithm scheme the application's battery consumption has improved by about 130%. Furthermore, the application can run for an extended period (about 60 hours of operation before consuming the smartphone battery), unlike the proposed studies [22], [42], [43] and [44].

6.8 Chapter Summary

In this chapter, we presented the amplitude-frequency algorithm scheme in detail. We illustrated the scheme's implementation and evaluation methodology. We presented and discussed the evaluation results and concluded that the FD threshold of 50% has better results than 70%. Moreover, the application efficiently consumed the smartphone's resources in terms of CPU, memory performance, and battery power consumption. Finally, the amplitude-frequency algorithm scheme has shown improvements in CPU and battery power consumption compared to the previously proposed system. In the next chapter, we will present the machine learning algorithm scheme.

Chapter 7

Machine Learning Algorithm Scheme

7.1 Introduction

As a subset of artificial intelligence, machine learning aims to automatically improve the performance of computer systems throughout a learning process to integrate domain knowledge [133][134]. Another definition of machine learning is the study of simulating human learning behaviour by learning from data to gain new knowledge or skills using analysis algorithms [135] [136].

Machine learning can be applied to nearly any field such as medicine, education, industry, automobiles or stock markets [136]. Furthermore, machine learning classification algorithms have been applied extensively in the medical field to help medical staff in disease prediction and diagnosis [137]. ML can be divided into supervised and unsupervised learning. Supervised learning is when the human intervenes in the learning process by labelling or classifying data into the algorithm. On the other hand, unsupervised learning occurs without human intervention by looking for a pattern within raw data. Supervised learning has two main areas: classification and regression. Examples of well-known and popular classification machine learning algorithms include support vector machine (SVM), random forest (RF), decision trees (DT), Naïve Bayes (NB) and k-nearest neighbours.

ML is applied in several healthcare applications, such as detecting diseases or predicting the health status of patients based on their medical history. One area we are interested in is applying ML to uterine EHG signals. Studies have been conducted to use the uterine EHG signals to identify contractions to help in monitoring pregnancy health status (please refer to Section 3.2.2 for more information). Data are fed to the ML algorithms for training to classify the data or create categories for future

predictions [138].

7.2 Proposed Scheme

Detecting and predicting premature labour, as established in Chapter 1, is a challenging task. Machine learning can identify or predict premature labour by analyzing EHG signals with high accuracy. After analyzing studies in the literature, we chose four machine learning classifiers that are widely used by researchers to classify EHG signals into labour and non-labour signals based on their accuracy and efficiency. The four classifiers are:

- Decision trees (DT)
- Random forest (RF)
- Support vector machine (SVM)
- Naïve Bayes (NB)

Similar to the previous scheme implementation described in Section 6.3, we will use the implemented proof-of-concept application built using the Android Studio programming platform for deployment and testing on an Asus Nexus 7 tablet with Android OS version 6.0.1.

To improve the simulation scenario, we used one of the tablets to mimic the WBS by wirelessly sending the EHG signal readings via Bluetooth for more accurate evaluation. The application will continuously receive the uterine contraction EHG data via Bluetooth for the duration of the 30-minute monitoring session. After the 30-minute monitoring session, the application will extract the selected features and feed them to the machine learning classifier implemented within the application to classify the EHG data and decide if the pregnant woman is in labour. If she is in labour, the application will trigger a warning to notify the pregnant woman to go to the hospital. Otherwise, the application will start a new monitoring session. Figure 7.1 shows the block diagram of the monitoring system architecture. In the following section, we will present the scheme UI.

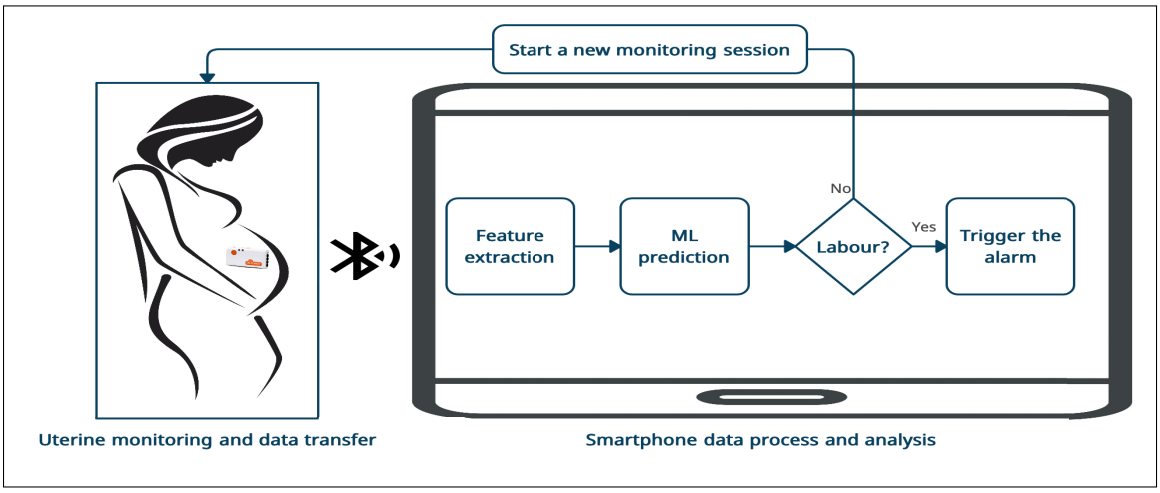

Figure 7.1: The monitoring system architecture

7.3 Scheme User Interface

The UI is the same as the previous scheme in Section 6.3.1 for interfaces 1 and 2. Interface 3 (the alarm interface) was modified and improved by adding Google Maps to guide pregnant women to the closest hospital. In Figure 7.2, we can see the IWK Health Centre's location in Halifax, Nova Scotia, Canada. In the next section, we will present the scheme's experimental framework.

7.4 Experimental Framework

The ML algorithm development cycle shown in Figure 7.3 has two main phases. The first phase deals with data preparation and ML algorithms building and testing. The second phase deals with converting the ML algorithm to TensorFlow Lite format to deploy it to the smartphone. In the next section, we will present the scheme's data selection and preprocessing.

7.4.1 Data Selection and Preprocessing

Data Selection

Similar to the previous scheme, we will use the three databases described in Section 6.4.1. In addition to these three databases, we added two more publicly available

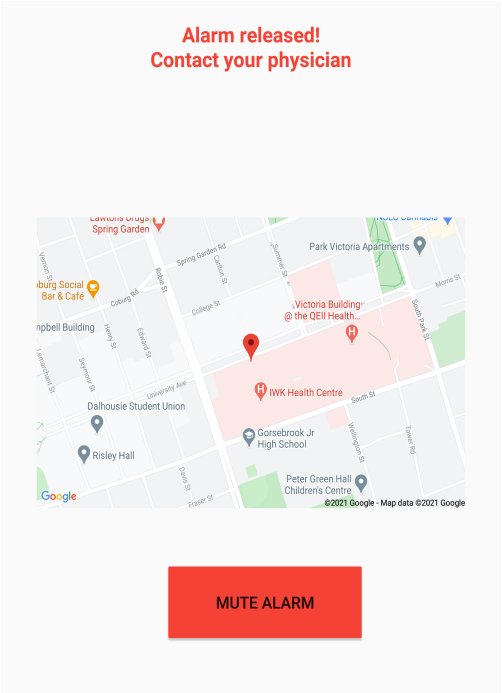

Figure 7.2: Application alarm interface with Google maps

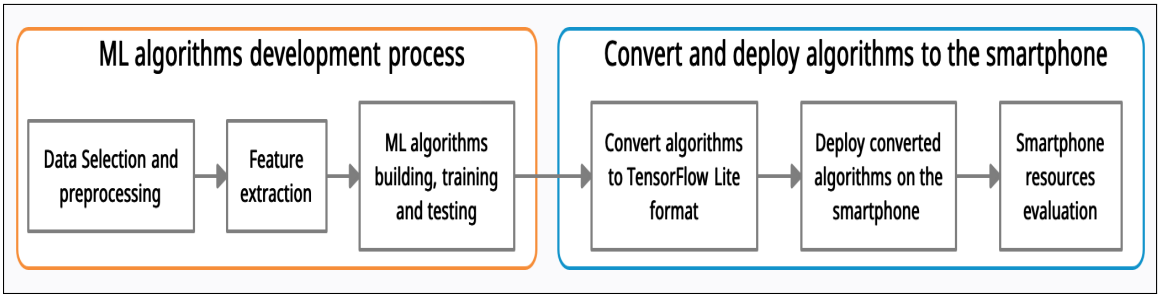

Figure 7.3: ML Algorithms development cycle

Elapsed time hh:mm:ss.mmm	FHR (bpm)	UC (nd)
0:00.000	150.500	7.000
0:00.250	150.500	8.500
0:00.500	151.000	8.500
0:00.750	151.250	7.500
0:01.000	151.250	9.500
0:01.250	150.250	8.500
0:01.500	150.250	10.500
0:01.750	150.250	12.000
0:02.000	148.750	11.000
0:02.250	148.750	11.500
0:02.500	149.500	13.500
0:02.750	147.750	12.000
0:03.000	147.750	13.000
0:03.250	147.250	12.000
0:03.500	147.250	13.500
0:03.750	146.500	15.000
0:04.000	146.500	15.000
0:04.250	146.500	15.000
0:04.500	145.750	14.500

Figure 7.4: CTU-CHB Intrapartum Cardiotocography data sample

Elapsed time hh:mm:ss.mmm	FECG (mV)	UC (mV)	
0:00.000	-104.315		60.875
0:00.002	0.150	1.315	
0:00.004	83.360	0.000	
0:00.006	0.060	0.000	
0:00.008	0.000	0.010	
0:00.010	0.000	0.005	
0:00.012	0.000	0.010	
0:00.014	0.010	0.010	
0:00.016	0.780	-145.760	
0:00.018	87.650	0.000	
0:00.020	4.845	0.725	
0:00.022	4.840	0.715	
0:00.024	4.815	0.725	
0:00.026	4.825	0.715	
0:00.028	4.810	0.720	
0:00.030	4.820	0.720	
0:00.032	4.850	0.715	
0:00.034	4.845	0.720	
0:00.036	4.845	0.725	
0:00.038	4.845	0.730	
0:00.040	4.840	0.730	
0:00.042	4.850	0.705	

Figure 7.5: OB-1 Fetal ECG data sample

databases from the PhysioNet repository [127] for a total of five databases:

- CTU-CHB Intrapartum Cardiotocography Database [139].
- OB-1 Fetal ECG Database [127].

The CTU-CHB Intrapartum Cardiotocography database contains 552 cardiotocography (CTG) recordings collected between 2010 and 2012 from Czech Technical University (CTU) in Prague and the University Hospital in Brno (UHB). Each recording has a fetal heart rate (FHR) time series and a uterine contraction (UC) signal. The length of the recording is 90 minutes at most. Figure 7.4 shows a data sample of uterine contractions EHG signals.

The OB-1 Fetal ECG database contains 5 hours and 42 minutes of fetal ECG signals and uterine contraction signals. Figure 7.5 shows the data sample of uterine contraction EHG signals. In the next section, we will explain the data preprocessing.

Data Preprocessing

The databases downloaded from the PhysioNet repository [127] are in the WFDB signal files format. To read and convert them into CSV format, we used a tool called **rdsamp** with the following command:

$$rdsamp\ -r\ record\ -c\ -H\ -f\ 0\ -v\ -pe\ > output\_file.csv \tag{7.1}$$

Where:

- **-r** reads the record.
- **-c** produces output in CSV.
- **-H** reads the signal files in high-resolution mode.
- **-f 0** begins at the specified time (0 means at the beginning of the record).
- **-v** prints column headings.
- **-pe** prints the elapsed time from the beginning of the record as hh:mm:ss.

In addition to the 6169 30-minute-long datasets from the three databases described in Section 6.4.2, we extracted an additional 1102 30-minute-long datasets from the two new databases, making 7271 30-minute-long datasets from all five databases. The ratio between the pattern and non-pattern datasets is 60% pattern to 40% non-pattern. The normal and premature labour ratio is 90% for the normal and 10% for the premature. In the next section, we will describe feature selection.

7.4.2 Feature Selection

Feature selection is the process of extracting or selecting a subset of features from data to use in model creation and training. Feature extraction can generate dense and improved information from raw EHG signals [140]. Furthermore, studies extracted EHG features based on the time domain, frequency domain, and time-frequency domain [140]. Table 7.1 summarizes the features used in the ML literature review studies.

The datasets we extracted have uterine contraction EHG raw signals, and we need to extract our features from them. As illustrated in Section 6.3, we need to extract

Proposed systems	1 [30]	2 [48]	3 [49]	4 [50]	5 [18]	6 [51]	7 [52]	8 [55]	9 [57]	10 [56]	11 [53]	12 [54]	13 [58]
Average Amplitude Change Of EMG Signal						✓						✓	
Autocorrelation zero-crossing												✓	
Centroid frequency											✓		
Difference Absolute Standard Deviation Value						✓							
Fourier Transform							✓						
Fractal Dimension				✓									
Fuzzy Entropy				✓									
Hilbert envelope													✓
Integrated EMG						✓							
Interquartile Range				✓									
Log Detector Of EMG Signal						✓							
Maximum Fractal Length Of EMG Signal						✓							
Mean Absolute Deviation				✓									
Mean Absolute Value						✓							
Mean Crossing Rate	✓				✓								
Mean frequency (MNF)												✓	
Mean Energy				✓									
Mean Teager-Kaiser Energy				✓									
Median frequency (MDF)						✓	✓			✓		✓	
Normalized Range	✓				✓								
Peak frequency (PF) Of EMG Signal						✓	✓			✓		✓	
Power Of The EHG Signal	✓				✓								
Root mean square (RMS)	✓				✓	✓	✓	✓		✓		✓	✓
Sample Entropy				✓			✓		✓	✓			
Simple Square Integral						✓							
Squared RMS													✓
Standard Deviation	✓			✓									
Teager energy													✓
Variance of EMG						✓							
Wavelet energy													✓
Wavelet Length of EMG Signal						✓			✓				

Table 7.1: Summary of the ML related work studies' feature selection

the EHG signals' amplitude and frequency to mimic obstetricians who use these two parameters to decide if the pregnant woman is in labour. Figure 7.6 visualizes the feature selection process. First, we will calculate the EHG signal's power spectrum using FFT for each dataset. Next, using the power spectrum, we will extract the following two features:

- Mean frequency (MNF), which represents the centroid frequency of the EHG signal's power spectrum.
- Peak frequency (PF), which represents the largest amplitude peaks of the EHG signal.

7.5 Machine Learning Classifiers

In this section, we will illustrate the chosen classifiers and our selection of hyper-parameters. Note that for all the classifiers, the split data ratio is 70% for training to 30% for testing. The implementation of the classifiers was done on a Windows 10 OS with a 3.60-GHz 8-Core Intel i7-9700KF processor, 128 GB of RAM and NVIDIA Quadro RTX 8000 48-GB GDDR6 memory GPU.

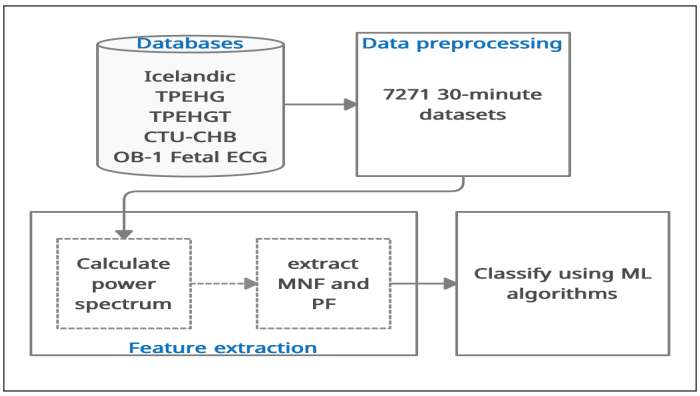

Figure 7.6: Feature selection process for ML

Package	Version	Description
scikit-learn	0.23.2	This is a Python integrated ML library. It includes various classification and regression algorithms such as RF, DT, NB and SVM. It also has various functions that we used for implementation and analysis.
tensorflow	2.6.0	This is an open-source ML library developed by the Google Brain team. It utilizes different programming languages such as Python, C++ and CUDA. Moreover, it can integrate ML algorithms on IoT, Android or iOS smartphones using TensorFlow Lite.

Table 7.2: ML implementation packages description

The coding was done in Python programming language version 3.7.11 using Jupyter Notebook environment version 6.4.3. Table 7.2 lists the packages used during implementation:

7.5.1 Hyper-parameters Search

Hyper-parameters are numeric or boolean values the user can set and configure before the classifier learning process. They help improve the training time, performance and prediction of the classifier. Examples of hyper-parameters are the learning rate, number of epochs or random state. Each hyper-parameter directly affects the classifier learning process, which means we need to make sure we choose the best hyper-parameters according to the data we are using.

To choose the optimum hyper-parameters for the classifiers, we will use a tuning technique called grid search. Grid search is a technique that calculates the optimum hyper-parameters for a given classifier through the exhaustive search of a given hyper-parameter. This technique can save time and resources when training the classifier.

Hyper-parameter	Definition	Values
criterion	The function is used to measure the quality of the split.	"gini" or "entropy'. default="gini"
max_depth	Represents the maximum depth of the tree.	int. default=None
min_samples_split	The minimum number of samples needed to split an internal node	int, float. default=2
min_samples_leaf	The minimum number of samples required to be at a leaf node (i.e. a node that has no children).	int or float. default=1
random_state	Controls the randomness of the estimator.	int, RandomState instance or None. default=None
n_estimators	The number of trees in the random forest.	int. default=100
kernel	The kernel to be used in the algorithm.	"linear", "poly", "rbf", "sigmoid" or "precomputed". default="rbf"
C	The regularization parameter.	float. default=1.0
gamma	The kernel coefficient for 'rbf', 'poly'and 'sigmoid'.	"scale", "auto" or float. default="scale"
probability	To enable or disable the probability estimates.	bool. default=False

Table 7.3: Hyper-parameters definitions

Table 7.3 defines the hyper-parameter used in the classifiers (more details on the use of these hyper-parameters will be provided in the following sections). Next, we will present ML classifiers and their optimized hyper-parameters.

7.5.2 Decision Trees

DT is a commonly used classifier tree that starts at the root, then each node represents an attribute test, and sorting down occurs until reaching a leaf node, which will provide a classification [141].

Selection of Hyper-parameters

The following key parameters were used for the DT classifier:

```
criterion = 'entropy', max_depth = 8, min_samples_split = 5,
min_samples_leaf=10 random_state = 0
```

The maximum depth for the tree was 8.

Moreover, we chose entropy for splitting as it performed better than gini in our experiment. Lastly, the minimum samples split is five, and the minimum samples leaf is ten according to the grid search we performed.

7.5.3 Random Forest

RF was proposed by Breiman in 2001 [142]. It is an ensemble DT using the bagging method. The goal of the bagging method is to increase the accuracy of the algorithm

by combining many classifiers. RF has advantages over DT by reducing data overfitting and increasing precision. It also does not require many configurations to produce accurate predictions. In addition, more trees mean more accurate results from the RF algorithm [142] [143].

Selection of Hyper-parameters

The following key parameters were used for the RF classifier:

```
n_estimators = 100, criterion = 'entropy', max_depth = 10,
min_samples_leaf = 1, min_samples_split = 15, random_state = 2
```

The algorithm performs the best with a maximum depth of 10 as recommended by the grid search. Moreover, the minimum samples split is 15, and the minimum samples leaf is 1. Lastly, the grid search recommended the number of trees to be 100, which is also the default value of the n_estimators hyper-parameter.

7.5.4 Support Vector Machine

The SVM classifier was introduced in 1995 [144]. It became popular due to its classification accuracy, robustness and indifference towards the input data type [145]. It is based on Vapnik statistical learning theory and can be applied to many classification and regression problems [146] [147].

SVM works by separating data into classes using support vectors and hyperplane. An SVM model can be linear (where the hyperplane is a straight line) and non-linear (where a straight line can not separate data). For the non-linear SVM, we use kernels to separate data. Kernels transform data into another dimension to be classified.

Selection of Hyper-parameters

The following key parameters were used for the SVM classifier:

```
C = 1000000, kernel = 'rbf', gamma = 1000, random_state = 0,
probability=True
```

Radial Basis Function (RBF) kernel is the best choice for our non-linear data.

Moreover, grid search confirmed that RBF is the best kernel for our model. When using RBF as the kernel, C and gamma are the two most important hyper-parameters to be considered. Both hyper-parameters have been tuned using grid search. Lastly, according to the sklearn's SVM documentation, the probability hyper-parameter should be enabled prior to calling the fit function when building and training the model.

7.5.5 Naïve Bayes

NB is one of the most widely used classifiers for many applications with a fast learning and testing process [148]. It is designed based on the Bayesian rule and probability theorems [148] [149]. The Bayes theorem assumes that the features are independent of each other. This assumption reduces the number of features and makes classification easier and more efficient.

Naïve Bayes has several variants such Gaussian Naive Bayes, Multinomial Naive Bayes or Complement Naive Bayes. The Gaussian Naive Bayes classifier, which we chose for classification, is used when the features have continuous values. It assumes that all the features follow a Gaussian distribution (also called normal distribution).

Selection of Hyper-parameters

We used the Gaussian NB classifier with the default hyper-parameters.

7.6 Convert and Deploy the MB Algorithm to the Smartphone

Android-based smartphones can run pre-trained ML algorithms. However, we need to convert the format of the ML algorithm into a compressed flat buffer using TensorFlow Lite converter with Python.

TensorFlow Lite is an open-source framework developed by Google to convert pre-trained ML models and deploy them into IoT devices and smartphones' OS such as Android and iOS.

There are three steps to convert the ML algorithm to the TensorFlow Lite format with the .tflite extension.

1. Save the pre-trained ML algorithm to produce the file my_model.sav.
2. Convert the file to TensorFlow Lite using the following Python commands:

```
converter =tf.lite.TFLiteConverter.from_saved_model('my_model')

tflite_model = converter.convert()
```

3. Save the converted model using the following Python command:

```
open("converted_model.tflite", "wb").write(tflite_model)
```

To deploy the converted_model.tflit file to the smartphone, we implement the following steps:

1. Implement the TensorFlow Lite library into the Android application's build gradel.
2. Add the converted_model.tflit file to the application's assets folder.
3. In the application's MainActivity Java file, we import the TensorFlow Interpreter to load the converted_model.tflit file into the Java environment.
4. We can now pass the values of the features to the loaded model and get the prediction after the 30-minute monitoring session.
5. The application will either trigger a warning or start a new monitoring session based on the prediction value.

7.7 Evaluation Methodology

To meet the research goals listed in Chapter 4, we need to evaluate the proposed scheme in terms of two aspects:

- Scheme algorithms' reliability and accuracy in detecting labour.
- Smartphone resources performance.

7.7.1 Reliability and Accuracy Analysis

We will be using the same evaluation methodology from the previous scheme illustrated in Section 6.5, namely the confusion matrix, AC, MisCl, R, P, F, FNR and FPR.

In addition to these evaluation criteria, we will be using the following two criteria:

- Receiver operating characteristic (ROC) is a performance evaluation measurement for binary classification algorithms. It is represented in a graphic plot between the true positive rate (TPR) and the false positive rate (FPR) within different thresholds.
- The area under the ROC curve (AUC) is a statistical value between 0 and 1 that measures the performance of a classifier. The classifier's probability ranking of a randomly chosen positive instance is higher than a randomly chosen negative instance [150]. A higher AUC value means better performance for the classifier. AUC is given by the following Equation 7.2; where TP stands for TP, FP stands for FP, P stands for positive, and N stands for negative:

$$AUC = \int_0^1 \frac{TP}{P} d\left(\frac{FP}{N}\right) \tag{7.2}$$

7.7.2 Smartphone Resources Performance

Chapter 4 previously illustrated that the proposed scheme should be cheap and reliable. Therefore, the proposed scheme should efficiently consume the limited smartphone resources.

We will be using the Android Profiler tool from the Android Studio integrated development environment (IDE) for the CPU and memory performance. For the battery power consumption, we will be using the Battery Historian tool. Next, we will illustrate each tool in detail. The Android Profiler and Battery Historian will be used separately. We used two identical Android tablets for the performance analysis to speed up the process: one tablet for the Android Profiler and the other for the Battery Historian tool. Figure 7.7 demonstrates the smartphone resources performance

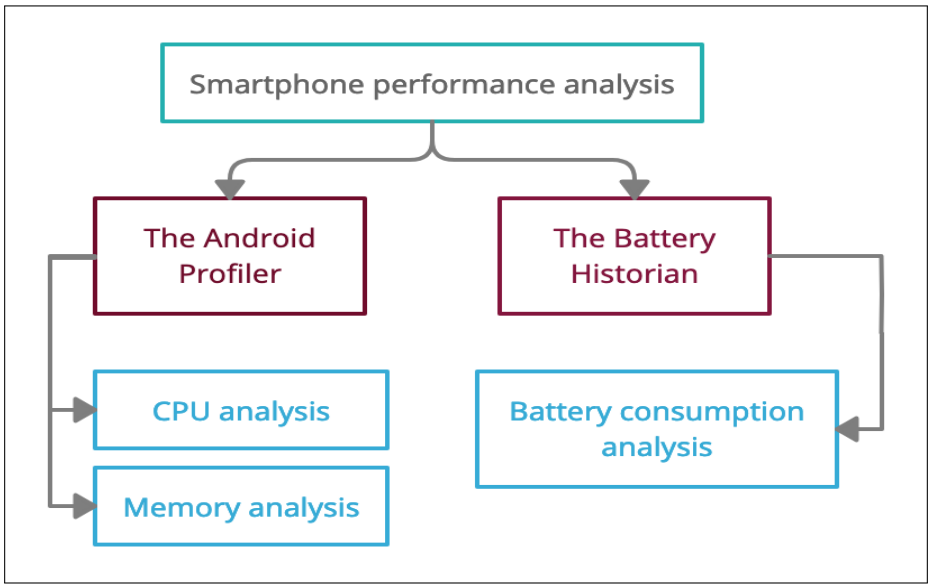

Figure 7.7: ML Algorithms development cycle

analysis.

The Android Profiler

The Android Profiler tool provides real-time data on the application usage of CPU, memory, network, and battery resources. It provides a visual representation of the application's performance. We will be using the CPU and memory resource usage from the Android Profiler tool in resources performance. We do not need to use the network analysis feature since we are not sending any data to the Internet. We cannot use the Android Profiler tool for the battery consumption analysis since it only supports Android version 8.0 and above, and our application's Android version is 5.0. In the next section, we will illustrate the Battery Historian tool.

To monitor the application CPU and memory usage, we first need to connect the device to the computer. Next, we will upload the application to the device and run the application. Once the application is running in ideal mode (i.e. we have not started the monitoring session yet), we will run the Android Profiler tool by clicking on View > Tool Windows > Profiler. We can then locate and choose the application for analysis and start the 30-minute monitoring session. The Android Profiler will

provide real-time analysis of the application's CPU usage percentage and allocated memory. Notice that the device should be connected to the computer throughout the monitoring session.

Battery Power Consumption

The Battery Historian tool can analyze the battery power consumption for Android device resources. It provides the battery consumption status as a percentage of the total battery capacity and the quantity of mAhs consumed during the application's running time.

To analyze battery consumption, we need to set up the smartphone with the following steps:

1. Connect the smartphone to the computer.
2. Type the following commands in the Android Studio terminal to reset the Battery Historian files: `adb kill-server`, `adb devices` and `adb shell dumpsys batterystats -reset`
3. Disconnect the smartphone from the computer and start the monitoring session.
4. Once the monitoring session is done, connect the smartphone to the computer and type the following commands in the terminal to dump the bugreport analysis files: `adb shell dumpsys batterystats > dir` and `adb bugreport > dir`
5. Start a localhost service such as docker and type the following terminal command: `docker run -p 9999:9999 gcr.io/android-battery-historian/stable:3.0 -port 9999`.
6. Use the browser to go to http://localhost:9999/
7. Upload the bugreport file and review the battery usage analysis report.

In the next section, we will present the results of the classifiers evaluation and the smartphone resource consumption.

	Classified pattern	**Classified no pattern**
Pattern	785	49
No pattern	52	1296

Table 7.4: DT classifier confusion matrix

Criteria	Result
AC	0.953
MisCl	0.046
R	0.941
P	0.937
F	0.939
FNR	0.058
FPR	0.038
AUC	0.98

Table 7.5: Reliability and accuracy evaluation results for the DT classifier

7.8 Results

In this section, we will present and compare the results of the classifiers' performance evaluation. Moreover, we will present smartphone resource consumption during the beginning, middle, and end of the monitoring session. The monitoring session length was 30 minutes, during which Bluetooth communication was sending EHG signals from one tablet to the other. The screen was off throughout the monitoring session.

7.8.1 Reliability and Accuracy Analysis

In this section, we will list the evaluation criteria listed in Section 7.7.1 for each classifier individually.

Decision Tree

Table 7.4 represents the DT classifier's confusion matrix, and Table 7.5 shows the reliability and accuracy of the evaluation results. Figure 7.8 shows the AUROC plot for the DT classifier.

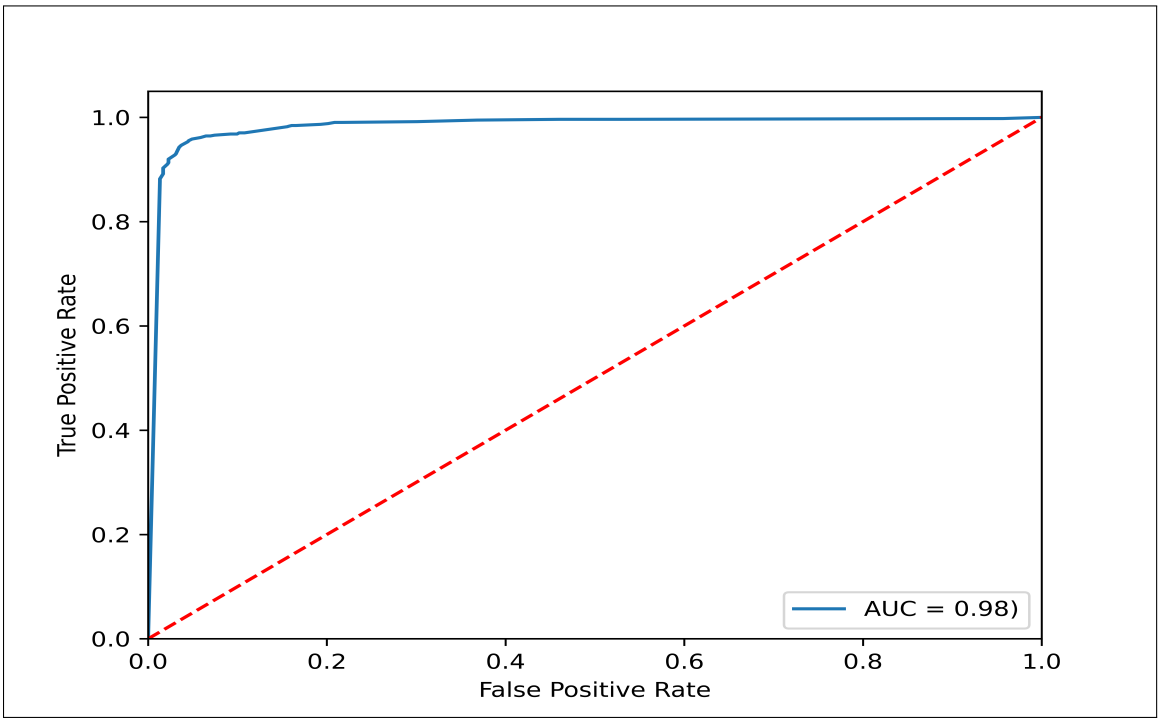

Figure 7.8: DT AUROC plot

	Classified pattern	Classified no pattern
Pattern	814	31
No pattern	62	1275

Table 7.6: RF classifier confusion matrix

Random Forest

Table 7.6 represents the RF classifier's confusion matrix, and Table 7.7 shows the reliability and accuracy evaluation results. Figure 7.9 shows the AUROC plot for the RF classifier.

Support Vector Machine

Table 7.8 represents the SVM classifier's confusion matrix, and Table 7.9 shows the reliability and accuracy analysis evaluation results. Figure 7.10 shows the AUROC plot for the SVM classifier.

Criteria	Result
AC	0.957
MisCl	0.042
R	0.963
P	0.929
F	0.945
FNR	0.036
FPR	0.046
AUC	0.99

Table 7.7: Reliability and accuracy analysis results for the RF classifier

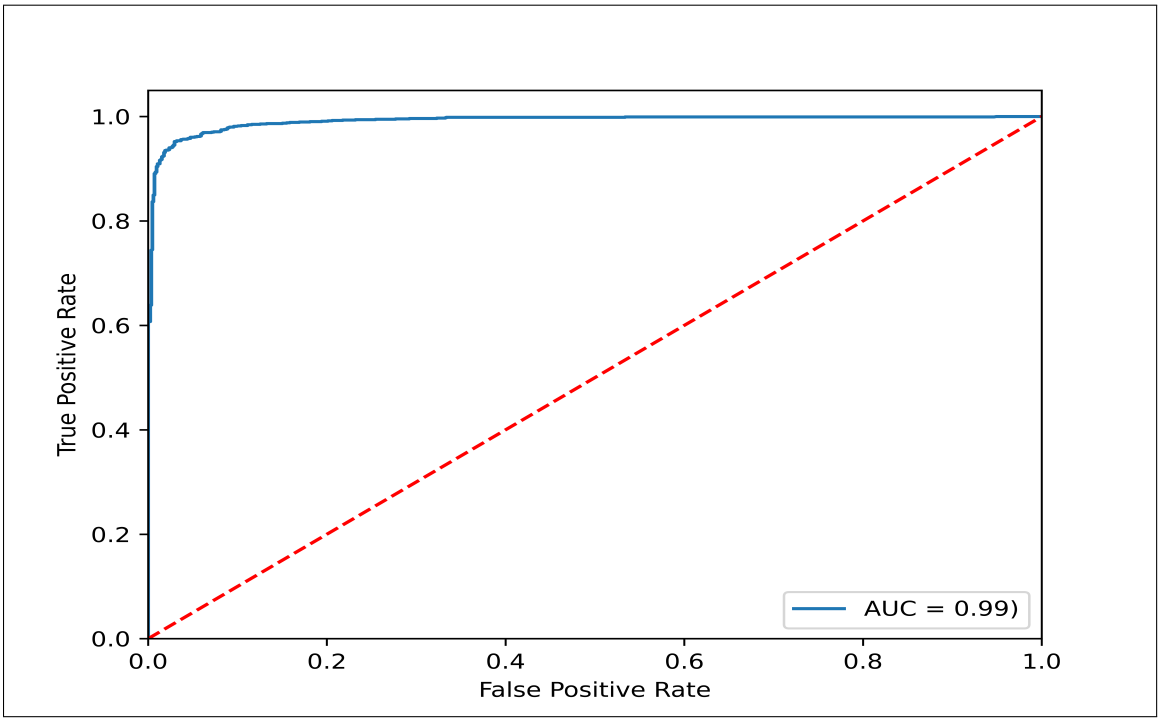

Figure 7.9: RF AUROC plot

	Classified pattern	**Classified no pattern**
Pattern	806	28
No pattern	102	1246

Table 7.8: SVM classifier confusion matrix

Criteria	Result
AC	0.940
MisCl	0.059
R	0.966
P	0.887
F	0.925
FNR	0.033
FPR	0.075
AUC	0.98

Table 7.9: Reliability and accuracy analysis evaluation results for the SVM classifier

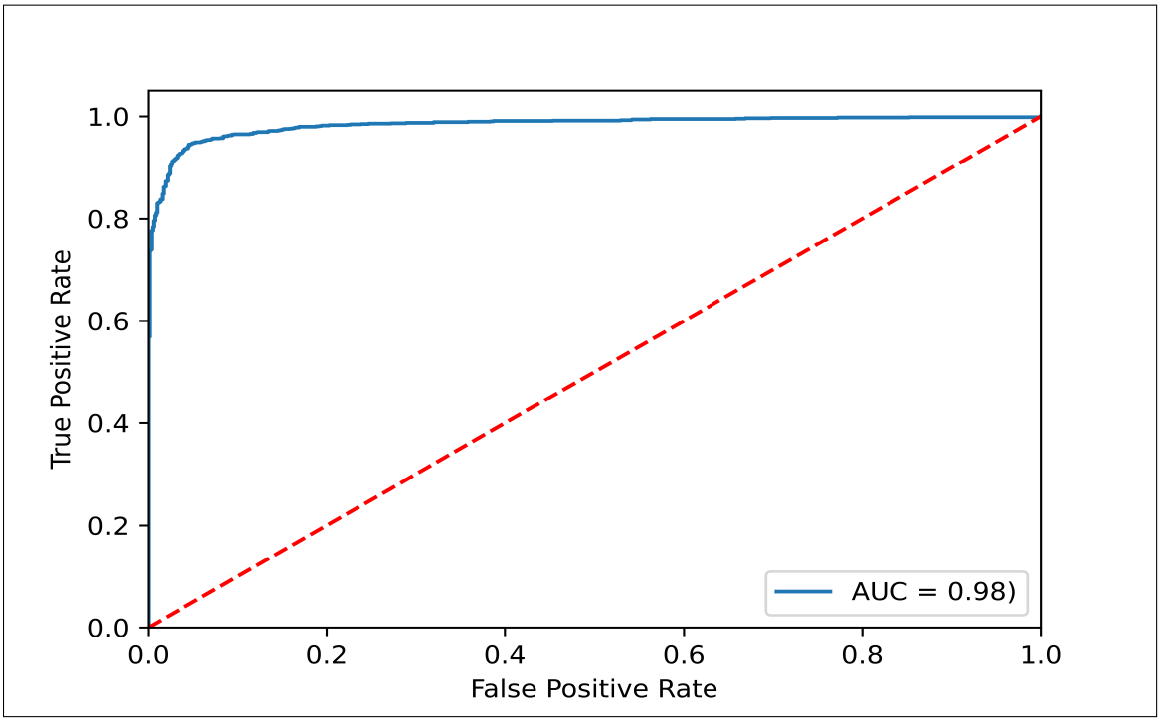

Figure 7.10: SVM AUROC plot

	Classified pattern	**Classified no pattern**
Pattern	811	23
No pattern	192	1156

Table 7.10: NB classifier confusion matrix

Criteria	Result
AC	0.901
MisCl	0.098
R	0.972
P	0.808
F	0.882
FNR	0.027
FPR	0.142
AUC	0.97

Table 7.11: Reliability and accuracy analysis evaluation results for the NB classifier

Naïve Bayes

Table 7.10 represents the NB classifier's confusion matrix, and Table 7.11 shows the reliability and accuracy analysis evaluation results. Figure 7.11 shows the AUROC plot for the NB classifier.

Table 7.12 summarizes all the criteria in terms of percentage and actual count from the confusion matrix tables. Moreover, Figure 7.12 shows the AUC and AUROC plot for all the classifiers.

7.8.2 Smartphone's Resources Performance

The following smartphone resources performance results apply to all the classifiers since there are no significant differences in performance between these classifiers. The testing was performed using twenty chosen datasets that represent all five databases.

Classifier	**AC**	**MisCl**	**R**	**P**	**F**	**FPR**	**FPR Count**	**FNR**	**FNR Count**
DT	0.953	0.046	0.941	0.937	0.939	0.038	52	0.058	49
RF	0.957	0.042	0.963	0.929	0.945	0.046	62	0.036	31
SVM	0.940	0.059	0.966	0.887	0.925	0.075	102	0.033	28
NB	0.901	0.098	0.972	0.808	0.882	0.142	192	0.027	23

Table 7.12: Machine learning classifiers comparison

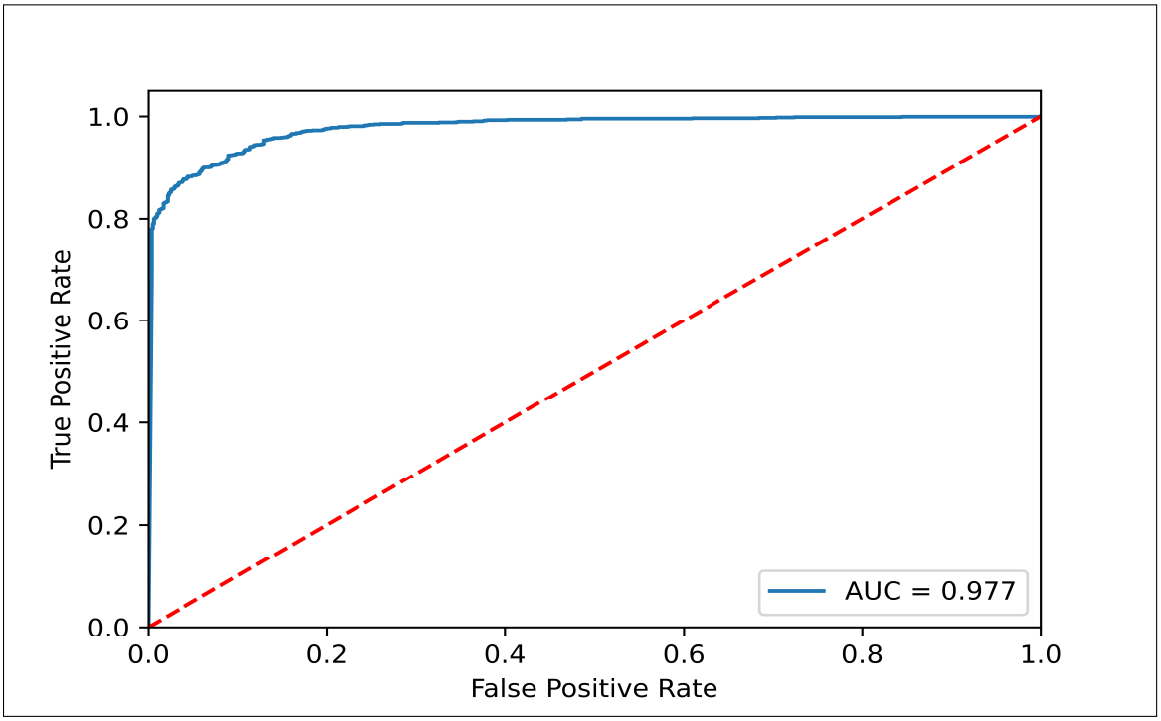

Figure 7.11: NB AUROC plot

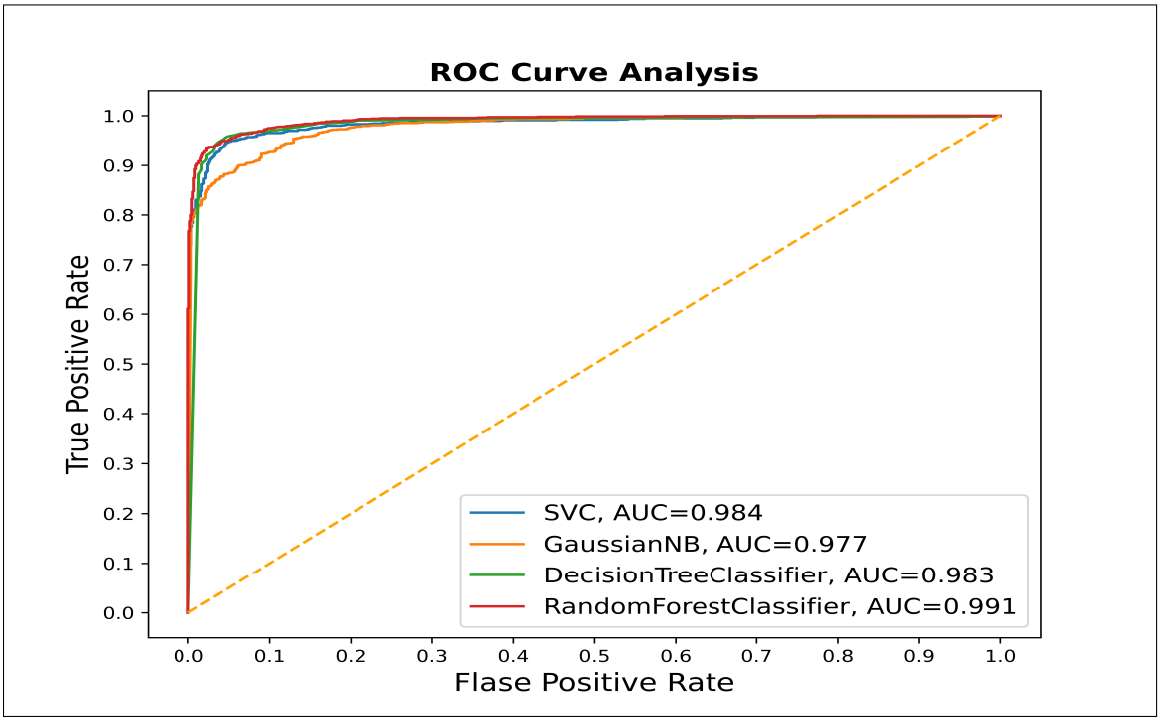

Figure 7.12: All classifiers AUROC plot

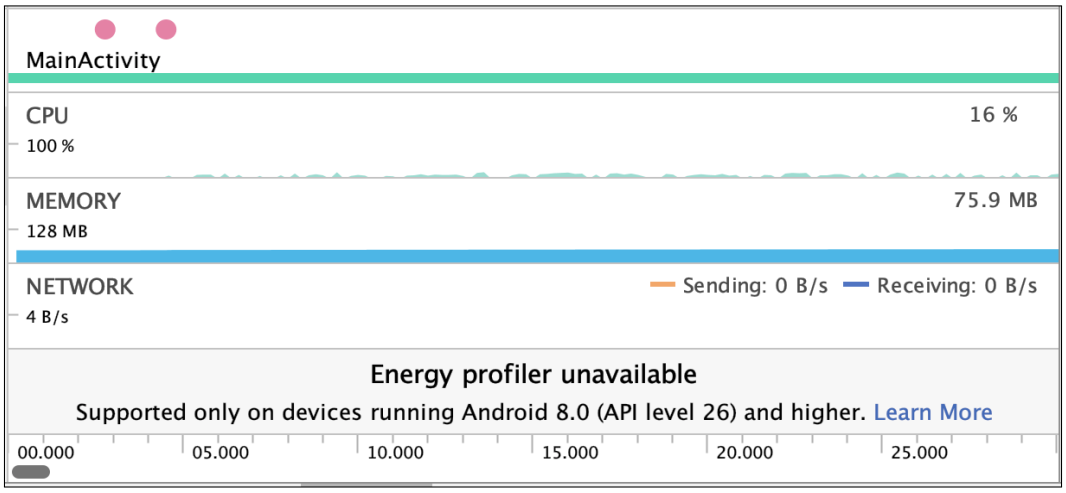

Figure 7.13: Beginning of the application's running time - machine learning algorithms

Ten of these datasets ended up with an alarm, and ten ended up with no alarm.

CPU and Memory Performance

At the start and the middle of the application's running time, the performance was similar whether the alarm was triggered or not.

Figure 7.13 shows that the application at the beginning uses 16% of the CPU power and allocates 75.9 MB out of 1.80 GB of the device's memory.

The application at the middle uses 16% of the CPU and allocates 75.9 MB out of 1.80 GB of the device's memory, as shown in Figure 7.14. The following section will present the application's performance with the alarm triggered at the end of the monitoring session.

With Alarm

Figure 7.15 shows that the application at the end uses 0% of the CPU (the application has ended) with the alarm triggered, as is shown at the top of the figure. Furthermore, the smartphone memory usage was reduced to 49.6 MB out of 1.80 GB after the application monitoring session.

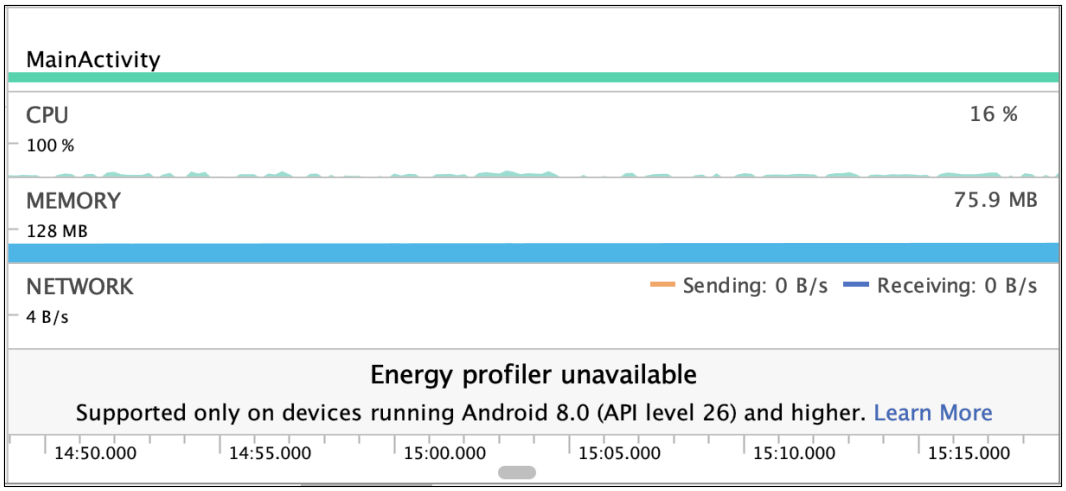

Figure 7.14: Middle of the application's running time - machine learning algorithms

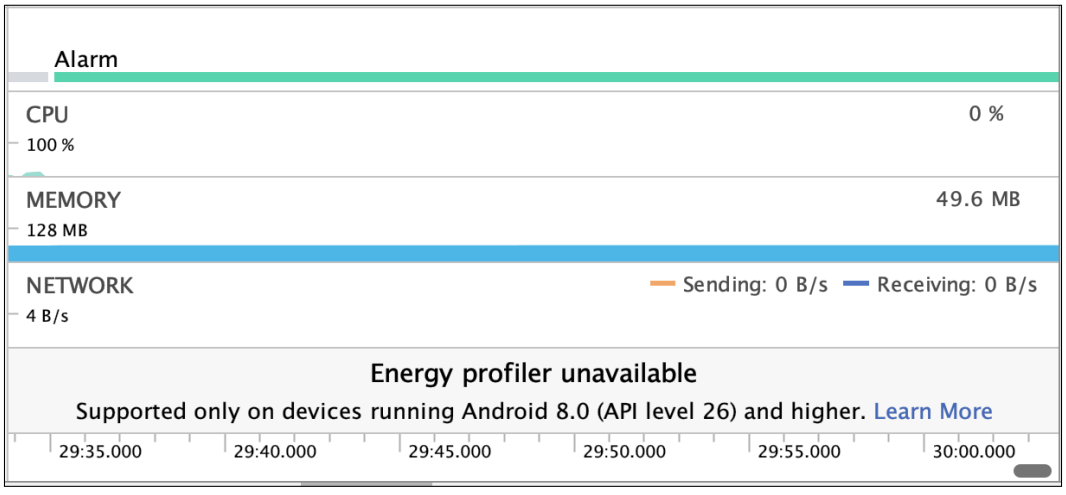

Figure 7.15: End of the application's running time - with alarm - machine learning algorithm

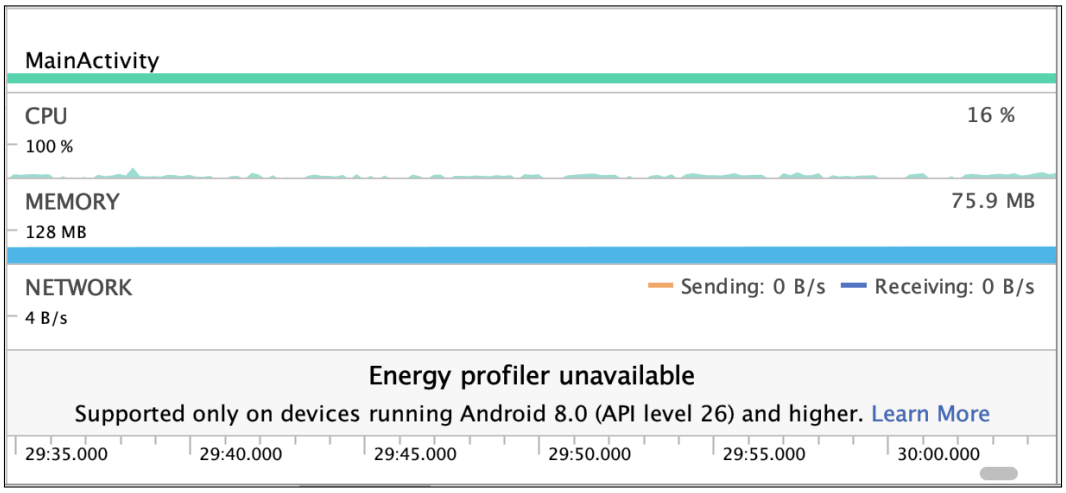

Figure 7.16: Beginning of the application's running time - with no alarm - machine learning algorithm

With no Alarm

Figure 7.16 shows that the application at the end continues using 16% of the CPU (the application did not end the monitoring session) with the alarm not triggered, as is shown at the top of the figure. Furthermore, the application allocates 75.9 MB out of 1.80 GB of the device's memory.

Battery Power Consumption

The smartphone has a battery capacity of 3448 mAh. On average, the application consumed 0.54% or 18.6 mAh of battery capacity. In the next section, we will discuss the results.

7.9 Discussion

In this section, we will discuss the scheme's results and how the scheme met the objectives set out in Section 4.2. We will compare the machine learning algorithms' results with the studies in the literature review and the results from the previously proposed scheme [130] detailed in Chapter 6. We will also discuss our choice of machine learning classifiers. In addition, we will discuss the smartphone resources performance results.

7.9.1 Reliability and Accuracy Analysis

In the proposal report, we chose the SVM classifier based on the literature review. In addition to the SVM classifier, we included the DT, RF and NB classifiers due to their excellent classification accuracy in general.

Based on the proposal report, we anticipated that the SVM would perform the best. To compare the four classifiers and determine which is the best, we need to compare the top significant rates for our proposed framework: higher AC, lower FPR and lower FNR. For example, a classifier could be better in AC; however, the FNR is higher than the classifier. In this case, the decision will be based on the user's preferences and whether they need higher accuracy in general or prefer to reduce the chance of the application not giving a warning while the pregnant woman is already in labour.

The RF performed the best in terms of the AC rate, the FPR rate and the FPR count among the four machine learning classifiers. In terms of FNR rate and FNR count, the NB classifier performed the best. Although NB has the lowest FNR and FNR count (i.e. there is a labour pattern, but no warning is given), RF is the best choice for our framework because it has higher AC and lower FPR. Moreover, the FNR difference between RF and NB is insignificant, making the RF our best choice of the four classifiers.

Furthermore, the RF classifier performed better in terms of the MisCl rate with 0.042, P rate with 0.929, F rate with 0.945 and AUC rate with 0.99. However, it came second after NB for the R rate with 0.963. The chart in Figure 7.17 visualizes the evaluation results.

Scheme Comparison with the Literature Review Studies

In this section, we will compare our chosen RF classifier to the studies from the literature review. The comparison will be on the criteria listed in Section 7.7.1. Table 7.13 shows the results of the RF classifier and the studies from the literature review.

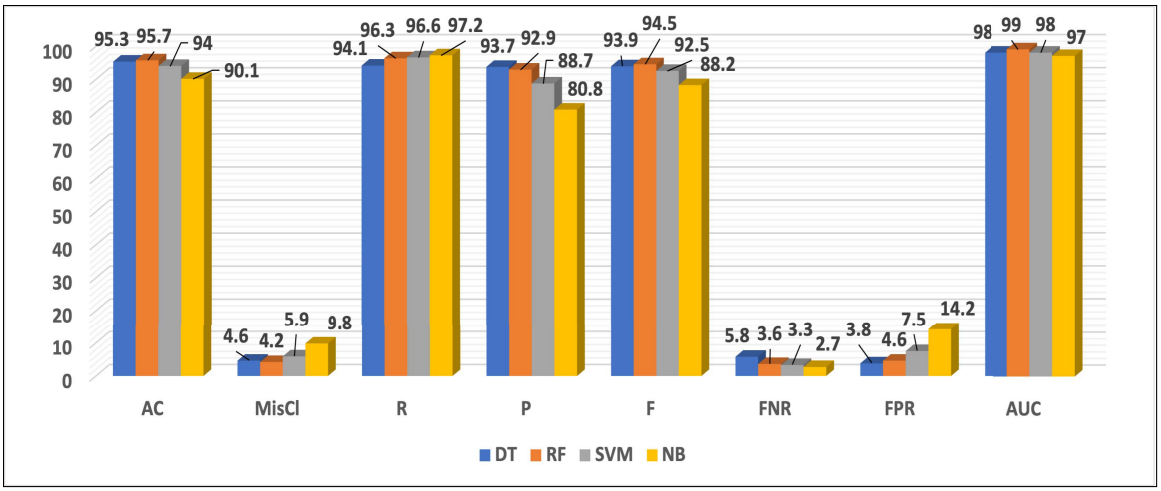

Figure 7.17: Machine learning classifiers results in comparison (in %)

Proposed systems	AC	MisCl	R	P	F	FNR	FPR	AUC
Proposed RF classifier	0.95	0.04	0.96	0.93	0.94	0.03	0.04	0.99
Idowu et al. [30]	x	x	0.97	x	x	x	x	0.94
Fergus et al.[48]	0.90	x	0.85	x	x	x	x	0.90
Acharya et al. [49]	0.96	x	0.95	x	x	x	x	x
Altini et al. [50]	0.87	x	x	x	x	x	x	x
Borowska et al. [18]	0.83	x	x	x	x	x	x	x
Altini et al. [51]	x	x	x	x	x	x	x	x
Hoseinzadeh and Amirani [52]	0.97	x	0.95	x	x	x	x	x
Degbedzui and Yüksel [53]	0.99	x	0.99	x	0.99	x	x	x
Peng et al. [54]	0.93	x	0.89	x	x	x	x	0.80
Shahbakhti et al. [55]	0.99	x	0.98	x	x	x	x	x
Sheryl Oliver et al. [56]	0.96	x	0.92	x	x	x	x	x
Chen et al. [57]	0.90	x	0.92	x	x	x	x	x
Esgalhado et al. [58]	0.97	x	x	x	x	x	x	x

Table 7.13: Comparative analysis of the proposed work with published state-of-the-art techniques

Table 7.13 shows that the studies did not provide some criteria, making their work more difficult to evaluate since we can not measure all the classifiers' performance results. For example, none of the studies reported MisCl, P, FNR or FPR rates. In this case, we can not compare our proposed work to the literature review studies regarding labour EHG signals being categorized by the classifier as non-labour, for example, since there is no FNR reported.

In terms of AC rate, six studies are better than our proposed scheme. However, when we perform a deeper analysis of the studies' design and implementation, we can see some advantages of our scheme over these studies. For instance, none of the studies used as many databases as we have used in our proposed scheme. Some of the studies used only one database. This could lead to a bias in the results due to the lack of diversity in the databases. The same concept applies to the R rate. The ratio is 60% pattern datasets to 40% non-pattern datasets in our datasets collection, implying no bias towards any dataset group. Finally, our proposed scheme achieved the highest AUC among the literature review studies.

7.9.2 Smartphone's Resources Performance

CPU

Throughout the monitoring session, the application used 16% of the CPU on average. Compared with 2% from the previous scheme in Chapter 6, this increase in CPU usage is due to the use of Bluetooth to simulate the sending of EHG signals from a WBS. However, the 16% usage is still considered low on average, especially when we notice from Figure 7.13, for example, that the CPU usage bar was consistently low throughout the monitoring session.

Memory Performance

The application memory usage increased from 60 to 75.9 MB compared to the previous scheme in Chapter 6. The increase in memory usage was only 15.9 MB or 4.2% of the smartphone memory capacity of 1.80 GB, which is still considered low and efficient.

Battery Power Consumption

The application efficiently consumed 0.54% or 18.6 mAh of the battery capacity on average. This is slightly lower than what the previous scheme in Chapter 6 consumed, which is 0.84%. The improvement was not significant; however, the application met the objective listed in Section 4.2 to use the smartphone's resources efficiently.

7.10 Chapter Summary

In this chapter, we presented the machine learning algorithm scheme in detail. We illustrated the scheme implementation and our choice of feature selection and machine learning classifiers. We presented and discussed the evaluation results and concluded that the RF classifier performed the best. Furthermore, we compared our results with the literature review studies. Moreover, the application efficiently consumed the smartphone's CPU, memory performance, and battery power consumption. In the next chapter, we will present the deep learning algorithm scheme.

Chapter 8

Deep Learning Algorithm Scheme

8.1 Introduction

Deep learning is a subfield of machine learning under the umbrella of artificial intelligence. Deep learning models learn from complex relationships or high-level features [138]. One example of a commonly used deep learning model is artificial neural network (ANN). ANN is a data processing archetype that mimics the biological nervous system of the human brain [151].

The ANN model consists of multiple layers: an input layer, several hidden layers and output layers [151] [152]. Each layer is comprised of neurons (also called nodes) that form parallel-connected neural networks to achieve superior computation speed and power [151]. A layer also has activation functions that are critical in designing the neural network. It is used to decide the neuron's output to the next layer depending on the activation function type. Two commonly used activation functions are:

- Rectified Linear Activation (ReLU): It makes the network training fast due to its simple and easy computation. If the input x is less than 0, then set the input to 0; otherwise, set the input to x. ReLU is given by the following equation:

$$relu(x) = max(0, x) \tag{8.1}$$

- Logistic (Sigmoid): It is best used for prediction since it produces a value between 0 and 1. Sigmoid is given by the following equation:

$$S(X) = \frac{1}{1 + e^{-x}} \tag{8.2}$$

When compiling the model, we use some parameters such as optimizers, loss functions and learning rate. Optimizers are methods used to minimize the losses by changing the attributes of the neural network. Commonly used optimizers are Adam, RMSprop and Stochastic Gradient Descent (SGD).

Loss functions are methods used to predict errors in the neural net and update their weights. Examples of loss functions are Mean Squared Error (MSE), Binary Cross-entropy (BCE) and Categorical Cross-entropy (CC). Learning rate refers to how much to update the neurons' weights when training the model, which ranges from 0.0 to 1.0. A lower learning rate means more training time. Finally, ANN has two phases: forward pass and backtrack. During the forward pass, the neural network outputs from the input layer to the ouput layer using activation functions. During the backtrack phase, we fine-tune the weights of the neural network using optimizers, loss functions and learning rates. One forward pass and backtrack is called an iteration, during which one batch of data is passed through.

8.2 Proposed Scheme

Like the previous machine learning scheme, the deep learning scheme aims to detect and predict premature labour. The difference between deep learning and machine learning is that deep learning is a more powerful and advanced technique. It utilizes big data to extract and form complex relationships between features to understand data better [153]. DL does not need feature engineering. We can feed the neural network with all the features, and it will identify the best features to use in classification.

We chose the ANN model for the DL scheme's implementation.

By utilizing the power of deep learning, we aim to personalize the scheme to fit pregnant women's different needs and characteristics. For example, a pregnant woman could have diabetes, be a smoker, have hypertension or have had a premature birth. In this case, deep learning could be fed with personal features, alongside the EHG signal features such as amplitude, to predict if the pregnant woman is at risk for premature labour.

Finally, to the best of our knowledge, only one study used EHG signals to identify uterine contractions using CNN. The issue with this study is that it can not be applied to a continuous monitoring scenario. More details can be found in Section 3.2.2. Our deep learning scheme contributes to the thesis by using ANN and EHG to predict premature labour. It also contributes by personalizing the scheme to the different health conditions of the pregnant woman. In the next section, we will present the scheme user interface.

8.3 Scheme User Interface

We will be using the same UI from the previous machine learning scheme in Section 7.3. In the next section, we will present the scheme's experimental framework.

8.4 Experimental Framework

In this section, we will illustrate the chosen DL model, feature selection and data selection. Note that the split data ratio is 70% for training to 30% for testing. The DL model development cycle is similar to the ML development cycle shown in Figure 7.3, with some differences illustrated in each section.

The implementation was done on a Windows 10 OS with a 3.60-GHz 8-Core Intel i7-9700KF processor, 128 GB of RAM and NVIDIA Quadro RTX 8000 48-GB GDDR6 memory GPU. The coding was done in Python programming language version 3.7.11 using Jupyter Notebook environment version 6.4.3. Table 8.1 lists the packages used during implementation:

8.4.1 Data Selection and Preprocessing

Data Selection

Similar to the previous scheme, we will use the five databases described in Section 6.4.1, which are:

- Icelandic 16-electrode Electrohysterogram Database [128].

Package	Version	Description
scikit-learn	0.23.2	This is a Python integrated ML library. It includes a wide variety of DL models such as ANN. It also has various functions that we used for implementation and analysis.
tensorflow	2.6.0	This is an open-source ML library developed by the Google Brain team. It utilizes different programming languages such as Python, C++ and CUDA. Moreover, it is capable of integrating ML algorithm on IoT, Android or iOS smartphones using a tool called TensorFlow Lite.

Table 8.1: ML implementation packages description

- Term-Preterm EHG Database [126].
- Term-Preterm EHG DataSet with Tocogram [131].
- CTU-CHB Intrapartum Cardiotocography Database [139].
- OB-1 Fetal ECG Database [127].

Data Preprocessing

We will use the same datasets previously extracted from the five databases for a total of 7271 30-minute-long EHG datasets detailed in Section 7.4.1. In the next section, we will list the selected features for the ANN algorithm.

8.4.2 Feature Selection

We will be using the two features from the previous scheme: MNF and PF with the addition of median frequency (MDF). Furthermore, to personalize the features for each pregnant woman, we need to add medical information regarding the pregnant woman's health, such as if she smokes or if she is diabetic. However, such information is not collected by all the five databases we use. Hence, we need to select common features between the five databases. Each database has a description record of the pregnant women, such as their gestational age, weight, or maternal risk factors. However, not all databases have the same record information. For example, one database has collected information about pregnant women's diabetes status, while other databases lack such information. Figure 8.1 visualizes the feature selection

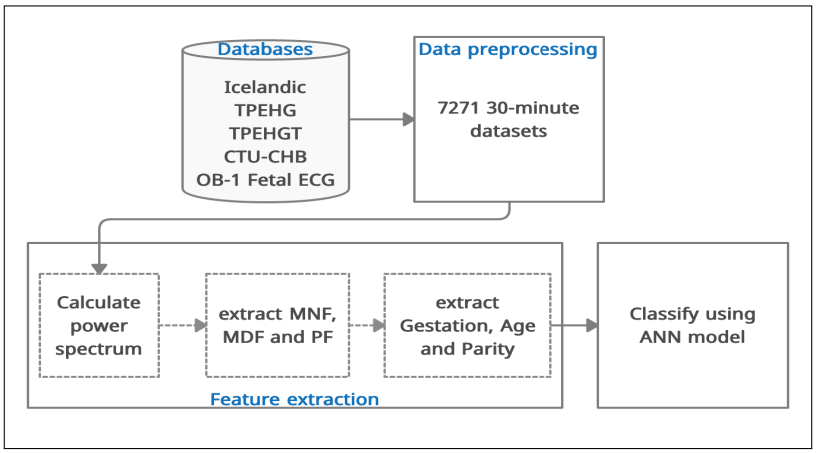

Figure 8.1: Feature selection process for DL

process.

We will only select features collected among all five databases to avoid any bias towards these features in the ANN model. In total, we will have six selected features as follows:

- **PF**.
- **MNF**.
- **MDF**.
- **Pregnancy gestational age**.
- **Pregnant woman's age**.
- **Parity**, which is the number of times a woman has given birth with a gestational age of 24 weeks or more and whether the child was born alive or was stillborn.

8.5 Hyper-parameter Searching and Setting

To choose the optimum hyper-parameters for the ANN model, we will use the Grid Search tuning technique similar to the previous Section 7.5.1. We will search for the best number of layers, neurons, activation functions, optimizers and loss functions.

The search range was as follows:

- The number of layers: 2, 3, 4 and 5.
- neurons: 16, 32, 64, 128 and 256.

- Activation functions: ReLU and sigmoid.
- Optimizers: SGD, RMSprop and Adam.
- Loss functions: Binary cross-entropy and Mean Squared Error.
- Learning rate: 1e-2, 1e-3 and 1e-4.

In the experiments, the network has shown excellent accuracy and precision results based on the following parameters:

- Four hidden layers.
- The number of nodes: 128.
- The activation functions: ReLU for the hidden layers and sigmoid for the output layer.
- Adam for the optimizer.
- The binary cross-entropy for the loss functions.
- Batch size of 20 with 50 epochs.
- Learning rate of 1e-3.

ReLU is expected to perform the best for the hidden layers as it is one of the most common and effective activation functions, as we explained in Section 8.1. Moreover, the sigmoid activation function is used for binary classification. Therefore, it performed the best for the output layer. Finally, the binary cross-entropy loss function is the best for binary classification.

8.6 Evaluation Methodology

Similar to the machine learning scheme, the deep learning scheme needs to meet the research goals listed in Chapter 4 by the evaluation of the proposed scheme for two aspects:

	Classified pattern	Classified no pattern
Pattern	839	9
No pattern	24	1306

Table 8.2: ANN confusion matrix

- Scheme algorithms' reliability and accuracy in detecting labour.
- Smartphone resources performance.

8.6.1 Reliability and Accuracy Analysis

We will be using the same evaluation methodology from the previous two schemes illustrated in Section 6.5 and Section 7.7, namely the confusion matrix, AC, MisCl, R, P, F, FNR, FPR, receiver operating characteristic (ROC) and AUC.

8.6.2 Smartphone Resources Performance

We will be using the same performance criteria illustrated in the previous machine learning scheme in Section 6.5.2. In the next section, we will present the results.

8.7 Results

In this section, we will present the evaluation results of the ANN model. Moreover, we will present the smartphone resource consumption during the monitoring session. The monitoring session length was 30 minutes, during which Bluetooth communication was sending EHG signals from one tablet to the other. The screen was off throughout the monitoring session.

8.7.1 Reliability and Accuracy Analysis

This section will list the results of the confusion matrix and derived equations explained in Section 8.6.1. Table 8.2 represents the ANN model's confusion matrix, and Table 8.3 shows the reliability and accuracy analysis results. Figure 8.2 shows the AUROC plot for the ANN model.

Criteria	Result
AC	0.984
MisCl	0.015
R	0.989
P	0.972
F	0.98
FNR	0.01
FPR	0.018
AUC	0.99

Table 8.3: Reliability and accuracy analysis evaluation results for the ANN model

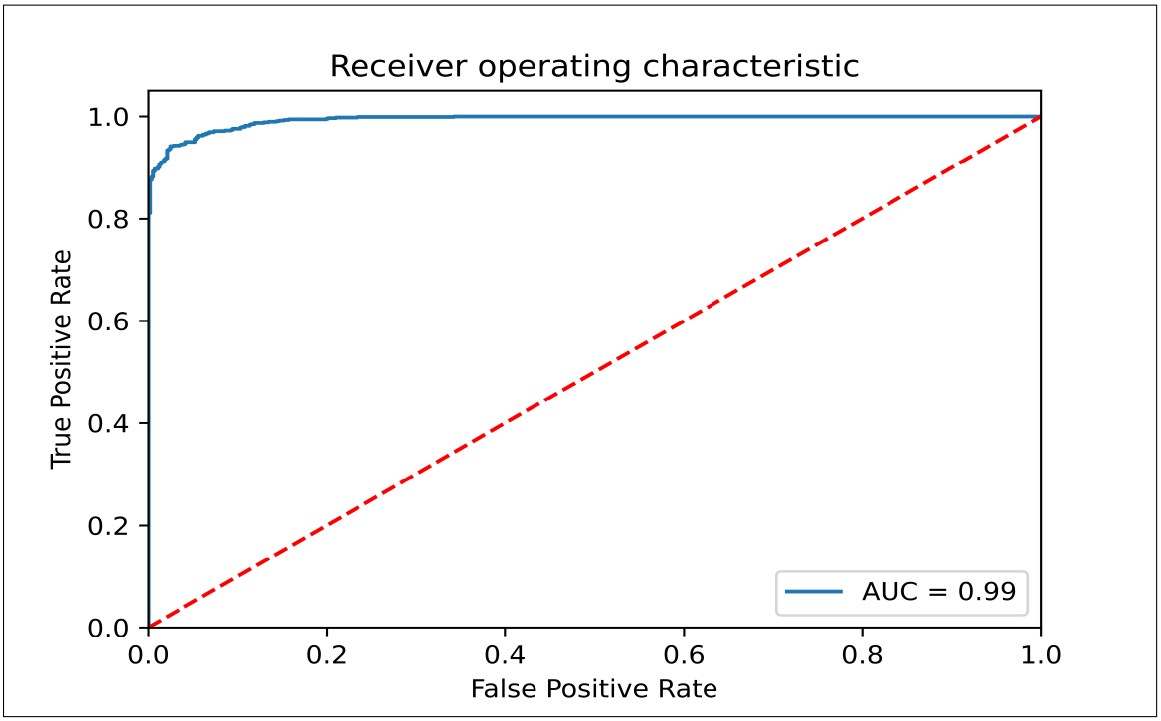

Figure 8.2: ANN AUROC plot

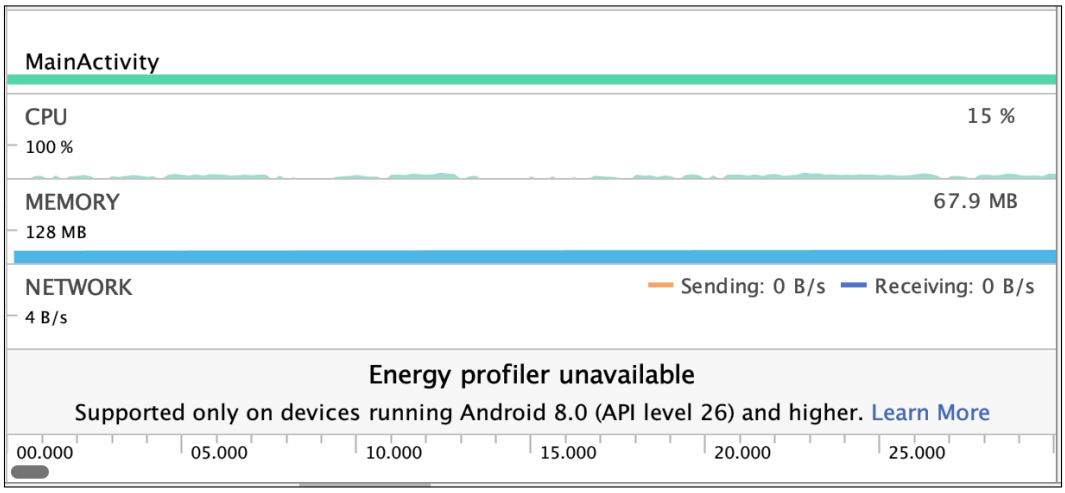

Figure 8.3: Beginning of the application's running time - machine learning algorithms

8.7.2 Smartphone's Resources Performance

The smartphone's resource consumption performance was similar to the performance of the previous machine learning scheme.

CPU and Memory Performance

As seen in Figures 8.3 and 8.4, the application's consumption of CPU and the memory resources from the beginning to the end of the monitoring session were very similar to the previous machine learning scheme. The CPU was 15% on average, and memory allocation was 67.9 MB.

Battery Power Consumption

The smartphone has a battery capacity of 3448 mAh. On average, the application consumed 0.50% or 18.6 mAh of the battery capacity. In the next section, we will discuss the results.

8.8 Discussion

In this section, we will discuss the scheme's results and how the scheme met the objectives set in Section 4.2. We will compare the results of the machine learning

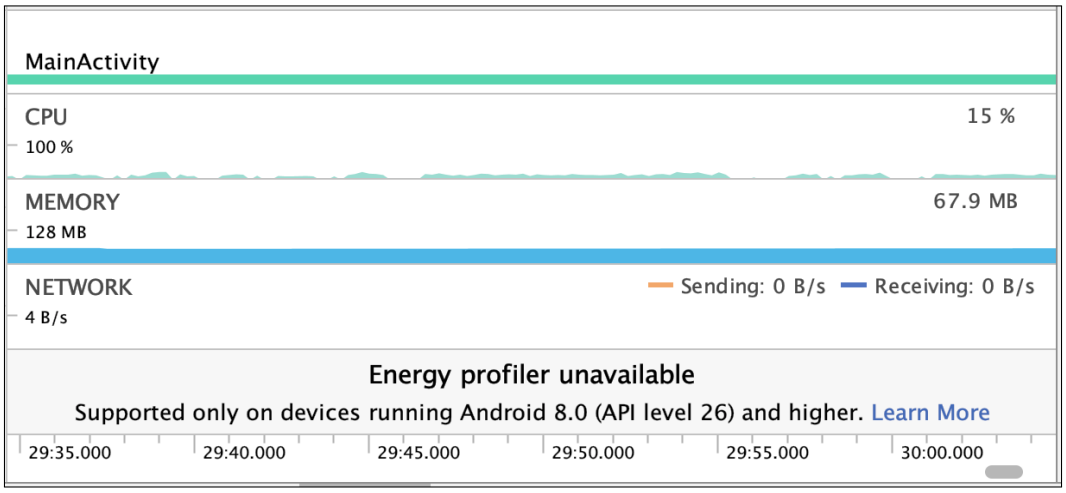

Figure 8.4: Beginning of the application's running time - with no alarm - machine learning algorithm

algorithms with the studies in the literature review. In addition, we will discuss the smartphone resources performance results.

8.8.1 Reliability and Accuracy Analysis

In the proposal report, our choice of deep learning model was the CNN model. However, we found that the CNN model is better for image recognition rather than pattern recognition. Therefore, we changed our choice to the ANN model since it is more suitable to the data type and the deep learning scheme's purpose.

We aim to improve the prediction and recognition of labour by personalizing the needs of each pregnant woman. Moreover, we want to use deep learning to further improve the outcome of the framework. As seen from the results in Table 8.3, the ANN improved the prediction in all the criteria compared to the RF algorithm from the machine learning scheme. The AC has improved from 0.95 to 0.98, FNR from 0.03 to 0.01 and FPR from 0.04 to 0.01.

FNR and FPR, as one of the top priority aspects in the framework, have been reduced by about 50% for the FNR and 75% for the FPR. The chart in Figure 8.5 visualizes the evaluation results. Finally, although we achieved good results using the deep learning approach, the size of our data could make the problem too easy for

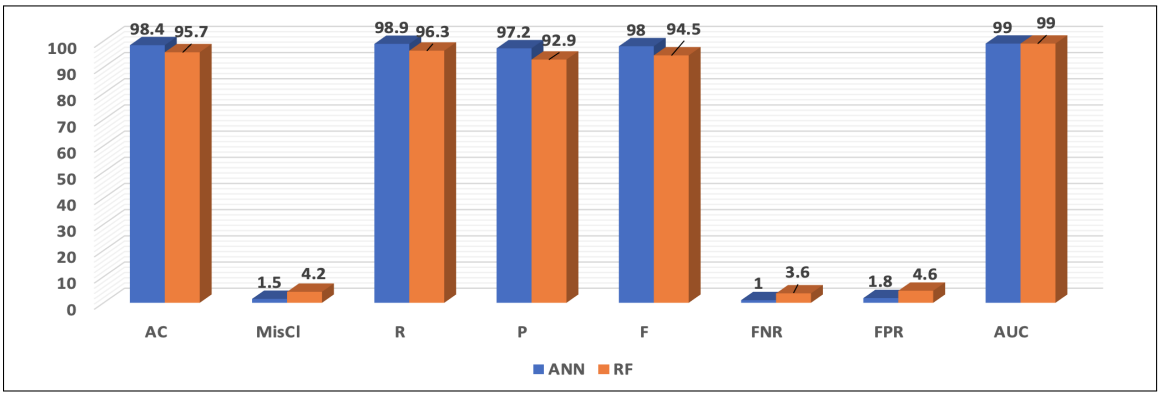

Figure 8.5: Results comparison between the ANN model and RF classifier

the deep learning models. Deep learning is powerful and needs big data to produce reliable results. We need more data to confirm our results for the deep learning approach, which we will discuss later in the chapter.

Scheme Comparison with the Literature Review Studies

Although the authors from [59] used a different approach in using the CNN model for image recognition of uterine contractions, their goal is similar to our approach to detect labour. Table 8.4 summarizes the comparison of the results between the two approaches. Our ANN and the CNN model have the same AC rate. Furthermore, our ANN model has a significantly better R rate and AUC value. The authors of the CNN model have not provided information about the MisCl, P, F, FNR and FPR rates. Although both models have a similar AC rate, other critical criteria such as FNR and FPR are missing, making the full comparison incomplete. Moreover, the R rate for the CNN model is below 90%. That means the probability of the model identifying a dataset as labour is lower than our ANN model by 11.2%. This further supports that we need more information on the CNN model's performance to analyze it comprehensively. In the next section, we will discuss big data and the issue of synthesizing EHG data.

Proposed systems	AC	MisCl	R	P	F	FNR	FPR	AUC
Proposed ANN model	0.98	0.01	0.98	0.97	0.98	0.01	0.01	0.99
CNN model [59]	0.98	x	0.87	x	x	x	x	0.92

Table 8.4: Summary of the related work studies

8.8.2 Big Data and Synthetic Data

One of the main aspects of deep learning is big data, as this is one of the main differences that distinguish it from machine learning. When it comes to medical data, obtaining big data on uterine EHG signals for pregnant women in general and pregnant women with a high risk of premature labour in particular is difficult. Moreover, the publicly available uterine EHG databases are limited. The vast majority of available databases collect data using the IUPC technique, which does not apply to our framework. For example, we contacted a pregnancy research group from Oxford University, and they agreed to share their big data with us; however, their data were on IUPC, not EHG. Furthermore, the lack of big data in our scheme is a limitation of our work. More data are needed to thoroughly utilize big data in our work.

To solve this issue, we proposed to generate our synthetic data using the five databases as seeds. We found Gretel Labs, Inc. (https://gretel.ai/), which provides a free service using Python. We were able to synthesize a few EHG datasets. However, after analyzing the synthesized datasets and consulting with our deep learning expert, Dr. Jaume Manero, about the quality of the synthesized datasets, he recommended that we would not be able to verify if the synthesized datasets are similar to the actual datasets of pregnant women. It is not easy to produce high-quality bio-synthetic data that are similar to the original data. This could be a limitation of the company's algorithms since they do not specialize in synthesizing biodata. Dr. Manero has also recommended that if we need to synthesize uterine EHG data, we would have to build our own deep learning synthetic model, which would take a long time.

Proposed systems	AC	MisCl	R	P	F	FNR	FPR	AUC
Proposed ANN model	0.98	0.01	0.98	0.97	0.98	0.01	0.01	0.99
Proposed RF classifier	0.95	0.04	0.96	0.93	0.94	0.03	0.04	0.99
CNN model [59]	0.98	x	0.87	x	x	x	x	0.92
Idowu et al. [30]	x	x	0.97	x	x	x	x	0.94
Fergus et al.[48]	0.90	x	0.85	x	x	x	x	0.90
Acharya et al. [49]	0.96	x	0.95	x	x	x	x	x
Altini et al. [50]	0.87	x	x	x	x	x	x	x
Borowska et al. [18]	0.83	x	x	x	x	x	x	x
Altini et al. [51]	x	x	x	x	x	x	x	x
Hoseinzadeh and Amirani [52]	0.97	x	0.95	x	x	x	x	x
Degbedzui and Yüksel [53]	0.99	x	0.99	x	0.99	x	x	x
Peng et al. [54]	0.93	x	0.89	x	x	x	x	0.80
Shahbakhti et al. [55]	0.99	x	0.98	x	x	x	x	x
Sheryl Oliver et al. [56]	0.96	x	0.92	x	x	x	x	x
Chen et al. [57]	0.90	x	0.92	x	x	x	x	x
Esgalhado et al. [58]	0.97	x	x	x	x	x	x	x

Table 8.5: Comparative analysis of the proposed work with published state-of-the-art techniques

8.8.3 Smartphone's Resources Performance

We maintained the same smartphone resource consumption as the previous machine learning scheme in Section 7.8.2. Furthermore, the CNN model might use more smartphone resources to extract images, requiring more CPU power and storage.

Table 8.5 summarizes the performance of all the ML and DL methods. In conclusion, the ANN model is the best choice given that all the methods from the literature review did not provide enough information for a complete comparison and good smartphone resource consumption.

8.9 Chapter Summary

In this chapter, we presented the deep learning algorithm scheme in detail. We illustrated the scheme implementation and our choice of feature selection and deep learning model. We also presented and discussed the evaluation results of the ANN model. Furthermore, we compared our results with the literature review studies. Moreover, the application efficiently consumed the smartphone's CPU, memory, and

battery power consumption. We concluded that the ANN deep learning model improved the detection and prediction compared to the machine learning scheme and the CNN model. In the next chapter, we will present experts' knowledge regarding the medical aspects of our framework.

Chapter 9

Experts Domain

In this chapter, we will present obstetricians' medical opinions on some aspects of our framework. We have contacted two obstetricians: Dr. Ebtehal Hussein Aljumaai, obstetric and gynecology registrar, Abha Maternity Children's Hospital, Saudi Arabia; and Dr. Mohamed Elsheikh, obstetrician and fetal medicine consultant, National Guard Hospital, MRCOG, SSCOG, DIP Prenatal genetics, Riyadh, Saudi Arabia.

9.1 Research Questions

To validate the medical aspects of the framework, we asked them the following questions:

1. Does the 30-minute monitoring session mimic the obstetrician's uterine contractions analysis to determine if a pregnant woman is in labour?
2. Are amplitude and frequency the most important parameters to use to decide if a pregnant woman is in labour?
3. Do you consider age, gestation and parity when evaluating the status of pregnant women with a high risk of premature labour?
4. Would you integrate our monitoring system to assist your patients?
5. How many stages does labour involve?
6. What is the window of time before the pregnant woman goes into labour?

In the following section, we will provide the obstetricians' answers to these questions.

9.2 Discussion

For question 1, the obstetrician will monitor the pregnant woman's contractions for a minimum of 30 to 40 minutes, then repeat the process. This process can take from 4 hours to 24 hours, depending on the pregnancy status. This supports our framework design, as the monitoring session is set to be 30 minutes long, and it is repeated if no alarm is triggered.

For question 2, both obstetricians acknowledged that amplitude and frequency are the top vital parameters when analyzing uterine contractions. That means our choice of having these two parameters as the basis for the machine learning and deep learning approaches is correct and mimics what an obstetrician would use to analyze uterine contractions.

Dr. Aljumaai also added that if the contractions pattern is regular or the amplitude is 60 millimetres of mercury (mmHg) or 200 Montevideo units (MVU) for IUPC, the pregnant woman is in labour. This is similar to our amplitude-frequency scheme, as we designed it to recognize regular contraction patterns.

For question 3, age was chosen by the obstetricians as the most important factor, especially if the pregnant woman's age is less than 18 or over 40. Gestation and parity are also important, especially if the pregnant woman has a history of premature labour.

For question 4, both obstetricians agreed that such a system is needed, and they would use it with their patients.

For question 5, obstetricians explained that there are four stages of labour:

1. Stage 1 (Latent): When the contractions start until the cervix widens to 6 cm.
2. Stage 2 (Active): When the cervix widens to 10 cm.
3. Stage 3: Starts when the baby is born until the placenta detaches.
4. Stage 4 (Afterbirth): Starts after the placenta comes out.

According to the obstetricians, our framework comes before stage 1 when the contractions start.

For question 6, obstetricians explained that the window before the pregnant

woman goes into stage 1 of labour depends on how many pregnancies the woman has had (Parity). If the pregnant woman is primigravida (it is her first pregnancy), the window is around 16 hours. If the pregnant woman is multigravida (it is her at least second pregnancy), the window is around 12 to 14 hours.

In the next chapter, we will present the concluding remarks and future work of the framework.

Chapter 10

Conclusion and Future Work

Premature birth is a global issue for pregnant women and babies that can lead to death or life-long health problems. Furthermore, there is no permanent solution or cure for premature birth because the cause is usually unknown. Moreover, even though premature birth more heavily affects women in developing countries, it is also an issue in developed countries and has a very high cost of treatment. For these reasons, we have proposed a framework for monitoring pregnant women with a high risk of premature birth using a WBS and a smartphone. We designed the framework to be continuous, home-comfortable, cost-effective, and reliable. The framework aims to detect labour patterns and send a warning to the pregnant woman by monitoring uterine EHG contractions. The framework has three schemes to use to analyze uterine contractions:

1. Amplitude-frequency algorithm scheme.
2. Machine learning algorithm scheme.
3. Deep learning algorithm scheme.

We have implemented a proof-of-concept smartphone application to test the framework's schemes. We used 7271 datasets of uterine EHG contractions obtained from the following five databases from [127]:

- Icelandic 16-electrode Electrohysterogram Database [128].
- Term-Preterm EHG Database [126].
- Term-Preterm EHG DataSet with Tocogram [131].
- CTU-CHB Intrapartum Cardiotocography Database [139].
- OB-1 Fetal ECG Database [127].

To evaluate the schemes, we calculated the accuracy and reliability of the analyzing algorithms and evaluated the smartphone's resources performance in terms of CPU,

memory and battery power consumption. The deep learning ANN model achieved better results in comparison to the machine learning RF classifier. In the next section, we will list the framework's future work.

10.1 Future Work

In future work, we will expand our smartphone usage to include iPhones and low-end cost-effective smartphones found largely in developing countries. We will also develop a deep learning model to synthesize EHG signals. Furthermore, we will identify and evaluate the privacy and security implications of the system design.

In addition, We will propose a user study to evaluate the system application UI ease of use. The following section will illustrate the user study to recruit pregnant women.

10.1.1 Study Proposal

In this section, we propose a user study to recruit pregnant women for EHG data collection and evaluation of how comfortable the sensor will be when attached to the pregnant woman. We were able to connect with some obstetricians to discuss the details of the study and the possibility of starting the recruitment. However, due to the unprecedented and very uncertain situation with the COVID-19 pandemic, we could not start the recruitment of pregnant women. According to the obstetricians, pregnant women can not be exposed to COVID-19 by any means, especially if they are at a high risk of premature labour. For that reason, we had to add recruitment as future work and apply our framework as a simulation. The following sections detail the study proposal for future work.

Objectives

As discussed in Chapter 2, pregnant women with a high risk of premature labour can have spontaneous labour as early as 19 weeks of gestational age. Furthermore, since EHG databases are limited in number, we can collect our data using WBSNs described

in Section 2.3. To collect the data, we propose a study design to recruit pregnant women with a high risk of premature labour. We will describe the WBS device we will be using to collect uterine contraction EHG data in the following section.

Data Collection

Any device we are going to use must have the following specifications in order to meet our research goals:

- Small in size so it does not restrict the pregnant woman's movement.
- Sends data wirelessly to the smartphone.
- Can be used non-invasively on the pregnant woman's abdomen.
- Safe to be used for both the pregnant woman and the fetus.
- Cost-effective to be applicable in developing countries.
- Easy to set up and launch.
- Collects data reliably and effectively for a long time.
- Stores data locally if unable to connect to the smartphone.

We will use a WBS device called the Shimmer3 Consensys EMG Development Kit. It consists of:

- The Shimmer3 EMG sensor.
- 5*9-inch biophysical leads.
- EMG electrodes.

The Shimmer3 EMG sensor can collect, filter, and send signals wirelessly via Bluetooth. Figure 10.1 shows the Shimmer3 device.

Patient Recruitment

Candidates for recruitment must be pregnant women with a history of premature labour. Due to this restriction, it might be challenging to recruit more than ten pregnant women with a high risk of premature labour. Therefore, we aim to recruit a minimum of five patients for a monitoring session every 30 minutes. The monitoring will start at the 19th week of gestational age and continue until the pregnant woman gives birth

Figure 10.1: The Shimmer3 EMG sensor

Appendix A

Publications

1. H. Allahem and S. Sampalli, "Automated Labour Detection Framework to Monitor Pregnant Women with a High Risk of Premature Labour Using Machine Learning and Deep Learning," *Informatics in Medicine Unlocked*, p. 100771, 2021. [Online]. Available: `https://doi.org/10.1016/j.imu.2021.100771`

2. H. Allahem and S. Sampalli, "Automated uterine contractions pattern detection framework to monitor pregnant women with a high risk of premature labour," *Informatics in Medicine Unlocked*, vol. 20, p. 100404, 2020. [Online]. Available: `https://doi.org/10.1016/j.imu.2020.100404`

3. H. Allahem and S. Sampalli, "Framework to monitor pregnant women with a high risk of premature labour using sensor networks," in *Proceedings of the IM 2017 - 2017 IFIP/IEEE International Symposium on Integrated Network and Service Management,* 2017, pp. 1178-1181. [Online]. Available: `https://ieeexplore.ieee.org/document/7987458`.

4. H. Allahem and S. Sampalli, "Survey of techniques for automatic detection of premature labour," The European Society of Medicine's Annual Congress (ESMED), Vienna, 2021.

Appendix B

Copyright Permissions

Transfer of Copyright to IFIP

PURPOSE

This form is to be used to transfer the copyright for a publication of the International Federation for Information Processing (IFIP), or the copyright for a separately-authored component of an IFIP publication, to IFIP. This form applies to IFIP publications not published by the IFIP publisher. There is a separate form for IFIP publications published by the IFIP publisher.

Title of Work: Framework to Monitor Pregnant Women with a High Risk of Premature Labour Using Sensor Networks

Author(s): Hisham Allahem and Srinivas Sampalli

Publication or Conference Name and Date:
PAPELE May 8th, 2017

TRANSFER OF COPYRIGHT AGREEMENT

Copyright to the above work (including without limitation, the right to publish the work in whole or in part in any and all forms of media, now or hereafter known) is hereby transferred to the International Federation for Information Processing (IFIP), effective as of the date of this agreement, on the understanding that the work has been accepted for inclusion in the IFIP Digital Library or the above referenced conference proceedings or other IFIP publication. For government work where transfer of copyright is restricted, the transfer of copyright is restricted as indicated in Part B below. All work included in the IFIP Digital Library is open access for the public.

However, each of the employer/author(s) retains the following rights:

1. All other proprietary rights to the work such as patent.
2. The right to reuse any portion of the work, without fee, in future works of the employer/author's own, including books, lectures and presentations in all media, provided that the IFIP citation and notice of the copyright are included (see Part A below).
3. The right to revise the work.

ELSEVIER

Publishing Agreement

Elsevier Ltd

Automated labour detection framework to monitor pregnant women with a high risk of premature labour using machine learning and deep learning

Corresponding author	Dr. Srinivas Sampalli
E-mail address	srini@cs.dal.ca

Journal	Informatics in Medicine Unlocked
Article number	100771
Our reference	IMU_100771
PII	S2352-9148(21)00244-6
DOI	10.1016/j.imu.2021.100771

Your Status

- I am one author signing on behalf of all co-authors of the manuscript

License of Publishing Rights

I hereby grant to Elsevier Ltd an exclusive publishing and distribution license in the manuscript identified above and any tables, illustrations or other material submitted for publication as part of the manuscript (the "Article") in print, electronic and all other media (whether now known or later developed), in any form, in all languages, throughout the world, for the full term of copyright, and the right to license others to do the same, effective when the Article is accepted for publication. This license includes the right to enforce the rights granted hereunder against third parties.

Supplemental Materials

"Supplemental Materials" shall mean materials published as a supplemental part of the Article, including but not limited to graphical, illustrative, video and audio material.

With respect to any Supplemental Materials that I submit, Elsevier Ltd shall have a perpetual worldwide non-exclusive right and license to publish, extract, reformat, adapt, build upon, index, redistribute, link to and otherwise use all or any part of the Supplemental Materials, in all forms and media (whether now known or later developed) and permit others to do so. The publisher shall apply the same end user license to the Supplemental Materials as to the Article where it publishes the Supplemental Materials with the Article in the journal on its online platforms on an Open Access basis.

Research Data

"Research Data" shall mean the result of observations or experimentation that validate research findings and that are published separate to the Article, which can include but are not limited to raw data, processed data, software, algorithms, protocols, and methods.

With respect to any Research Data that I wish to make accessible on a site or through a service of Elsevier Ltd, Elsevier Ltd shall have a perpetual worldwide, non-exclusive right and license to publish, extract, reformat, adapt, build upon, index, redistribute, link to and otherwise use all or any part of the Research Data in all forms and media (whether now known or later developed), and to permit others to do so. Where I have selected a specific end user license under which the Research Data is to be made available on a site or through a service, the publisher shall apply that end user license to the Research Data on that site or service.

Scholarly Communication Rights

I understand that I retain the copyright in the Article and that no rights in patents, trademarks or other intellectual property rights are transferred to Elsevier Ltd. As the author of the Article, I understand that I shall have: (i) the same rights to reuse the Article as those allowed to third party users of the Article under the CC BY-NC-ND License, as well as (ii) the right to use the Article in a subsequent compilation of my works or to extend the Article to book length form, to include the Article in a thesis or dissertation, or otherwise to use or re-use portions or excerpts in other works, for both commercial and non-commercial purposes. Except for such uses, I understand that the license of publishing rights I have granted to Elsevier Ltd gives Elsevier Ltd the exclusive right to make or sub-license commercial use.

User Rights

The publisher will apply the *Creative Commons Attribution-Noncommercial-NoDerivative Works 4.0 International License* (CC BY-NC-ND) to the Article where it publishes the Article in the journal on its online platforms on an Open Access basis. For further information, see http://www.elsevier.com/about/open-access/open-access-options.

The CC BY-NC-ND license allows users to copy and distribute the Article, provided this is not done for commercial purposes and further does not permit distribution of the Article if it is changed or edited in any way, and provided the user gives appropriate credit (with a link to the formal publication through the relevant DOI), provides a link to the license, and that the licensor is not represented as endorsing the use made of the work. The full details of the license are available at http://creativecommons.org/licenses/by-nc-nd/4.0.

Reversion of Rights

Articles may sometimes be accepted for publication but later rejected in the publication process, even in some cases after public posting in "Articles in Press" form, in which case all rights will revert to the author. See https://www.elsevier.com/about/our-business/policies/article-withdrawal.

Revisions and Addenda

I understand that no revisions, additional terms or addenda to this License Agreement can be accepted without Elsevier Ltd's express written consent. I understand that this License Agreement supersedes any previous agreements I have entered into with Elsevier Ltd in relation to the Article from the date hereof.

Copyright Notice

The publisher shall publish and distribute the Article with the appropriate copyright notice.

Author Representations / Ethics and Disclosure / Sanctions

I affirm the Author Representations noted below, and confirm that I have reviewed and complied with the relevant Instructions to Authors, Ethics in Publishing policy, Declarations of Interest disclosure and information for authors from countries affected by sanctions (Iran, Cuba, or Syria). Please note that some journals may require that all co-authors sign and submit Declarations of Interest disclosure forms. I am also aware of the publisher's policies with respect to retractions and withdrawal (https://www.elsevier.com/about/our-business/policies/article-withdrawal).

For further information see the publishing ethics page at https://www.elsevier.com/about/our-business/policies/publishing-ethics and the journal home page. For further information on sanctions, see https://www.elsevier.com/about/our-business/policies/trade-sanctions

Author representations

- The Article I have submitted to the journal for review is original, has been written by the stated authors and has not been previously published.
- The Article was not submitted for review to another journal while under review by this journal and will not be submitted to any other journal.
- The Article and the Supplemental Materials do not infringe any copyright, violate any other intellectual property, privacy or other rights of any person or entity, or contain any libellous or other unlawful matter.

- I have obtained written permission from copyright owners for any excerpts from copyrighted works that are included and have credited the sources in the Article or the Supplemental Materials.
- Except as expressly set out in this License Agreement, the Article is not subject to any prior rights or licenses.
- If I and/or any of my co-authors reside in Iran, Cuba, or Syria, the Article has been prepared in a personal, academic or research capacity and not as an official representative or otherwise on behalf of the relevant government or institution.
- If I am using any personal details or images of patients, research subjects or other individuals, I have obtained all consents required by applicable law and complied with the publisher's policies relating to the use of such images or personal information. See https://www.elsevier.com/about/our-business/policies/patient-consent for further information.
- Any software contained in the Supplemental Materials is free from viruses, contaminants or worms.
- If the Article or any of the Supplemental Materials were prepared jointly with other authors, I have informed the co-author(s) of the terms of this License Agreement and that I am signing on their behalf as their agent, and I am authorized to do so.

Governing Law and Jurisdiction

This License Agreement will be governed by and construed in accordance with the laws of the country or state of Elsevier Ltd ("the Governing State"), without regard to conflict of law principles, and the parties irrevocably consent to the exclusive jurisdiction of the courts of the Governing State.

For information on the publisher's copyright and access policies, please see http://www.elsevier.com/copyright.

☑ **I have read and agree to the terms of the License Agreement.**

23 December 2021 T-copyright license-v5/2017

References

[1] M. Mischi, C. Rabotti, L. P. Vosters, S. G. Oei, and J. W. Bergmans, "Electrohysterographic conduction velocity estimation," *Proceedings of the 31st Annual International Conference of the IEEE Engineering in Medicine and Biology Society: Engineering the Future of Biomedicine, EMBC 2009*, pp. 6934–6937, 2009.

[2] M. T. Garcia-Gonzalez, S. Charleston-Villalobos, C. Vargas-Garcia, R. Gonzalez-Camarena, and T. Aljama-Corrales, "Characterization of EHG contractions at term labor by nonlinear analysis," *Proceedings of the Annual International Conference of the IEEE Engineering in Medicine and Biology Society, EMBS*, pp. 7432–7435, 2013.

[3] M. Hassan, J. Terrien, B. Karlsson, and C. Marque, "Application of wavelet coherence to the detection of uterine electrical activity synchronization in labor," *Irbm*, vol. 31, no. 3, pp. 182–187, 2010. [Online]. Available: http://dx.doi.org/10.1016/j.irbm.2009.12.004

[4] M. Shahrdad and M. C. Amirani, "Detection of preterm labor by partitioning and clustering the EHG signal," *Biomedical Signal Processing and Control*, vol. 45, pp. 109–116, 2018. [Online]. Available: https://doi.org/10.1016/j.bspc.2018.05.044

[5] N. Nader, M. Hassan, W. Falou, A. Diab, S. Al-Omar, M. Khalil, and C. Marque, "Classification of pregnancy and labor contractions using a graph theory based analysis," *Proceedings of the Annual International Conference of the IEEE Engineering in Medicine and Biology Society, EMBS*, vol. 2015-Novem, pp. 2876–2879, 2015.

[6] M. Hassan, J. Terrien, C. Muszynski, A. Alexandersson, C. Marque, and B. Karlsson, "Better pregnancy monitoring using nonlinear correlation analysis of external uterine electromyography," *IEEE Transactions on Biomedical Engineering*, vol. 60, no. 4, pp. 1160–1166, 2013.

[7] A. G. Batista, S. Najdi, D. M. Godinho, C. Martins, F. C. Serrano, M. D. Ortigueira, and R. T. Rato, "A multichannel time–frequency and multi-wavelet toolbox for uterine electromyography processing and visualisation," *Computers in Biology and Medicine*, vol. 76, pp. 178–191, 2016. [Online]. Available: http://dx.doi.org/10.1016/j.compbiomed.2016.07.003

[8] N. Sadi-Ahmed, B. Kacha, H. Taleb, and M. Kedir-Talha, "Relevant Features Selection for Automatic Prediction of Preterm Deliveries from Pregnancy ElectroHysterograhic (EHG) records," *Journal of Medical Systems*, vol. 41, no. 12, 2017.

[9] H. Ganer Herman, H. Miremberg, A. Dekalo, G. Barda, J. Bar, and M. Kovo, "Preterm uterine contractions ultimately delivered at term: Safe but not out of danger," *European Journal of Obstetrics Gynecology and Reproductive Biology*, vol. 199, pp. 1–4, 2016. [Online]. Available: http://dx.doi.org/10.1016/j.ejogrb.2016.01.019

[10] M. Yochum, J. Laforêt, and C. Marque, "An electro-mechanical multiscale model of uterine pregnancy contraction," *Computers in Biology and Medicine*, vol. 77, pp. 182–194, 2016. [Online]. Available: http://dx.doi.org/10.1016/j.compbiomed.2016.08.001

[11] W. H. Organization. (2015) Preterm birth. [Accessed 23 August 2016]. [Online]. Available: http://www.who.int/mediacentre/factsheets/fs363/en/

[12] A. López Bernal, "Overview. Preterm labour: mechanisms and management," *BMC Pregnancy and Childbirth*, vol. 7, no. Suppl 1, p. S2, 2007. [Online]. Available: http://bmcpregnancychildbirth.biomedcentral.com/articles/10.1186/1471-2393-7-S1-S2

[13] J. P. Vogel, S. Chawanpaiboon, K. Watananirun, P. Lumbiganon, M. Petzold, A. B. Moller, J. Thinkhamrop, M. Laopaiboon, A. H. Seuc, D. Hogan, O. Tunçalp, E. Allanson, A. P. Betrán, M. Bonet, O. T. Oladapo, and A. M. Gülmezoglu, "Global, regional and national levels and trends of preterm birth rates for 1990 to 2014: Protocol for development of World Health Organization estimates," *Reproductive Health*, vol. 13, no. 1, pp. 1–9, 2016. [Online]. Available: http://dx.doi.org/10.1186/s12978-016-0193-1

[14] N. Nader, C. Marque, M. Hassan, W. Falou, A. Diab, and M. Khalil, "Pregnancy monitoring using graph theory based analysis," *2015 International Conference on Advances in Biomedical Engineering, ICABME 2015*, pp. 73–76, 2015.

[15] A. J. Hussain, P. Fergus, H. Al-Askar, D. Al-Jumeily, and F. Jager, "Dynamic neural network architecture inspired by the immune algorithm to predict preterm deliveries in pregnant women," *Neurocomputing*, vol. 151, no. P3, pp. 963–974, 2015. [Online]. Available: http://dx.doi.org/10.1016/j.neucom.2014.03.087

[16] N. Nader, M. Hassan, W. Falou, C. Marque, and M. Khalil, "A node-wise analysis of the uterine muscle networks for pregnancy monitoring," *Proceedings of the Annual International Conference of the IEEE Engineering in Medicine and Biology Society, EMBS*, vol. 2016-Octob, pp. 712–715, 2016.

[17] M. Zhang, V. Tidwell, P. S. La Rosa, J. D. Wilson, H. Eswaran, and A. Nehorai, "Modeling magnetomyograms of uterine contractions during pregnancy using a multiscale forward electromagnetic approach," *PLoS ONE*, vol. 11, no. 3, pp. 1–23, 2016.

[18] M. Borowska, E. Brzozowska, P. Kuć, E. Oczeretko, R. Mosdorf, and P. Laudański, "Identification of preterm birth based on RQA analysis of electrohysterograms," *Computer Methods and Programs in Biomedicine*, vol. 153, pp. 227–236, 2018.

[19] R. E. Garfield and W. L. Maner, "Physiology and electrical activity of uterine contractions," *Seminars in Cell and Developmental Biology*, vol. 18, no. 3, pp. 289–295, 2007.

[20] A. C. of Obstetricians and Gynecologists. (2016) Preterm birth definition. [Accessed 25 April 2017]. [Online]. Available: http://www.acog.org/Patients/FAQs/Preterm-Premature-Labor-and-Birth

[21] D. Alamedine, M. Khalil, and C. Marque, "Parameters extraction and monitoring in uterine EMG signals. Detection of preterm deliveries," *Irbm*, vol. 34, no. 4-5, pp. 322–325, 2013. [Online]. Available: http://dx.doi.org/10.1016/j.irbm.2013.08.003

[22] D. C. Dyson, K. H. Danbe, J. A. Bamber, Y. M. Crites, D. R. Field, J. A. Maier, L. A. Newman, D. A. Ray, D. L. Walton, and M. A. Armstrong, "Monitoring Women at Risk for Preterm Labor," *New England Journal of Medicine*, vol. 338, no. 1, pp. 15–19, 1998. [Online]. Available: http://www.nejm.org/doi/full/10.1056/NEJM199801013380103{%}5Cnhttp://www.nejm.org/doi/pdf/10.1056/NEJM199801013380103

[23] P. S. La Rosa, H. Eswaran, H. Preissl, and A. Nehorai, "Multiscale forward electromagnetic model of uterine contractions during pregnancy." *BMC medical physics*, vol. 12, p. 4, 2012. [Online]. Available: http://www.pubmedcentral.nih.gov/articlerender.fcgi?artid=3605117{&}tool=pmcentrez{&}rendertype=abstract

[24] R.-J. Kuon and R. E. Garfield, "Actions of progestins for the inhibition of cervical ripening and uterine contractions to prevent preterm birth," *Facts, views & vision in ObGyn*, vol. 4, no. 2, pp. 110–9, 2012. [Online]. Available: https://www.ncbi.nlm.nih.gov/pmc/articles/PMC3987504/

[25] P. Rozenberg, A. Chauveaud, P. Deruelle, M. Capelle, N. Winer, R. Desbrire, F. Perrotin, C. Bohec, L. Connan, C. Vayssire, B. Langer, A. Mantel, S. Azimi, R. Porcher, and E. Azria, "Prevention of preterm delivery after successful tocolysis in preterm labor by 17 alpha-hydroxyprogesterone caproate: A randomized controlled trial," *American Journal of Obstetrics and Gynecology*, vol. 206, no. 3, pp. 206.e1–206.e9, 2012. [Online]. Available: http://dx.doi.org/10.1016/j.ajog.2011.12.026

[26] A. Lemancewicz, M. Borowska, P. Kuć, E. Jasińska, P. Laudański, T. Laudański, and E. Oczeretko, "Early diagnosis of threatened premature labor by electrohysterographic recordings - The use of digital signal processing," *Biocybernetics and Biomedical Engineering*, vol. 36, no. 1, pp. 302–307, 2016.

[27] J. Mas-Cabo, Y. Ye-Lin, J. Garcia-Casado, J. Alberola-Rubio, A. Perales, and G. Prats-Boluda, "Uterine contractile efficiency indexes for labor prediction: A bivariate approach from multichannel electrohysterographic records," *Biomedical Signal Processing and Control*, vol. 46, pp. 238–248, 2018. [Online]. Available: https://doi.org/10.1016/j.bspc.2018.07.018

[28] K. Horoba, J. Jezewski, A. Matonia, J. Wrobel, R. Czabanski, and M. Jezewski, "Early predicting a risk of preterm labour by analysis of antepartum electrohysterograhic signals," *Biocybernetics and Biomedical Engineering*, vol. 36, no. 4, pp. 574–583, 2016. [Online]. Available: http://dx.doi.org/10.1016/j.bbe.2016.06.004

[29] J. Karsdon, M. El Daouk, W. M. Huang, and G. G. Ashmead, "Electrical pacemaker as a safe and feasible method for decreasing the uterine contractions of human preterm labor," *Journal of Perinatal Medicine*, vol. 40, no. 6, pp. 697–700, 2012.

[30] I. O. Idowu, P. Fergus, A. Hussain, C. Dobbins, M. Khalaf, R. V. Eslava, and R. Keight, "Artificial intelligence for detecting preterm uterine activity in gynacology and obstertric care," *Proceedings - 15th IEEE International Conference on Computer and Information Technology, CIT 2015, 14th IEEE International Conference on Ubiquitous Computing and Communications, IUCC 2015, 13th IEEE International Conference on Dependable, Autonomic and Se*, pp. 215–220, 2015.

[31] B. Latré, B. Braem, I. Moerman, C. Blondia, and P. Demeester, "A survey on wireless body area networks," *Wireless Networks*, vol. 17, no. 1, pp. 1–18, 2011.

[32] B. Vermeulen-Giovagnoli, C. Peters, M. B. van der Hout-van der Jagt, M. Mischi, C. van Pul, E. J. E. Cottaar, and S. G. Oei, "The development of an obstetric tele-monitoring system," in *2015 37th Annual International Conference of the IEEE Engineering in Medicine and Biology Society (EMBC)*. IEEE, aug 2015, pp. 177–180. [Online]. Available: http://ieeexplore.ieee.org/document/7318329/

[33] D. Schlembach, W. L. Maner, R. E. Garfield, and H. Maul, "Monitoring the progress of pregnancy and labor using electromyography," *European Journal of Obstetrics Gynecology and Reproductive Biology*, vol. 144, no. SUPPL 1, pp. 2–8, 2009.

[34] J. Nicholl, J. West, S. Goodacre, and J. Turner, "The relationship between distance to hospital and patient mortality in emergencies: An observational study," *Emergency Medicine Journal*, vol. 24, no. 9, pp. 665–668, 2007.

[35] L. F. Bastos, W. van Meurs, and D. Ayres-de Campos, "A model for educational simulation of the evolution of uterine contractions during labor," *Computer Methods and Programs in Biomedicine*, vol. 107, no. 2, pp. 242–247, aug 2012. [Online]. Available: http://dx.doi.org/10.1016/j.cmpb.2011.09.016https://linkinghub.elsevier.com/retrieve/pii/S016926071100263X

[36] S. A. Vora, O. C. Montgomery, and T. P. Kurzweg, "Method for uterine contraction monitoring with passive RFID tags," *2017 IEEE EMBS International Conference on Biomedical and Health Informatics, BHI 2017*, pp. 213–216, 2017.

[37] D. Verner, "What Factors Influence World Literacy ?" *World Bank Policy Research Working Paper*, no. January, pp. 1–25, 2005.

[38] I. Medhi, A. Prasad, and K. Toyama, "Optimal audio-visual representations for illiterate users of computers," *16th International World Wide Web Conference, WWW2007*, pp. 873–882, 2007.

[39] I. Medhi, A. Sagar, and K. Toyama, "Text-free user interfaces for illiterate and semi-literate users," *2006 International Conference on Information and Communication Technology and Development, ICTD2006*, pp. 72–82, 2006.

[40] M. I. P. Nasution, S. D. Andriana, P. D. Syafitri, E. Rahayu, and M. R. Lubis, "Mobile device interfaces illiterate," *Proceedings of the 2015 International Conference on Technology, Informatics, Management, Engineering and Environment, TIME-E 2015*, pp. 117–120, 2016.

[41] M. A. Ahmed, M. N. Islam, F. Jannat, and Z. Sultana, "Towards Developing a Mobile Application for Illiterate People to Reduce Digital Divide," *2019 International Conference on Computer Communication and Informatics, ICCCI 2019*, pp. 0–4, 2019.

[42] B. C. Jacod, E. M. Graatsma, E. Van Hagen, and G. H. A. Visser, "A validation of electrohysterography for uterine activity monitoring during labour," *Journal of Maternal-Fetal and Neonatal Medicine*, vol. 23, no. 1, pp. 17–22, 2010.

[43] C. Urquhart, R. Currell, F. Harlow, and L. Callow, "Home uterine monitoring for detecting preterm labour," in *Cochrane Database of Systematic Reviews*, C. Urquhart, Ed. Chichester, UK: John Wiley & Sons, Ltd, feb 2017. [Online]. Available: http://doi.wiley.com/10.1002/14651858.CD006172.pub4

[44] J. J. P. C. Rodrigues, A. M. B. Oliveira, and K. Saleem, "Smart Mobile System for Pregnancy Care Using Body Sensors," *International Conference on Selected Topics in Mobile & Wireless Networking (MoWNeT)Short Papers*, pp. 1–4, 2016.

[45] A. Ni, M. C. R. I. An-vida, and L. Stoicu-tivadar, "Integrated Wireless Sensor Network for Monitoring Pregnant Women," pp. 354–358, 2015.

[46] F. Sarhaddi, I. Azimi, S. Labbaf, H. Niela-Vilén, N. Dutt, A. Axelin, P. Liljeberg, and A. M. Rahmani, "Long-term iot-based maternal monitoring: System design and evaluation," *Sensors*, vol. 21, no. 7, pp. 1–21, 2021.

[47] S. Veena and D. J. Aravindhar, "Remote Monitoring System for the Detection of Prenatal Risk in a Pregnant Woman," *Wireless Personal Communications*, no. 0123456789, 2021. [Online]. Available: https://doi.org/10.1007/s11277-021-08249-x

[48] P. Fergus, I. Idowu, A. Hussain, and C. Dobbins, "Advanced artificial neural network classification for detecting preterm births using EHG records," *Neurocomputing*, vol. 188, pp. 42–49, 2016.

[49] U. R. Acharya, V. K. Sudarshan, S. Q. Rong, Z. Tan, C. M. Lim, J. E. Koh, S. Nayak, and S. V. Bhandary, "Automated detection of premature delivery using empirical mode and wavelet packet decomposition techniques with uterine electromyogram signals," *Computers in Biology and Medicine*, vol. 85, no. April, pp. 33–42, 2017. [Online]. Available: http://dx.doi.org/10.1016/j.compbiomed.2017.04.013

[50] M. Altini, E. Rossetti, M. Rooijakkers, J. Penders, D. Lanssens, L. Grieten, and W. Gyselaers, "Combining electrohysterography and heart rate data to detect labour," *2017 IEEE EMBS International Conference on Biomedical and Health Informatics, BHI 2017*, pp. 149–152, 2017.

[51] M. Altini, E. Rossetti, M. J. Rooijakkers, and J. Penders, "Towards Non-invasive Labour Detection: A Free-Living Evaluation," *Proceedings of the Annual International Conference of the IEEE Engineering in Medicine and Biology Society, EMBS*, vol. 2018-July, pp. 2841–2844, 2018.

[52] S. Hoseinzadeh and M. C. Amirani, "Use of Electro Hysterogram (EHG) Signal to Diagnose Preterm Birth," *26th Iranian Conference on Electrical Engineering (ICEE2018)*, pp. 1477–1481, 2018. [Online]. Available: https://ieeexplore.ieee.org/document/8472416/

[53] D. K. Degbedzui and M. E. Yüksel, "Accurate diagnosis of term–preterm births by spectral analysis of electrohysterography signals," *Computers in Biology and Medicine*, vol. 119, no. February, p. 103677, 2020. [Online]. Available: https://doi.org/10.1016/j.compbiomed.2020.103677

[54] J. Peng, D. Hao, L. Yang, M. Du, X. Song, H. Jiang, Y. Zhang, and D. Zheng, "Evaluation of electrohysterogram measured from different gestational weeks for recognizing preterm delivery: a preliminary study using random Forest," *Biocybernetics and Biomedical Engineering*, vol. 40, no. 1, pp. 352–362, 2020. [Online]. Available: https://doi.org/10.1016/j.bbe.2019.12.003

[55] M. Shahbakhti, M. Beiramvand, M. R. Bavi, and S. Mohammadi Far, "A New Efficient Algorithm for Prediction of Preterm Labor," *Proceedings of the Annual International Conference of the IEEE Engineering in Medicine and Biology Society, EMBS*, pp. 4669–4672, 2019.

[56] A. Sheryl Oliver, U. Ashwanthika, and R. Aswitha, "Labor Prediction in pregnant woman based on ElectroMyoGram and ElectroHysteroGram using Machine Learning Techniques," *2020 Fourth International Conference on Inventive Systems and Control (ICISC)*, pp. 77–82, 2020. [Online]. Available: https://ieeexplore.ieee.org/abstract/document/9171128

[57] L. Chen, Y. Hao, and X. Hu, "Detection of preterm birth in electrohysterogram signals based on wavelet transform and stacked sparse autoencoder," *PLoS ONE*, vol. 14, no. 4, pp. 1–17, 2019. [Online]. Available: http://dx.doi.org/10.1371/journal.pone.0214712

[58] F. Esgalhado, A. G. Batista, H. Mouriño, S. Russo, C. R. P. dos Reis, F. Serrano, V. Vassilenko, and M. Duarte Ortigueira, "Automatic contraction detection using uterine electromyography," *Applied Sciences*, vol. 10, no. 20, 2020. [Online]. Available: https://www.mdpi.com/2076-3417/10/20/7014

[59] D. Hao, J. Peng, Y. Wang, J. Liu, X. Zhou, and D. Zheng, "Evaluation of convolutional neural network for recognizing uterine contractions with electrohysterogram," *Computers in Biology and Medicine*, vol. 113, no. August, p. 103394, 2019. [Online]. Available: https://doi.org/10.1016/j.compbiomed.2019.103394

[60] C. Rabotti, M. Mischi, J. Van Laar, G. Oei, and J. Bergmans, "On the propagation analysis of electrohysterographic signals," *Conference Proceedings of the International Conference of IEEE Engineering in Medicine and Biology Society*, vol. 2008, pp. 3868–3871, 2008. [Online]. Available: http://www.ncbi.nlm.nih.gov/pubmed/19163557

[61] X. Wei, Z. Zhao, and X. Zhang, "Design of a remote monitoring platform for uterine contraction pressure based on virtual instrument," *Proceedings - 2014 7th International Conference on BioMedical Engineering and Informatics, BMEI 2014*, no. Bmei, pp. 534–539, 2014.

[62] J. Alberola-Rubio, G. Prats-Boluda, Y. Ye-Lin, J. Valero, A. Perales, and J. Garcia-Casado, "Comparison of non-invasive electrohysterographic recording techniques for monitoring uterine dynamics," *Medical Engineering and Physics*, vol. 35, no. 12, pp. 1736–1743, 2013. [Online]. Available: http://dx.doi.org/10.1016/j.medengphy.2013.07.008

[63] M. W. Vlemminx, K. M. Thijssen, G. I. Bajlekov, J. P. Dieleman, M. B. Van Der Hout-Van Der Jagt, and S. G. Oei, "Electrohysterography for uterine monitoring during term labour compared to external tocodynamometry and intra-uterine pressure catheter," *European Journal of Obstetrics and Gynecology and Reproductive Biology*, vol. 215, pp. 197–205, 2017. [Online]. Available: http://dx.doi.org/10.1016/j.ejogrb.2017.05.027

[64] C. Rabotti, M. Mischi, J. Van Laar, G. Oei, and J. Bergmans, "Electrohysterographic analysis of uterine contraction propagation with labor progression: A preliminary study," *Annual International Conference of the IEEE Engineering in Medicine and Biology - Proceedings*, pp. 4135–4138, 2007.

[65] M. Liu, L. A. Belfore, Y. Shen, and M. W. Scerbo, "Uterine Contraction Modeling and Simulation," *Computer Methods and Programs in Biomedicin*, vol. 107, no. 2, pp. 242 – 247, 2012.

[66] R. Halabi, M. O. Diab, B. Moslem, M. Khalil, and C. Marque, "Cross-correlation analysis of multichannel uterine EMG signals," *Proceedings of the Annual International Conference of the IEEE Engineering in Medicine and Biology Society, EMBS*, pp. 3106–3109, 2012.

[67] A. Diab, M. Hassan, B. Karlsson, and C. Marque, "Effect of decimation on the classification rate of non-linear analysis methods applied to uterine EMG signals," *Irbm*, vol. 34, no. 4-5, pp. 326–329, 2013. [Online]. Available: http://dx.doi.org/10.1016/j.irbm.2013.07.010

[68] G. Haran, M. Elbaz, M. D. Fejgin, and T. Biron-Shental, "A comparison of surface acquired uterine electromyography and intrauterine pressure catheter to assess uterine activity," *American Journal of Obstetrics and Gynecology*, vol. 206, no. 5, pp. 412.e1–412.e5, 2012. [Online]. Available: http://dx.doi.org/10.1016/j.ajog.2011.12.015

[69] B. Vasak, E. M. Graatsma, E. Hekman-Drost, M. J. Eijkemans, J. H. Schagen Van Leeuwen, G. H. Visser, and B. C. Jacod, "Uterine electromyography for identification of first-stage labor arrest in term nulliparous women with spontaneous onset of labor," *American Journal of Obstetrics and Gynecology*, vol. 209, no. 3, pp. 232.e1–232.e8, 2013. [Online]. Available: http://dx.doi.org/10.1016/j.ajog.2013.05.056

[70] B. Moslem, M. Khalil, C. Marque, and M. O. Diab, "Complexity analysis of the uterine electromyography," *2010 Annual International Conference of the IEEE Engineering in Medicine and Biology Society, EMBC'10*, pp. 2802–2805, 2010.

[71] P. S. La Rosa, A. Nehorai, H. Eswaran, C. L. Lowery, and H. Preissl, "Detection of uterine MMG contractions using a multiple change point estimator and the K-means cluster algorithm," *IEEE Transactions on Biomedical Engineering*, vol. 55, no. 2, pp. 453–467, 2008.

[72] T. Y. Euliano, D. Marossero, M. T. Nguyen, N. R. Euliano, J. Principe, and R. K. Edwards, "Spatiotemporal electrohysterography patterns in normal and arrested labor," *American Journal of Obstetrics and Gynecology*, vol. 200, no. 1, pp. 54.e1–54.e7, 2009. [Online]. Available: http://dx.doi.org/10.1016/j.ajog.2008.09.008

[73] J. Terrien, C. Marque, and G. Germain, "Ridge extraction from the time-frequency representation (TFR) of signals based on an image processing approach: Application to the analysis of uterine electromyogram AR TFR," *IEEE Transactions on Biomedical Engineering*, vol. 55, no. 5, pp. 1496–1503, 2008.

[74] G. I. Bajlekov, C. Rabotti, S. G. Oei, and M. Mischi, "[7]-Electrohysterographic Detection of Uterine Contractions in Term Pregnancy," *Embc*, pp. 5851–5854, 2015.

[75] H. Léman, C. Marque, and J. Gondry, "Use of the electrohysterogram signal for characterization of contractions during pregnancy," *IEEE Transactions on Biomedical Engineering*, vol. 46, no. 10, pp. 1222–1229, 1999.

[76] T. Y. Euliano, M. T. Nguyen, S. Darmanjian, S. P. McGorray, N. Euliano, A. Onkala, and A. R. Gregg, "Monitoring uterine activity during labor: A comparison of 3 methods," *American Journal of Obstetrics and Gynecology*, vol. 208, no. 1, pp. 66.e1–66.e6, 2013. [Online]. Available: http://dx.doi.org/10.1016/j.ajog.2012.10.873

[77] D. D. Taralunga, M. Ungureanu, B. Hurezeanu, I. Gussi, and R. Strungaru, "Empirical mode decomposition applied for non-invasive electrohysterograhic signals denoising," *Proceedings of the Annual International Conference of the IEEE Engineering in Medicine and Biology Society, EMBS*, vol. 2015-Novem, pp. 4134–4137, 2015.

[78] J. Duchêne, D. Devedeux, S. Mansour, and C. Marque, "Analyzing Uterine EMG: Tracking Instantaneous Burst Frequency," *IEEE Engineering in Medicine and Biology Magazine*, vol. 14, no. 2, pp. 125–132, 1995.

[79] Z. Liu, D. Hao, L. Zhang, J. Liu, X. Zhou, L. Yang, Y. Yang, X. Li, S. Zhang, and D. Zheng, "Comparison of electrohysterogram characteristics during uterine contraction and non-contraction during labor," *Proceedings of the Annual International Conference of the IEEE Engineering in Medicine and Biology Society, EMBS*, pp. 2924–2927, 2017.

[80] M. Diab, C. Marque, and M. Khalil, "Unsupervised Classification in Uterine Electromyography Signal: Toward The Detection of Preterm Birth," *2005 IEEE Engineering in Medicine and Biology 27th Annual Conference*, pp. 5660–5663, 2005. [Online]. Available: http://ieeexplore.ieee.org/document/1615770/

[81] D. L. Carnì, G. Fortino, R. Gravina, D. Grimaldi, A. Guerrieri, and F. Lamonaca, "Continuous, real-time monitoring of assisted livings through wireless body sensor networks," *Proceedings of the 6th IEEE International Conference on Intelligent Data Acquisition and Advanced Computing Systems: Technology and Applications, IDAACS'2011*, vol. 2, no. September, pp. 872–877, 2011.

[82] H. Alemdar and C. Ersoy, "Wireless sensor networks for healthcare: A survey," *Computer Networks*, vol. 54, no. 15, pp. 2688–2710, 2010. [Online]. Available: http://dx.doi.org/10.1016/j.comnet.2010.05.003

[83] H. Reza Naj and M. Aminian, "A Hospital Healthcare Monitoring System Using Wireless Sensor Networks," *Journal of Health & Medical Informatics*, vol. 04, no. 02, pp. 4–9, 2013. [Online]. Available: http://www.omicsonline.org/2157-7420/2157-7420-4-121.digital/2157-7420-4-121.html

[84] S. Movassaghi, M. Abolhasan, J. Lipman, D. Smith, and A. Jamalipour, "Wireless Body Area Networks: A Survey," *Ieee Communications Surveys and Tutorials*, vol. 16, no. 3, pp. 1658–1686, 2014.

[85] D. Adams, H. Zheng, M. Sinclair, M. Murphy, and J. McCullough, "Integrated care for pregnant women with Type one diabetes using wearable technology," *BIBE 2019; The Third International Conference on Biological Information and Biomedical Engineering*, pp. 1–5, 2019. [Online]. Available: https://ieeexplore.ieee.org/document/8903360

[86] A. A. Boatin, B. J. Wylie, I. Goldfarb, R. Azevedo, E. Pittel, C. Ng, and J. E. Haberer, "Wireless Vital Sign Monitoring in Pregnant Women: A Functionality and Acceptability Study," *Telemedicine and e-Health*, no. July, p. tmj.2015.0173, 2016. [Online]. Available: http://online.liebertpub.com/doi/10.1089/tmj.2015.0173

[87] R. Braojos, I. Beretta, J. Constantin, A. Burg, and D. Atienza, "A Wireless Body Sensor Network for Activity Monitoring with Low Transmission Overhead," *2014 12th IEEE International Conference on Embedded and Ubiquitous Computing*, pp. 265–272, 2014. [Online]. Available: http://ieeexplore.ieee.org/lpdocs/epic03/wrapper.htm?arnumber=6962296

[88] M. Lucovnik, R. J. Kuon, L. R. Chambliss, W. L. Maner, S. Q. Shi, L. Shi, J. Balducci, and R. E. Garfield, "Use of uterine electromyography to diagnose term and preterm labor," *Acta Obstetricia et Gynecologica Scandinavica*, vol. 90, no. 2, pp. 150–157, 2011.

[89] Healthcare Denmark, "Denmark - A Telehealth Nation," 2018.

[90] M. Lucovnik, W. L. Maner, L. R. Chambliss, R. Blumrick, J. Balducci, Z. Novak-Antolic, and R. E. Garfield, "Noninvasive uterine electromyography for prediction of preterm delivery," *American Journal of Obstetrics and Gynecology*, vol. 204, no. 3, pp. 228.e1–228.e10, 2011. [Online]. Available: http://dx.doi.org/10.1016/j.ajog.2010.09.024

[91] C. Urquhart, R. Currell, E. Callow, and F. Harlow, "Home uterine monitoring for detecting preterm labour," *Cochrane Database of Systematic Reviews*, no. 4, 2006.

[92] U. U. Sajjad and S. Shahid, "Baby+: A mobile application to support pregnant women in Pakistan," *Proceedings of the 18th International Conference on Human-Computer Interaction with Mobile Devices and Services Adjunct, MobileHCI 2016*, pp. 667–674, 2016.

[93] W. Yang, K. Yang, H. Jiang, Z. Wang, Q. Lin, and W. Jia, "Fetal heart rate monitoring system with mobile internet," *Proceedings - IEEE International Symposium on Circuits and Systems*, pp. 443–446, 2014.

[94] Y. Ye-Lin, J. Alberola-Rubio, G. Prats-Boluda, J. M. Barrachina, A. Perales, J. Valero, D. Desantes, and J. Garcia-Casado, "Non-invasive electrohysterogram recording using flexible concentric ring electrode," *2014 36th Annual International Conference of the IEEE Engineering in Medicine and Biology Society, EMBC 2014*, pp. 4050–4053, 2014.

[95] A. Pawlak, K. Horoba, J. Jezewski, J. Wrobel, and A. Matonia, "Telemonitoring of pregnant women at home - Biosignals acquisition and measurement," *Proceedings of the 22nd International Conference Mixed Design of Integrated Circuits and Systems, MIXDES 2015*, pp. 83–87, 2015.

[96] K. Zhang, M. Jiang, and Z. Ma, "The monitoring system for Pregnancy-induced Hypertension based on Mobile Communication Technology," *2015 7th International Conference on Advanced Computational Intelligence, ICACI 2015*, pp. 263–266, 2015.

[97] K. Karagiannaki, S. Chonianakis, E. Patelarou, A. Panousopoulou, and M. Papadopouli, "MMamee: A mHealth platform for monitoring and assessing maternal environmental exposure," *Proceedings - IEEE Symposium on Computer-Based Medical Systems*, vol. 2015-July, pp. 163–168, 2015.

[98] P. Norasethasopon, K. Chitsakul, and S. Tretriluxana, "A development of real-Time fetal movement detector," *IECBES 2016 - IEEE-EMBS Conference on Biomedical Engineering and Sciences*, pp. 637–640, 2016.

[99] B. Lakshmi, T. Indumathi, and N. Ravi, "An Hybrid Approach for Prediction Based Health Monitoring in Pregnant Women," *Procedia Technology*, vol. 24, pp. 1635–1642, 2016. [Online]. Available: http://dx.doi.org/10.1016/j.protcy.2016.05.171

[100] Y. C. Du and P. W. Wu, "Novel wearable uterine contractions detection using positive force measurement," *2016 13th International Conference on Electrical Engineering/Electronics, Computer, Telecommunications and Information Technology, ECTI-CON 2016*, pp. 1–4, 2016.

[101] S. Kumaresh, M. Sabareesh, and R. Srihari, "Non-invasive fetus heart rate and growth measurement with abnormality detection using IoT," *International Conference on Electrical, Electronics, and Optimization Techniques, ICEEOT 2016*, pp. 3655–3659, 2016.

[102] S. Amirneni, B. S. Sundari, and S. Ravindran, "Post and pre natal tracking in rural areas using cloud computing and ICT," in *2016 International Conference on Inventive Computation Technologies (ICICT)*, vol. 3. IEEE, aug 2016, pp. 1–5. [Online]. Available: http://ieeexplore.ieee.org/document/7830101/

[103] B. N. Lakshmi, T. S. Indumathi, and N. Ravi, "Prediction based health monitoring in pregnant women," *Proceedings of the 2015 International Conference on Applied and Theoretical Computing and Communication Technology, iCATccT 2015*, pp. 594–598, 2016.

[104] E. Lq, D. P. Xpdu, X. Á. Loedj, D. Dp, Q. Df, L. Q. Udphvknxpduphhqd, J. Frp, Á. S. Qlwm, D. F. Lq, V. Qlwm, D. F. Lq, Z. V. Olylqj, L. Q. Uhprwh, D. Kdyh, and U. Dffhvv, "An IoT Based Multi-Parameter Data Acquisition System for Efficient Bio-Telemonitoring of Pregnant Women at Home," pp. 618–624, 2018.

[105] O. S. Lupşe and L. Stoicu-Tivadar, "Profiling in obstetrics for premature birth risk patients," *2017 E-Health and Bioengineering Conference, EHB 2017*, pp. 289–292, 2017.

[106] Y. A. Zhivolupova and Y. O. Bobrova, "The concept of the fetal remote monitoring system development," *Proceedings of 2017 IEEE 2nd International Conference on Control in Technical Systems, CTS 2017*, pp. 360–362, 2017.

[107] S. Sribhavani, H. Sunitha, and B. Subhiksha, "Providing a friendly e-health care environment to rural women during preganncyand child growth," in *2017 IEEE Technological Innovations in ICT for Agriculture and Rural Development (TIAR)*. IEEE, apr 2017, pp. 215–217. [Online]. Available: http://ieeexplore.ieee.org/document/8273718/

[108] Y. O. Bobrova and Y. A. Zhivolupova, "Automatic detection of abnormal fetal states by means of a personal monitoring system," *Proceedings of 2017 20th IEEE International Conference on Soft Computing and Measurements, SCM 2017*, pp. 782–784, 2017.

[109] G. K. Endo, I. Oluwayomi, V. Alexandra, Y. Athavale, and S. Krishnan, "Technology for continuous long-term monitoring of pregnant women for safe childbirth," *IHTC 2017 - IEEE Canada International Humanitarian Technology Conference 2017*, pp. 6–10, 2017.

[110] A. Abid and S. Shahid, "Helping pregnant women in the rural areas of Pakistan using a low-cost interactive system," *ACM International Conference Proceeding Series*, vol. Part F1320, 2017.

[111] S. Mondal and N. Mukherjee, "A framework for ICT-based primary healthcare delivery for children," *2017 9th International Conference on Communication Systems and Networks, COMSNETS 2017*, pp. 525–529, 2017.

[112] V. Shulgin and O. Viunytskyi, "Spatio-temporal signal processing for fetus and mother state monitoring during pregnancy," *Proceedings of 2018 IEEE 9th International Conference on Dependable Systems, Services and Technologies, DESSERT 2018*, no. Cv, pp. 641–644, 2018.

[113] I. Marin and N. Goga, "Healthcare System Based on the Smart Monitoring Bracelets and Sentiment Analysis," *2018 International Symposium on Fundamentals of Electrical Engineering, ISFEE 2018*, 2018.

[114] N. Mathew, "A Boosting Approach for Maternal Hypertensive Disorder Detection," *Proceedings of the International Conference on Inventive Communication and Computational Technologies, ICICCT 2018*, no. Icicct, pp. 1474–1477, 2018.

[115] G. Wicahyono, A. Setyanto, S. Raharjo, and A. Munandar, "Pregnancy monitoring mobile application user experience assessment," *2019 International Conference on Information and Communications Technology, ICOIACT 2019*, pp. 872–877, 2019.

[116] A. Munandar, A. Setyanto, S. Raharjo, and G. Wicahyono, "Pregnancy mapping and monitoring web based geographic's information system," *2019 4th International Conference on Information Technology, Information Systems and Electrical Engineering, ICITISEE 2019*, vol. 6, pp. 490–494, 2019.

[117] Y. C. Jo, H. Na Kim, W. H. Hwang, H. Ki Hong, Y. S. Choi, and S. Won Jung, "Wearable Patch Device for Uterine EMG and Preterm Birth Monitoring Applications," *IEEE Region 10 Annual International Conference, Proceedings/TENCON*, vol. 2018-Octob, no. October, pp. 1127–1130, 2019.

[118] O. Oti, I. Azimi, A. Anzanpour, A. M. Rahmani, A. Axelin, and P. Liljeberg, "Iot-based healthcare system for real-Time maternal stress monitoring," *Proceedings - 2018 IEEE/ACM International Conference on Connected Health: Applications, Systems and Engineering Technologies, CHASE 2018*, pp. 57–62, 2019.

[119] T. Rahman, A. Anjum, R. Rahman, and R. R. Khan, "A proposed integrated system towards digitizing the maternal health and children support process in developing countries," *2019 5th IEEE International WIE Conference on Electrical and Computer Engineering, WIECON-ECE 2019 - Proceedings*, pp. 2–5, 2019.

[120] I. Marin, B. I. Pavaloiu, C. V. Marian, V. Racovita, and N. Goga, "Early detection of preeclampsia based on a machine learning approach," *2019 7th E-Health and Bioengineering Conference, EHB 2019*, pp. 21–24, 2019.

[121] Y. Gupta, S. Kumar, and V. Mago, "Pregnancy health monitoring system based on biosignal analysis," *2019 42nd International Conference on Telecommunications and Signal Processing, TSP 2019*, pp. 664–667, 2019.

[122] S. Kumar, Y. Gupta, and V. Mago, "Health-monitoring of pregnant women: Design requirements, and proposed reference architecture," *2019 16th IEEE Annual Consumer Communications and Networking Conference, CCNC 2019*, 2019.

[123] S. Prasath Surendhar, B. Baby, and S. Jesna, "Smart mobile system for pregnancy care using body sensors," *International Journal of Innovative Technology and Exploring Engineering*, vol. 8, no. 9 Special Issue 3, pp. 1091–1092, 2019.

[124] A. R. Sazali and R. Al-Ashwal, "Fetal movement simulator for fetal monitoring system testing," *2018 IEEE EMBS Conference on Biomedical Engineering and Sciences, IECBES 2018 - Proceedings*, pp. 544–547, 2019.

[125] J. B. Tylcz, C. Muszynski, J. Dauchet, D. Istrate, and C. Marque, "An Automatic Method for the Segmentation and Classification of Imminent Labor Contraction from Electrohysterograms," *IEEE Transactions on Biomedical Engineering*, vol. 67, no. 4, pp. 1133–1141, 2020.

[126] G. Fele-Žorž, G. Kavšek, Ž. Novak-Antolič, and F. Jager, "A comparison of various linear and non-linear signal processing techniques to separate uterine EMG records of term and pre-term delivery groups," *Medical and Biological Engineering and Computing*, vol. 46, no. 9, pp. 911–922, 2008.

[127] A. L. Goldberger, L. A. N. Amaral, L. Glass, J. M. Hausdorff, P. C. Ivanov, R. G. Mark, J. E. Mietus, G. B. Moody, C.-K. Peng, and H. E. Stanley, "Physiobank, physiotoolkit, and physionet: Components of a new research resource for complex physiologic signals," *Circulation*, vol. 101, no. 23, pp. e215–e220, 2000. [Online]. Available: http://circ.ahajournals.org/content/101/23/e215

[128] A. Alexandersson, T. Steingrimsdottir, J. Terrien, C. Marque, and B. Karlsson, "The icelandic 16-electrode electrohysterogram database," *Scientific Data*, vol. 2, pp. 150 017 EP –, 04 2015. [Online]. Available: http://dx.doi.org/10.1038/sdata.2015.17

[129] H. Allahem and S. Sampalli, "Framework to monitor pregnant women with a high risk of premature labour using sensor networks," in *Proceedings of the IM 2017 - 2017 IFIP/IEEE International Symposium on Integrated Network and Service Management*, 2017, pp. 1178–1181. [Online]. Available: https://ieeexplore.ieee.org/document/7987458

[130] H. Allahem and S. Sampalli, "Automated uterine contractions pattern detection framework to monitor pregnant women with a high risk of premature labour," *Informatics in Medicine Unlocked*, vol. 20, p. 100404, 2020. [Online]. Available: https://doi.org/10.1016/j.imu.2020.100404

[131] F. Jager, S. Libenšek, and K. Geršak, "Characterization and automatic classification of preterm and term uterine records," vol. 13, no. 8, pp. 1–49, 2018.

[132] C. Sammut and G. I. Webb, Eds., *Encyclopedia of Machine Learning*. Boston, MA: Springer US, 2010.

[133] K. Sharma and R. Nandal, "A literature study on machine learning fusion with IoT," *Proceedings of the International Conference on Trends in Electronics and Informatics, ICOEI 2019*, vol. 2019-April, no. Icoei, pp. 1440–1445, 2019.

[134] O. Simeone, "A Very Brief Introduction to Machine Learning With Applications to Communication Systems," *IEEE Transactions on Cognitive Communications and Networking*, vol. 4, no. 4, pp. 648–664, 2020.

[135] Y. Wu, "Based on machine learning of data mining to further explore," *Proceedings - 2012 International Conference on Computer Science and Information Processing, CSIP 2012*, pp. 1235–1238, 2012.

[136] C. Malhotra, "Ethical Framework for Machine Learning Charru Malhotra," *Machine Learning for a 5G Future*, pp. 26–28, 2018.

[137] P. Singh, S. P. Singh, and D. S. Singh, "An introduction and review on machine learning applications in medicine and healthcare," *2019 IEEE Conference on Information and Communication Technology, CICT 2019*, 2019.

[138] A. R. Rout and S. B. Bagal, "Natural Scene Classification Using Deep Learning," *2017 International Conference on Computing, Communication, Control and Automation, ICCUBEA 2017*, 2018.

[139] V. Chudáček, J. Spilka, M. Burša, P. Janků, L. Hruban, M. Huptych, and L. Lhotská, "Open access intrapartum CTG database," *BMC Pregnancy and Childbirth*, vol. 14, no. 1, 2014.

[140] A. Phinyomark and E. Scheme, "EMG Pattern Recognition in the Era of Big Data and Deep Learning," *Big Data and Cognitive Computing*, vol. 2, no. 3, p. 21, 2018.

[141] S. S. Gavankar and S. D. Sawarkar, "Eager decision tree," *2017 2nd International Conference for Convergence in Technology, I2CT 2017*, vol. 2017-Janua, pp. 837–840, 2017.

[142] S. Kabiraj, M. Raihan, N. Alvi, M. Afrin, L. Akter, S. A. Sohagi, and E. Podder, "Breast Cancer Risk Prediction using XGBoost and Random Forest Algorithm," *2020 11th International Conference on Computing, Communication and Networking Technologies, ICCCNT 2020*, pp. 1–4, 2020.

[143] S. Ghosh and C. Banerjee, "A Predictive Analysis Model of Customer Purchase Behavior using Modified Random Forest Algorithm in Cloud Environment," *2020 IEEE International Conference for Convergence in Engineering, ICCE 2020 - Proceedings*, pp. 239–244, 2020.

[144] S. F. Ding, X. L. Liu, and L. W. Zhang, "Research on Ranking Support Vector machine and prospects," *Proceedings of the 29th Chinese Control Conference, CCC'10*, no. 9, pp. 2829–2831, 2010.

[145] A. C. Braun, U. Weidner, and S. Hinz, "Support Vector Machines, Import Vector Machines And Relevance Vector Machines For Hyperspectral Classification - A Comparison," vol. 2, no. 3, pp. 36–39, 2011.

[146] S.-x. Lu, J. Meng, and G.-e. Cao, "Support vector machine based on a new reduced samples method," in *2010 International Conference on Machine Learning and Cybernetics*, vol. 3. IEEE, jul 2010, pp. 1510–1514. [Online]. Available: http://ieeexplore.ieee.org/document/5580828/

[147] S. Balasundaram and N. Kapil, "Application of Lagrangian Twin Support Vector Machines for Classification," in *2010 Second International Conference on Machine Learning and Computing*. IEEE, 2010, pp. 193–197. [Online]. Available: http://ieeexplore.ieee.org/document/5460743/

[148] A. H. Jahromi and M. Taheri, "A non-parametric mixture of Gaussian naive Bayes classifiers based on local independent features," *19th CSI International Symposium on Artificial Intelligence and Signal Processing, AISP 2017*, vol. 2018-Janua, no. 1, pp. 209–212, 2018.

[149] T. M. Ma, K. Yamamori, and A. Thida, "A Comparative Approach to Naïve Bayes Classifier and Support Vector Machine for Email Spam Classification," *2020 IEEE 9th Global Conference on Consumer Electronics, GCCE 2020*, pp. 324–326, 2020.

[150] T. Fawcett, "An introduction to roc analysis," *Pattern Recognition Letters*, vol. 27, no. 8, pp. 861–874, 2006, rOC Analysis in Pattern Recognition. [Online]. Available: https://www.sciencedirect.com/science/article/pii/S016786550500303X

[151] M. Majumder, "Artificial Neural Network," pp. 49–54, 2015.

[152] H. A. Mesrabadi and K. Faez, "Improving early prostate cancer diagnosis by using Artificial Neural Networks and Deep Learning," *Proceedings - 2018 4th Iranian Conference of Signal Processing and Intelligent Systems, ICSPIS 2018*, pp. 39–42, 2018.

[153] F. Chollet, *Deep Learning with Python*, 1st ed. USA: Manning Publications Co., 2017.